



UNIVERSITÀ DEGLI STUDI DI MILANO  
FACOLTÀ DI SCIENZE MATEMATICHE,  
FISICHE E NATURALI

# Spanning Trees and Forests on genus-weighted Random Lattices

Relatore: Prof. Sergio Caracciolo

Correlatore: Dott. Andrea Sportiello

Roberto Bondesan  
Matricola 736421  
A.A. 2008/2009

PACS: 05.50.+q,  
75.10.Hk, 02.10.Ox

# Contents

<b>Introduction</b>	<b>1</b>
Outline of the thesis . . . . .	2
<b>1 Random Matrices and Combinatorics</b>	<b>5</b>
1.1 Wick's theorem and Feynman diagrams as tools for enumerating graphs	5
1.1.1 Catalan numbers . . . . .	9
1.2 EGF for fat-graphs . . . . .	10
1.3 Multi-matrix integrals . . . . .	11
1.3.1 $\mathcal{O}(n)$ loop-gas model on random lattices . . . . .	12
1.3.2 Potts model on random lattices . . . . .	14
<b>2 Solution of the <math>\mathcal{O}(n)</math> loop-gas model for <math>n = 0, -2</math></b>	<b>17</b>
2.1 Saddle point equation . . . . .	18
2.2 The $\mathcal{O}(0)$ loop-gas model, i.e. the one-matrix model . . . . .	20
2.2.1 Wigner semicircle law and quartic potential . . . . .	21
2.2.2 The continuum limit . . . . .	22
2.3 The $\mathcal{O}(-2)$ loop-gas model . . . . .	23
2.3.1 Eigenvalue density . . . . .	23
2.3.2 Singularity structure . . . . .	24
<b>3 Counting unicellular maps</b>	<b>27</b>
3.1 An exponential generating function from matrix integrals . . . . .	27
3.2 More facts about counting unicellular maps . . . . .	30
<b>4 Random matrix approach to spanning forests on random lattices</b>	<b>34</b>
4.1 General background and motivations . . . . .	34
4.2 The model . . . . .	37
4.3 Useful counting problems . . . . .	38
4.3.1 Counting non-intersecting trees in $\mathbb{H}$ . . . . .	38
4.3.2 Counting non-intersecting trees in $\mathbb{D}$ . . . . .	40
4.4 A matrix integral for the partition function . . . . .	40
4.5 Critical structure of spanning forests . . . . .	43
4.5.1 Equivalence with the $\mathcal{O}(-2)$ loop-gas model . . . . .	43

4.5.2	Mapping to flat lattice . . . . .	44
<b>5</b>	<b>Exploring the universality class <math>\gamma = -1</math></b>	<b>49</b>
5.1	Spanning trees on random planar graphs . . . . .	49
5.1.1	Critical coupling and string susceptibility exponent . . . . .	50
5.2	Spanning hypertrees on random planar hypergraphs . . . . .	51
5.2.1	Two combinatorial results for spanning hypertrees . . . . .	52
5.2.2	Computation of the partition function and critical behaviour . . . . .	57
5.3	Hamiltonian cycles . . . . .	59
5.4	Discussions . . . . .	61
<b>6</b>	<b>Spanning trees on random lattices of arbitrary genus</b>	<b>62</b>
6.1	Analysis at fixed genus . . . . .	62
6.1.1	Thermodynamic limit . . . . .	64
6.1.2	Partition function as sum over triangulations . . . . .	64
6.2	All genus partition function . . . . .	68
6.2.1	Divergent series and Borel summability . . . . .	68
6.2.2	Critical behaviour of the exponential generating function . . . . .	71
6.2.3	Subleading corrections as sums over polygons . . . . .	75
6.3	Discussions . . . . .	78
	<b>Conclusion and outlook</b>	<b>80</b>
<b>A</b>	<b>Basic notions about graphs and maps</b>	<b>82</b>
A.1	Graphs . . . . .	82
A.2	Maps . . . . .	84
A.2.1	Fat-graphs . . . . .	84
A.2.2	Automorphism group . . . . .	85
A.2.3	Dual map . . . . .	86
<b>B</b>	<b>The Tutte polynomial</b>	<b>87</b>
B.1	Relation with the Potts model and spanning forests . . . . .	87
B.2	Spanning trees expansion . . . . .	90
B.2.1	Definition for embedded graphs . . . . .	91
	<b>Bibliography</b>	<b>95</b>

# List of Figures

1.1	Pictorial representation of matrix elements as double opposite oriented lines. Propagators force to contract the half-edges according to arrows. . . . .	7
1.2	The graphical representation of $\langle \text{Tr} M^6 \rangle$ as a sum over $(6 - 1)!! = 15$ labelled one-vertex fat-graphs with 3 edges. . . . .	8
1.3	On top, there is a link pattern with $n = 8$ arcs. On bottom there is depicted the procedure of removal of the rightmost arc that leaves two link patterns. . . . .	9
1.4	A configuration of self-avoiding loops on a random triangulated surface of genus 1 in the $\mathcal{O}(n)$ loop-gas model on random lattices. . . . .	14
1.5	A configuration of the Potts model on random graphs. Edges colored in one color weight $e^k$ , while edges that links vertices with different colors weight 1. . . . .	15
2.1	The terms in the expansion (2.28) up to $n = 2$ . Under every graph there is its weight. . . . .	22
3.1	A representation of the partition $\lambda = (4, 3, 2, 1, 1)$ of 11 by its Ferrers' diagram. . . . .	31
4.1	On top, there is a cubic tree ( $h = 1$ ) with $n = 8$ vertices and 10 leaves on $\partial\mathbb{H}$ . On bottom, we depicted the procedure of removal of the rightmost leaf and the resulting trees that remains. . . . .	39
4.2	The identification of a component of a forest on a random cubic graph with a tree on the disk. The edges of the tree are marked in bold and the region enclosed by the shaded line is the tree with its border legs. . . . .	41
4.3	The procedure for shrinking the trees. Given a spanning forest $\mathcal{F}$ over a graph $\mathcal{G}$ , we mark the components of the forest (here in bold) , and we shrink the trees with their leaves to single vertices respecting the ordering of the the border legs. Then we obtain $\mathcal{G}/\mathcal{F}$ (graph on the bottom). The figure on top right is an intermediate step, where we deform the graph and color in gray the region to be shrunked, to better visualize the procedure. . . . .	42

4.4	The phase diagram of the Potts model on the square lattice. There are four regions, corresponding to a ferromagnetic phase (F), a high temperature phase (HT), an antiferromagnetic phase (AF), and a non physical region (NP) where $v < -1$ . The blue solid curve are the ferromagnetic and antiferromagnetic transition curves of the Baxter solution. We enlarge the phase diagram near the origin related to spanning forests. The two regions corresponding to a high temperature phase and a massless low temperature phase, are colored respectively in light red and light blue. Note that there are not critical points between $w = +\infty$ (spanning trees, $c = -2$ ) and $w = -1/4$ (antiferromagnetic transition, $c = -1$ ), beside the trivial point $w = 0$ , thus confirming asymptotic freedom. The point $v = e^K - 1 = 0$ ( $w = 0$ ) is the infinite temperature point, and the arrows determine the stability of critical points according to the renormalization group analysis of the $\mathcal{O}(n)$ $\sigma$ -model. . . . .	46
4.5	A rooted cubic random planar graph with 6 vertices ad a spanning tree over it that has no internal embedding-active edges and then contributes to the partition function of spanning forests on random planar graphs at $t = -1$ . External embedded-active edges are marked with a star. The blue line starting at the root (red half-edge) is the walk that defines the ordering and consequently the activity. . . . .	48
5.1	On the left a spanning tree (with edges in bold) on a random cubic planar graph. The gray region becomes a point when the tree is shrinked. Then we are left with a planar one-vertex diagram with petals juxtaposed or included into one-another. . . . .	50
5.2	A spanning hypertree on a 3-uniform cubic random hypergraph. Hyperedges of the spanning tree are in black. . . . .	53
5.3	On top a hyperlink pattern with $m = 5$ 3-hyperarcs. On bottom the removal procedure of the rightmost hyperarc that leaves $l = 3$ remaining component. . . . .	53
5.4	On top the generating function $F_{k,l}(z)$ . It is a sum over $m$ of the configurations of hypertrees with $m$ border legs rooted on $\partial\mathbb{H}$ . On bottom the auxiliary generating function $F_{k,l}^*(z)$ . Here the sum is over configurations constrained to have a vertex as the rightmost point in $\partial\mathbb{H}$ . . . . .	55
5.5	On top the graphical explanation of equation (5.14). The $k - 1$ objects attached to the vertex of the rightmost leg (in red) can be part of a hyperedge or a border leg. This binary choice produces the factor $(z + F_{k,l}^*(z))^{k-1}$ on the right hand side of the equation. On bottom the illustration of equation (5.15). We remove the hyperedge (in red) containing the rightmost vertex and substitute the hyperedge with $l - 1$ border legs (here $l = 3$ ). This operation brings the term $1/z$ for every leg that was not rooted. . . . .	56

5.6	The shrinking procedure and the resulting one-vertex planar hypergraph. In dark gray the region to be shrunked. . . . .	58
5.7	A cubic random planar graph with $2n = 20$ vertices that possesses a Hamiltonian cycle over it (marked in bold), is equal to two sequences of link patterns defined as the inner (marked in blue) and outer (marked in red) configurations of the cycle. . . . .	60
6.1	A spanning tree over a graph embedded in a surface of genus 3. The gray region encloses the tree with its leaves to be shrunked. After the shrinking we have a one-vertex graph on that surface. . . . .	63
6.2	The two steps for replacing $G'$ with $G'''$ . . . . .	66
6.3	The circle over which the integral in equation 6.15 is performed. It is between the branch cuts of $Q_-(z)$ and $a(z)$ . . . . .	67
6.4	The $N^{2/3}$ vs. $\tilde{g}$ phase diagram. The region filled is where the integral converges. The boundary of this region is the critical curve, equation (6.38). Of course this analysis is not valid for values of $N^{2/3}$ near the origin. . . . .	74
A.1	Deletion and contraction of the edge marked in blue. . . . .	83
A.2	A graph, together with a spanning tree (middle) and a spanning forest with three connected components (right) over it. . . . .	83
A.3	The complete graph $K_4$ drawn on the sphere and on the torus corresponds to two maps of different genus. . . . .	85
A.4	On the left, three edges that meet at a vertex defining a cyclic ordering. On the right, a face. . . . .	85
A.5	At the left top corner there is a one-vertex map of genus 1 with 3 edges. We can draw it on the torus, as at the top of the middle column, where the torus is as usual seen as the quotient space of the square where black and white arrows indicate how to glue the sides. This map has two faces both of degree 3 corresponding to the filled and non filled region. Then we construct the dual map by inserting a dual vertex (white circle) in every face. Dual edges are represented as shaded lines and connect dual vertices on the two sides of the edges of the one-vertex map. The figure at the bottom of the middle column is the resulting dual map with one face, drawn on the torus. If we draw it on the plane as in the right bottom corner, non-planarity imposes that its edges intersect not only in their endpoints. . . . .	86
B.1	The 16 spanning subgraphs of $C_4$ . Elements of the subgraphs are marked in red. . . . .	88
B.2	Examples of fundamental cycle and cocycle for edges of the graph in figure B.2(a). . . . .	90
B.3	The walk along the tree that starts from the root (red half-edge) is marked in blue. We order the edges according to their order of appearance around the tree and mark the resulting embedding-active edges with a star. . . . .	92

B.4	A rooted cubic random planar graph with embedding-active edges marked with a star. It has 4 internal and 3 external embedding-active edges. As before the root is in red and the walk along the tree in blue. The external edges form link patterns on the boundary of the upper half-plane. . . . .	92
B.5	The configurations that lead to internal and external embedding-active edges on random planar graphs. Filled regions correspond to arbitrary configurations and the the root is marked in red. . . . .	93

# Introduction

Within the context of statistical mechanics in two dimensions, one of the topics that deserved a lot of interest during the last thirty years is the study of statistical systems on random lattices, that is accomplished by replacing the fixed lattice on which a model is defined with its spatial fluctuations. The computations of the thermodynamical quantities in this case can be pursued using the techniques of the so called *random matrix theory* since the partition function of a model can be expressed as a suitable integral over one or more matrices.

The idea behind this identification dates back to a work by 't Hooft on quantum chromodynamics [1]. 't Hooft showed that the Feynman diagrams of a matrix field theory can be interpreted as double line graphs called fat-graphs, setting the basis for the enumeration of graphs according to their genera (topological expansion) needed to study models on random graphs.

The precise connection between a matrix field theory and the enumeration of graphs was established by Brezin *et. al* in [2] where they computed exactly a sum over planar graphs solving a matrix integral in the limit of large dimension of the matrix. Their breakthrough result inspired Kazakov who few years later solved the Ising model on fluctuating lattices [3]. Since then a plethora of statistical models, such as the  $\mathcal{O}(n)$  or the Potts model, were solved on random graphs.

The study of this branch of statistical mechanics is of interest for a wide range of physical and mathematical research areas. Random lattices are dual to dynamical triangulations that can be interpreted as discretized version of surfaces. There are indeed many of two dimensional systems that can be understood in terms of statistical mechanics of fluctuating surfaces, such as biological membranes, 2D quantum gravity and string theory [4].

The connection with 2D quantum gravity was the most investigated and a lot of checks between its continuum formulation, Liouville field theory, and the results obtained with matrix models were performed, ensuring that the discrete approach is valuable and important. In string theory one dimensional objects called strings evolve in time describing a 2D world-sheet, that is a surface on which is defined the  $d$ -dimensional vector field that describes the string. Then also string theories can be discretized as random lattices, but the applicability of this discrete approach is limited to  $d \leq 1$  [5].

A great interest about physical systems on random lattices comes also from their flat space counterpart since the critical properties of a model on fixed and random graphs



can be related with the KPZ relations [6]. If the discrete formulation of 2D quantum gravity and string theory have eventually been not so successful, this connection is in principle very fruitful since models on random lattices are generally easier to solve than their partners on the plane, the deep reason being their larger symmetry, the discrete version of the general covariance.

Random matrices, the most important tool to deal with statistical mechanics on random lattices, were first introduced in physics by Wigner [7], for explaining the energy level distribution in heavy nuclei. Since then, they were useful not only in statistical mechanics, but also in different aspects of quantum physics [8] and in integrable systems [9] to mention some of the applications<sup>1</sup>.

Random graphs are studied also by mathematicians, and from their point of view the partition function of a model on fluctuating lattices is the generating function of decorated random graphs. Then during the last years direct combinatorial methods has entered the field beside random matrix techniques. Combinatorics and random matrices have been applied together for solving different enumeration problems of both mathematical and physical interest, such as the enumeration of maps [11], the counting of knots and tangles [12] and the meander problem, directly related with the folding of polymers and membranes [13]. The intimate connection between combinatorics and statistical physics led also to new combinatorial solutions of statistical models, as in [14, 15].

Given this background, in this thesis we will turn our attention to the study of spanning forests and spanning trees on random lattices. A spanning forest is a subgraph without cycles that has the same vertex set of the underlying graph, and a tree is a forest with only one connected component. Spanning forests are an important and interesting topic in graph theory and combinatorics, but not only in these fields. They are also important in statistical physics, where the partition function of spanning forests arises in the limit  $q \rightarrow 0$  of the Potts model in the Fortuin-Kasteleyn representation [16]. Moreover the same partition function can be represented as a fermionic theory, that resembles the  $\mathcal{O}(n)$  invariant non linear  $\sigma$ -model at  $n = -1$  [17]. Studying spanning forests then gives information on the phase diagram of these models. The connection with the  $\mathcal{O}(n)$   $\sigma$ -model model makes also clear that at least perturbatively spanning forests are asymptotically free for positive values of the fugacity of the trees. Asymptotic freedom is a not yet completely understood feature shared also by non abelian gauge theories, and the simplicity of forests can potentially give new insights on this important aspect. Moreover, a good reason for studying spanning trees is that they are related to further different topics of 2D statistical mechanics, such as logarithmic conformal field theories and stochastic Loewner evolution (SLE).

---

<sup>1</sup>For an extensive treatise on random matrices, see Mehta [10]

## Outline of the thesis

In this thesis we will explain how to deal with spanning forests and spanning trees when considered on random lattices. It will turn out that in most cases simple combinatorial considerations can be used to solve the models. We will try to follow the implications of our results and in particular we would like to have a better understanding of the critical behaviour on both random and flat lattices.

In chapter 1 we explain the connection between combinatorics and random matrices. We first show how averages with respect to a Gaussian measure over a  $N \times N$  Hermitian matrix generate random fat-graphs weighted by powers of  $N$  according to their genus, and we give an expression for the generating function of fat-graphs. Then we put loops and spin variables on the lattices, using multi-matrix models. These are interpreted as the partition functions of the  $\mathcal{O}(n)$  loop-gas and Potts model on fluctuating surfaces.

Chapter 2 concerns the solution of the matrix integral of the  $\mathcal{O}(n)$  loop-gas model with the saddle point technique. We show how to derive the saddle point equation in the general case, and we solve it in the special cases  $n = 0$  and  $n = -2$ . The specialization to  $n = 0$  is equivalent to a one-matrix model and its solution is a pedagogical introduction of the relevant concepts, such as the spectral density of eigenvalues and the string susceptibility exponent. The solution of the  $\mathcal{O}(-2)$  loop-gas model is then pursued following Kostov [18], and we show how to derive the critical points of the model.

Chapter 3 will be devoted to some results in the enumeration of unicellular maps. Maps are embedded graphs and their counting can be pursued using matrix integrals as shown in chapter 1. We first present the early work of Harer and Zagier that involved random matrices [11]. Then we turn to purely combinatorial formulas and give the results obtained by Walsh and Lehman [19] and Goupil and Schaeffer [20] who express the number of unicellular maps of given genus as sum over integer partitions of the genus. Along with the trend of using combinatorial methods in statistical mechanics, we will use these results later to compute the partition function of spanning trees on random lattices of arbitrary genus.

In chapter 4 we will deal with the model of spanning forests on random lattices. After a brief revision of the actual state of the art in understanding spanning forests, we derive a matrix integral to represent the partition function, as done by Caracciolo and Sportiello in [21]. This derivation consists in shrinking the trees to points and study the resulting ensemble of graphs with effective vertices, the whole procedure being controlled using basic results in the combinatorics of trees. Then we expose our original contribution to this problem. We make the connection with the  $\mathcal{O}(-2)$  loop-gas model and use its solution presented in chapter 2 to obtain the critical behaviour of spanning forests on random lattices. This analysis joint with the KPZ relations confirms asymptotic freedom and predicts the existence of a critical point for negative value of the fugacity whose interpretation is discussed.

Chapter 5 and 6 present the combinatorial methods to deal with spanning trees and

related models on random lattices. Starting from the combinatorial solution of trees on random planar graphs presented in [21], we are able to solve also other models pertaining to the same universality class,  $\gamma = -1$ . We first generalize the analysis to hypertrees on random planar hypergraphs, thanks to the derivation of more general combinatorics about hypertrees and hyperlink patterns, and then we easily solve Hamiltonian cycles. The solution of these two models are original work. Chapter 6 is entirely original. There we will extend the analysis of spanning trees from planar to positive genus lattices, showing that we can compute exactly the partition function at every genus using the results of chapter 3. The critical exponents computed are in agreement with the literature and our previous analysis. It is also shown that the analysis at generic genus in the thermodynamic limit can be carried out by considering only one-vertex triangulations of a surface. We will also try to understand the possibility of a non perturbative solution from the topological expansion we have computed. We study the exponential generating function of spanning trees of given genus, deriving its critical behaviour and explaining a method to keep track of the subleading corrections.

In appendix A we give some standard notions about graphs and maps that will be useful in the whole work, explaining concepts such as duality and automorphism of a map. In appendix B the Tutte polynomial of a graph and its relation with spanning forests is presented. In particular we specialize to the spanning trees expansion in the case of random planar graphs.

# Chapter 1

## Random Matrices and Combinatorics

Integrals over the ensemble of random matrices are intimately connected with the enumeration of graphs [13, 22]. Wick's theorem and Feynman diagrams allow to associate to every matrix integral a generating function for decorated graphs of given genus that are interpreted as statistical models on fluctuating surfaces, namely the discretization of 2D Quantum Gravity coupled to matter model [5]. The idea underlying the diagrammatics of matrix integrals dates back to the work of 't Hooft in the context of large  $N$  QCD [1]. Subsequently, starting from the fundamental works of Bessis [23] and Brezin *et. al* [2] this subject deserved a lot of interest during the last thirty years, and a lot of solutions of several statistical models on random lattices were exposed.

### 1.1 Wick's theorem and Feynman diagrams as tools for enumerating graphs

We start considering a normalized Gaussian measure over the real line and we want to compute averages of monomials  $x^{2n}$  w.r.t it:

$$\langle x^{2n} \rangle = \frac{1}{\sqrt{2\pi}} \int_{-\infty}^{+\infty} x^{2n} e^{-\frac{1}{2}x^2} dx. \quad (1.1)$$

To compute this integral introduce the generating function  $\Sigma(s) = \langle e^{sx} \rangle = e^{s^2/2}$ , so that  $\langle x^{2n} \rangle$  will be given by the  $2n$ -th derivative of  $\Sigma(s)$  evaluated in  $s = 0$ . Note that derivatives must be taken by pairs one on the exponential and one on the term thus created, to yield a nonzero result. Since every pair of derivative contributes as  $(d^2/ds^2)\Sigma(s)|_{s=0} = 1$ , integral (1.1) will be equal to the number of pairings of  $2n$  objects,  $(2n - 1)!!$ . We can describe the computation of  $\langle x^{2n} \rangle$  pictorially associating a half-edge attached to a single vertex to every term  $x$ . Then a pair of derivatives will correspond to a matching between two half-edges and each of the  $(2n - 1)!!$  possible

saturation of these half-edges will produce a one-vertex graph with  $n$  edges. This interpretation lead to the one-dimensional version of the *Wick's theorem*:

$$\langle x^{2n} \rangle = \sum_P \prod_{e \in P} \langle x^2 \rangle \quad (1.2)$$

where the sum is over all possible pairings  $P$  that saturate the  $2n$  half-edges and the product is over the set of edges  $e$  thus formed. We have then reduced the computation of the integral (1.1) to that of  $\langle x^2 \rangle = (d^2/ds^2)\Sigma(s)|_{s=0} = 1$ .

Wick's theorem is a fundamental result in quantum field theory (QFT) which expresses the averages of polynomials w.r.t a Gaussian measure (finite or infinite dimensional). In the language of QFT each saturation of the half-edges is a *Feynman diagram* of this theory and to every edge corresponds a propagator  $\langle xx \rangle = 1$ .

Now, we substitute to the integration over the line an integration over  $N \times N$  Hermitian matrices  $M$  and we would like to generalize the analysis above. Using a matrix notation, the normalized Gaussian probability measure we will use is<sup>1</sup>:

$$\frac{1}{Z_0} e^{-\frac{1}{2} N \text{Tr} M^2} \mathcal{D}M \quad (1.3)$$

where  $Z_0 = (2\pi/N)^{N^2} 2^{(N-N^2)/2}$  and  $\mathcal{D}M = \prod_i dM_{ii} \prod_{i < j} d\Re M_{ij} d\Im M_{ij}$  is the Haar measure of the group of Hermitian matrices invariant under  $U(N)$ . We are interested in computing

$$\langle f(M) \rangle = \frac{1}{Z_0} \int f(M) e^{-\frac{1}{2} N \text{Tr} M^2} \mathcal{D}M. \quad (1.4)$$

To generalize Wick's theorem to the matrix case, introduce as above a generating function  $\Sigma(S) = \langle e^{\text{Tr} SM} \rangle = e^{\frac{\text{Tr} S^2}{2N}}$ . Deriving  $\Sigma(S)$  by  $S$  and evaluating in  $S = 0$  gives the averages of product of matrices and again we have to take derivatives by pairs to have a nonzero result. So, analogously to the uni-dimensional case, we can easily state the Wick's theorem for matrix fields:

$$\left\langle \prod_{(ij) \in J} M_{ij} \right\rangle = \sum_P \prod_{(ij,kl) \in P} \langle M_{ij} M_{kl} \rangle \quad (1.5)$$

where  $J$  is a list of indices and the sum is over all the possible pairings  $P$  of pairs of indices in  $J$  and the propagator is<sup>2</sup>:

$$\langle M_{ij} M_{kl} \rangle = \left. \frac{\partial}{\partial S_{ji}} \frac{\partial}{\partial S_{lk}} \langle e^{\text{Tr} SM} \rangle \right|_{S=0} = \frac{1}{N} \delta_{il} \delta_{kj}. \quad (1.6)$$

Following 't Hooft [1], the Feynman diagrams of this matrix field theory can be constructed by associating to every term  $M_{ij}$  a half-edge composed of two double lines

<sup>1</sup> We introduced a factor  $N$  in the exponential to yield a non trivial limit  $N \rightarrow \infty$ , since  $\mathcal{D}M$  consists of  $N^2$  terms and behaves like  $e^{N^2}$ .

<sup>2</sup>Note that to obtain a factor  $M_{ij}$  we have to derive  $\Sigma(S)$  by  $S_{ji}$ .

carrying indices  $i$  and  $j$  in opposite directions (Fig. 1.1(a)). According to (1.6), nonzero contractions of the half-edges are the ones where they are joined according to the arrows orientations to form  $\langle M_{ij}M_{ji} \rangle$  (Fig. 1.1(b)). In this way,  $\text{Tr}(M^n)$  will be represented by a star diagram with  $n$  half-edges made of oriented double lines in such a way to respect the identification of the indices (see figure 1.1(c) for an example in the case  $n = 6$ ).

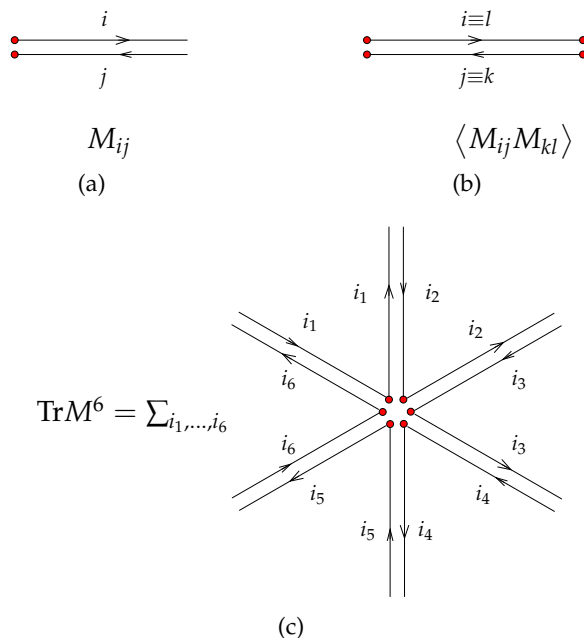


Figure 1.1: Pictorial representation of matrix elements as double opposite oriented lines. Propagators force to contract the half-edges according to arrows.

To compute the average of  $\text{Tr}M^n$

$$\langle \text{Tr}(M^n) \rangle = \sum_{i_1, \dots, i_n} \langle M_{i_1 i_2} \cdots M_{i_n i_1} \rangle, \quad (1.7)$$

we contract the half-edges in all possible ways that conserve indices along the lines and weight diagrams with the following Feynman rules:

- Associate a factor  $N^{-1}$  to every propagator (see eq. (1.6))
- Faces (cycles formed by single line) brings a factor  $\sum_i \delta_{ii} = N$ .

The pictorial representation outlined above associate to the Feynman diagrams of the zero-dimensional matrix field theory described by (1.4) one-vertex fat-graphs, graphs with oriented double lines.

These fat-graphs  $\mathcal{G}$  thanks to the “thickened” oriented structure specify an ordering at the edges at vertices, and thus can be seen as piecewise linear surfaces of Euler characteristics

$$\chi(\mathcal{G}) = 2 - 2h(\mathcal{G}) = V(\mathcal{G}) - E(\mathcal{G}) + F(\mathcal{G}) \quad (1.8)$$

where we call  $V$ ,  $E$  and  $F$  respectively the number of vertices, edges and faces, and  $\mathfrak{h}(\mathcal{G})$  is the genus of the surface, its number of handles. Then, in the computation of (1.7) every labelled fat-graph produced by the contractions of the half-edges will be weighted by  $N^{-E+F} = N^{1-2\mathfrak{h}}$ . For a discussion on graphs and their embedding, called in the mathematical language maps, see A.2. However please note that in this thesis we will use the word graph also to indicate its embedding on surfaces.

We remark that  $\langle \text{Tr} M^n \rangle$  has an important combinatorial meaning; it is written as a sum of powers of  $N$  and the coefficient of  $N^{1-2\mathfrak{h}}$  gives the number of one-vertex labeled graphs with  $n/2$  edges that can be drawn on a surface of genus  $\mathfrak{h}$ .

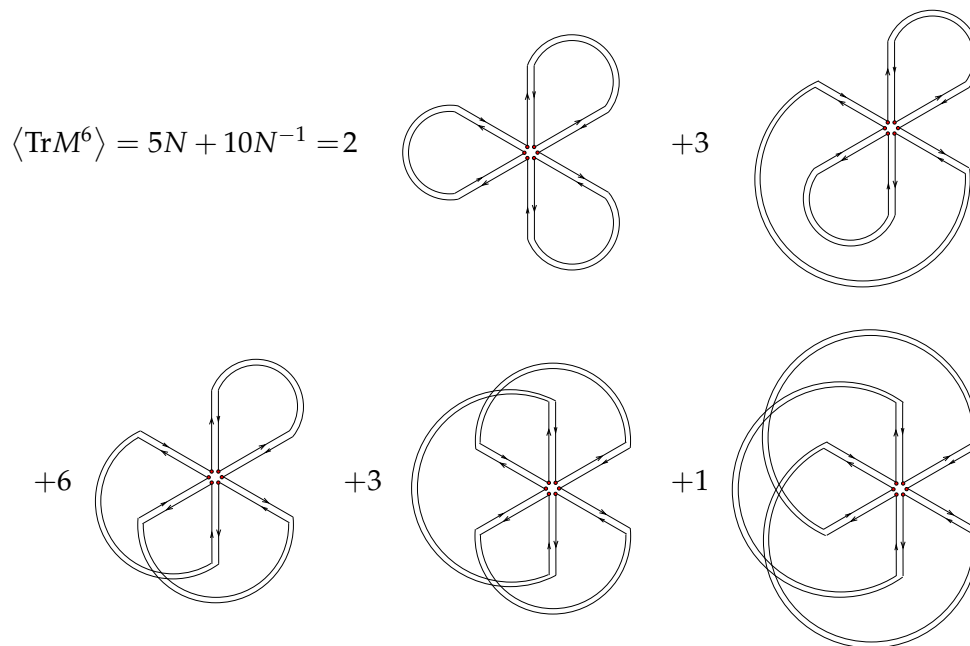


Figure 1.2: The graphical representation of  $\langle \text{Tr} M^6 \rangle$  as a sum over  $(6 - 1)!! = 15$  labelled one-vertex fat-graphs with 3 edges.

In figure 1.2 we represent graphically  $\langle \text{Tr} M^6 \rangle$ . Note that the number of the possible contractions is correctly  $(6 - 1)!! = 15$ . Out of this 15, 5 diagrams are planar, and 10 are of genus 1, as we can read from the coefficient of the term  $N$  and  $N^{-1}$ . Integrating on the space of Hermitian matrices rather than on the line has so allowed us to separate the ways of contracting half-edges according to the genus of the resulting graph.

Now we specialize to the planar case, namely we consider graphs that can be embedded in the Riemann sphere ( $\mathfrak{h} = 0$ ). This is the subset of the  $(n - 1)!!$  one-vertex diagrams in which petals are juxtaposed or included into one-another. If we set  $\chi = 2$  and  $V = 1$  in (1.8), we have that planar graphs contribute as  $N$ , while if  $\mathfrak{h}$  is higher the diagrams contribute with a lower exponent of  $N$ . This means that if we perform the limit  $N \rightarrow \infty$  in (1.7), only the class of planar diagrams survives, and we are left with the enumeration of planar contraction of half-edges of a one-vertex graph. In the next

paragraph we will see how to solve this counting problem.

### 1.1.1 Catalan numbers

Consider the problem of enumerating the planar contractions of half-edges of a one-vertex graph. To better visualize the configurations, we fix a half-edge of an edge (say at position 1) and open the petals respecting their positions. What remains is counting the resulting non-intersecting arcs with extremities on the border of the upper half plane, called *link patterns* (top of figure 1.3, where we switched from the double to the single line representation).

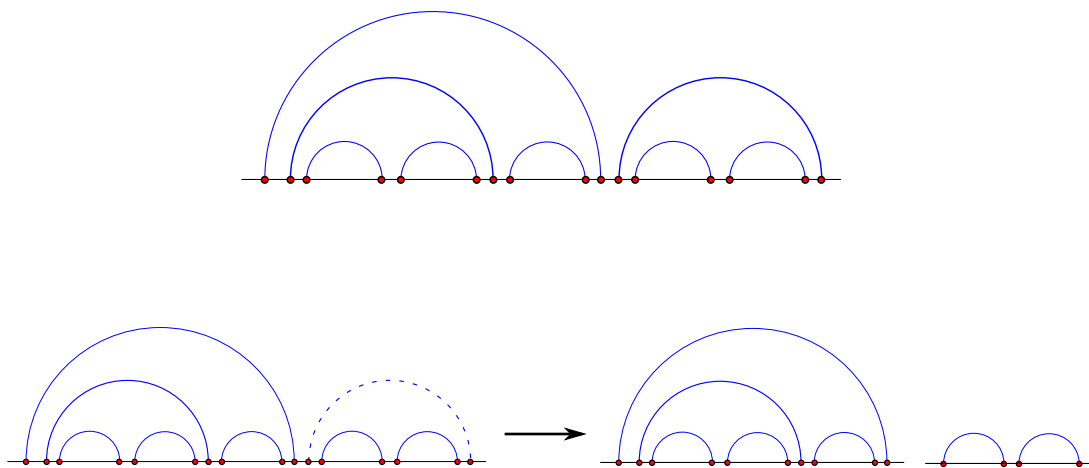


Figure 1.3: On top, there is a link pattern with  $n = 8$  arcs. On bottom there is depicted the procedure of removal of the rightmost arc that leaves two link patterns.

Call  $C_n$  the number of link patterns with  $n$  arcs and set  $C_0 = 1$ , since we have only one empty configuration. Given a configuration with  $n > 0$ , remove the rightmost arc. Then we are left with two smaller link patterns (bottom of figure 1.3) and this translates into this convolutional formula for the coefficient  $C_n$ :

$$C_n = \sum_{n_1=0}^{n-1} C_{n_1} C_{n-1-n_1}. \quad (1.9)$$

Introducing the generating function  $C(q) = \sum_{n \geq 0} C_n q^n$ , (1.9) can be rewritten as

$$C(q) = 1 + qC(q)^2 \quad (1.10)$$

and the solution that is coherent with the condition  $C(0) = 1$  is

$$C(q) = \frac{1 - \sqrt{1 - 4q}}{2q}. \quad (1.11)$$



The coefficient of the Taylor series of the function  $C(q)$  above can be expressed as a Cauchy integral:

$$C_n = \oint \frac{dz}{2\pi iz} \frac{1 - \sqrt{1 - 4z}}{2z} z^{-n}. \quad (1.12)$$

The integration is performed on a circle that encloses the singularity at the origin and since the integrand has a branch cut from  $1/4$  to  $\infty$ , we can deform the contour of integration up to encircle the whole plane except the cut. For any integer  $n$  the integral on the large circle vanishes and what remains are the integrals on the two sides of the cut. Setting  $z = x \pm i\epsilon$ , with  $x \in (1/4, \infty)$  and  $\epsilon > 0$  infinitesimal, we have  $\sqrt{1 - 4(x \pm i\epsilon)} = \mp i|\sqrt{4x - 1}| + O(\epsilon)$ . Then, we can write:

$$\begin{aligned} C_n &= \int_{\frac{1}{4}}^{\infty} \frac{dx}{2\pi} \frac{\sqrt{4x - 1}}{x^{n+2}} \\ &= \frac{1}{n+1} \binom{2n}{n}. \end{aligned} \quad (1.13)$$

These numbers are called the Catalan numbers (sequence [A000108](#) in [24]) and are a very famous integer sequence in combinatorics, since they solve a lot of combinatorial problems.

Once enumerated the planar pairings of a one-vertex diagram, we can immediately obtain the value of  $\frac{1}{N} \langle \text{Tr} M^n \rangle$  in the planar limit:

$$\lim_{N \rightarrow \infty} \frac{1}{N} \langle \text{Tr} M^n \rangle = \begin{cases} C_p = \frac{1}{p+1} \binom{2p}{p} & \text{if } n = 2p \\ 0 & \text{otherwise} \end{cases}. \quad (1.14)$$

## 1.2 EGF for fat-graphs

With the formalism of the previous section, we can write a formal expression for the exponential generating function (EGF) for fat-graphs. Consider the following average:

$$e^{Z_N(\{g_i\})} = \left\langle e^{N \sum_{i \geq 1} g_i \frac{\text{Tr} M^i}{i}} \right\rangle \quad (1.15)$$

which is to be intended as a formal expression defined by its perturbative expansion. When we expand the exponential, we have to compute averages of products of matrices using (1.5) that will instruct us to contract together half-edges of a set of star diagrams in all possible ways. Doing so, (1.15) can be written as a sum over fat-graphs and using Euler relation, we have:

$$e^{Z_N(\{g_i\})} = \sum_{V_1, \dots, V_i, \dots} \prod_i \frac{(Ng_i)^{V_i}}{i^{V_i} V_i!} \left\langle \prod_i (\text{Tr} M^i)^{V_i} \right\rangle \quad (1.16)$$

$$= \sum_{\mathcal{G}} \frac{1}{|\text{Aut}(\mathcal{G})|} \prod_i g_i^{V_i(\mathcal{G})} N^{2-2h(\mathcal{G})}. \quad (1.17)$$

Note that summing over Wick contractions produces labelled graphs, but in (1.17) we are left with a sum over unlabelled fat-graphs  $\mathcal{G}$  weighted by  $1/|\text{Aut}(\mathcal{G})|$ , where  $|\text{Aut}(\mathcal{G})|$  is the order of the automorphism group of  $\mathcal{G}$ , that is the discrete group of symmetries of  $\mathcal{G}$  (see A.2.2). The same happens in QFT where symmetric diagrams does not cancel completely the factor  $1/n!$  in the perturbative expansion of the exponential of the interaction term.

The sum in (1.17) contains also disconnected graphs, and as usual we take the logarithm to have the exponential generating function of connected fat-graphs. Further, we can express it as a sum over topologies:

$$Z_N(\{g_i\}) = \sum_{\mathfrak{h}=0}^{+\infty} N^{2-2\mathfrak{h}} Z_{\mathfrak{h}}(\{g_i\}) \quad (1.18)$$

where we call  $Z_{\mathfrak{h}}$  the partition function of connected fat-graphs of fixed genus  $\mathfrak{h}$ . As well as performing a power series expansion in terms of the couplings  $g_i$ , we can regard the diagrammatic expansion as a perturbation series in  $1/N^2$ , called the *topological expansion*.

Dual fat-graphs give a polygonal tessellation of the Riemann surface in which are embedded (see A.2.3 for the definition of duality). Consider the ensemble of triangulations  $\mathcal{T}$  and the partition function

$$Z_N(g) = \sum_{\mathcal{T}} \frac{g^{A(\mathcal{T})}}{|\text{Aut}(\mathcal{T})|} N^{2-2\mathfrak{h}(\mathcal{T})}. \quad (1.19)$$

This is equal to (1.17) restricted to cubic graphs ( $g_i = 0$  if  $i \neq 3$ ,  $g_3 = g$ ) if we identify  $V(\mathcal{G}) = A(\mathcal{T})$ , for  $\mathcal{T}$  and  $\mathcal{G}$  dual. Equation (1.19) is the partition function of *pure gravity*, the model that describes the structure of the vacuum in 2D quantum gravity<sup>3</sup>

### 1.3 Multi-matrix integrals

Considering ensembles of more than one Hermitian matrix will give us the possibility of specifying decorations on graphs, that will be interpreted as statistical systems defined on fluctuating lattices.

---

<sup>3</sup> Indeed 2D quantum gravity is described formally as a sum over topologies of the path integral over the metrics  $g$  of fixed topology:

$$Z_{QG} = \sum_{\mathfrak{h}=0}^{+\infty} \int \mathcal{D}g e^{-S_E}$$

The action  $S_E$  is the Einstein action, that in 2 dimension is

$$S_E = \Lambda \int_{\mathcal{S}} dx^2 \sqrt{|g|} + \frac{\mathcal{N}}{4\pi} \int_{\mathcal{S}} dx^2 R = \Lambda A(\mathcal{S}) + \mathcal{N}(2 - 2\mathfrak{h}(\mathcal{S}))$$

where  $\Lambda$  is the cosmological constant coupled to the area  $A(\mathcal{S})$  of the surface  $\mathcal{S}$ ,  $R$  is its scalar curvature and  $\mathcal{N}$  is the Newton constant. If we set  $g = e^{-\Lambda}$  and  $N = e^{-\mathcal{N}}$  in (1.19), we recover the discrete version of the functional integration over the metrics. [4]

We now address our interest to generalization of (1.4) of the form

$$\langle f(M_1, \dots, M_p) \rangle = \frac{\int f(M_1, \dots, M_p) e^{-\frac{N}{2} \sum_{a,b=1}^p \text{Tr} M_a Q_{ab} M_b} \mathcal{D}M_1 \dots \mathcal{D}M_p}{\int e^{-\frac{N}{2} \sum_{a,b=1}^p \text{Tr} M_a Q_{ab} M_b} \mathcal{D}M_1 \dots \mathcal{D}M_p} \quad (1.20)$$

where  $M_1, \dots, M_p$  are  $p$  Hermitian matrices and  $Q_{ab}$  is a positive-definite quadratic form. Following our derivation of (1.5) we introduce the source

$$\Sigma(S_1, \dots, S_p) = \left\langle e^{\sum_{a=1}^p \text{Tr} S_a M_a} \right\rangle = e^{\frac{1}{2N} \sum_{a,b=1}^p \text{Tr} S_a Q_{ab}^{-1} S_b} \quad (1.21)$$

and its derivatives in zero will yield the desired averages. The propagator is

$$\langle (M_a)_{ij} (M_b)_{kl} \rangle = \left. \frac{\partial}{\partial (S_a)_{ji}} \frac{\partial}{\partial (S_b)_{lk}} \Sigma(S_1, \dots, S_p) \right|_{S_a=0, S_b=0} = \frac{1}{N} \delta_{il} \delta_{kj} (Q^{-1})_{ab} \quad (1.22)$$

and Wick's theorem for multi-matrix integrals will tell us to sum over possible pairings weighting by (1.22). Different traces of matrices will then represent different types of vertices (and labels  $a, b, \dots$  are attached to half-edges, or *legs*) and we now have the freedom of forbidding the link between legs of type  $a$  and  $b$  by setting  $(Q^{-1})_{ab} = 0$ . This is a way to represent the partition function of statistical systems on fluctuating lattices. We will now see how to construct a matrix integral for the partition function of the  $\mathcal{O}(n)$  loop-gas and Potts model on random lattices. In the  $\mathcal{O}(n)$  loop-gas model studied in this thesis it is sufficient to consider only the case in which  $Q_{ab}$  is a diagonal matrix. More generally, a possible simplification comes from regarding the off-diagonal part as bivalent interaction vertices.

### 1.3.1 $\mathcal{O}(n)$ loop-gas model on random lattices

The  $\mathcal{O}(n)$  loop-gas model is described on a graph  $\mathcal{G}$ , say on the honeycomb lattice, by

$$Z_{\mathcal{G}}^{\mathcal{O}(n)} = \int \prod_{i \in V(\mathcal{G})} d\mu(\vec{\sigma}_i) e^{S_{\mathcal{G}}} \quad (1.23)$$

where the spherical measure  $d\mu(\vec{\sigma}_i)$  is

$$d\mu(\vec{\sigma}_i) = \frac{2}{\Omega_n} \delta(\vec{\sigma}_i^2 - 1) d^n \vec{\sigma}_i, \quad (1.24)$$

$\Omega_n = \frac{2\pi^{n/2}}{\Gamma(n/2)}$ . The model is specified by a logarithmic action,

$$S_{\mathcal{G}} = \sum_{(i,j) \in E(\mathcal{G})} \log(1 + n\beta \vec{\sigma}_i \cdot \vec{\sigma}_j) \quad (1.25)$$

so that (1.23) is

$$Z_{\mathcal{G}}^{\mathcal{O}(n)}(\beta) = \int \prod_{i \in V(\mathcal{G})} d\mu(\vec{\sigma}_i) \prod_{(i,j) \in E(\mathcal{G})} (1 + n\beta \vec{\sigma}_i \cdot \vec{\sigma}_j). \quad (1.26)$$

Expanding in terms of  $\beta$  we obtain a loop model. Since we are on a cubic graph, integrating the terms coming from this expansion involves only the first three moments of (1.24),  $\langle \sigma^a \rangle = 0$ ,  $\langle \sigma^a \sigma^b \rangle = \frac{1}{n} \delta_{ab}$ ,  $\langle \sigma^a \sigma^b \sigma^c \rangle = 0$ . Interpreting the term  $n\beta \sigma_i^a \sigma_j^a$  as a marked edge with color  $a$ , the integration over the spherical measure forces to mark edges with the same color and to have self-avoiding loops. Marked edges get a factor  $\beta$  and the sum over colorings produces a topological factor  $n$  per loop:

$$Z_{\mathcal{G}}^{\mathcal{O}(n)}(\beta) = \sum_{l \in L(\mathcal{G})} \beta^{E(l)} n^{c(l)}. \quad (1.27)$$

$L(\mathcal{G})$  is the set of possible configurations of self-avoiding loops on  $\mathcal{G}$ ,  $E(l)$  the number of edges of  $\mathcal{G}$  occupied by the loops and  $c(l)$  the number of loops. Now the model can be formally extended to values of  $n$  not integer.

The random graph counterpart of (1.27) is easy to figure out, we just have to replace the honeycomb lattice with its spatial fluctuations into cubic graphs of arbitrary genera [25]:

$$Z_N^{\mathcal{O}(n)}(g, \beta) = \sum_{\mathcal{G}} \frac{1}{|\text{Aut}(\mathcal{G})|} g^{A(\mathcal{G})} N^{2-2h(\mathcal{G})} \sum_{l \in L(\mathcal{G})} \beta^{E(l)} n^{c(l)} \quad (1.28)$$

where the first sum is over connected cubic graphs. We now want to write a multi-matrix integral to reproduce this partition function. We introduce a matrix  $B$  that describes the fluctuations of the graphs and  $n$  matrices  $A_c$ ,  $c = 1, \dots, n$  that generates self-avoiding loops with  $n$  colors. This is done by considering two types of vertices  $\frac{g}{3} B^3$  and  $g B A_c^2$ . The first type describes unoccupied vertices, while the second vertices with two half-edges colored with colour  $c$  and a third not occupied. To reproduce self-avoiding loops on cubic lattices we consider propagators that connect only matrices with the same color and unoccupied half-edges only to unoccupied ones

$$\begin{aligned} \langle (A_c)_{ij} (A_d)_{kl} \rangle &= \frac{\beta}{N} \delta_{il} \delta_{jk} \delta_{cd} \\ \langle B_{ij} B_{kl} \rangle &= \frac{1}{N} \delta_{il} \delta_{jk} \\ \langle (A_c)_{ij} B_{kl} \rangle &= 0 \end{aligned}$$

where we give an additional factor  $\beta$  for  $A_c$  propagators. These equations define the quadratic form  $Q_{ab}$ ,  $a, b = 1, \dots, n$ . As before, the sum over all possible colorings will give the topological factor  $n^{c(l)}$ . For a typical configuration see figure 1.4.

The matrix integral that gives (1.28) from its Feynman expansion is:

$$\begin{aligned} Z_N^{\mathcal{O}(n)}(g, \beta) &= \log \frac{\int \mathcal{D}A_1 \dots \mathcal{D}A_n \mathcal{D}B e^{-N \text{Tr} V(A_1, \dots, A_n, B)}}{\int \mathcal{D}A_1 \dots \mathcal{D}A_n \mathcal{D}B e^{-N \text{Tr} V_0(A_1, \dots, A_n, B)}} \quad (1.29) \\ V(A_1, \dots, A_n, B) &= \frac{1}{2} B^2 + \frac{1}{2\beta} \sum_{c=1}^n A_c^2 - \frac{g}{3} B^3 - g B \sum_{c=1}^n A_c^2 \\ V_0(A_1, \dots, A_n, B) &= \frac{1}{2} B^2 + \frac{1}{2\beta} \sum_{c=1}^n A_c^2. \end{aligned}$$

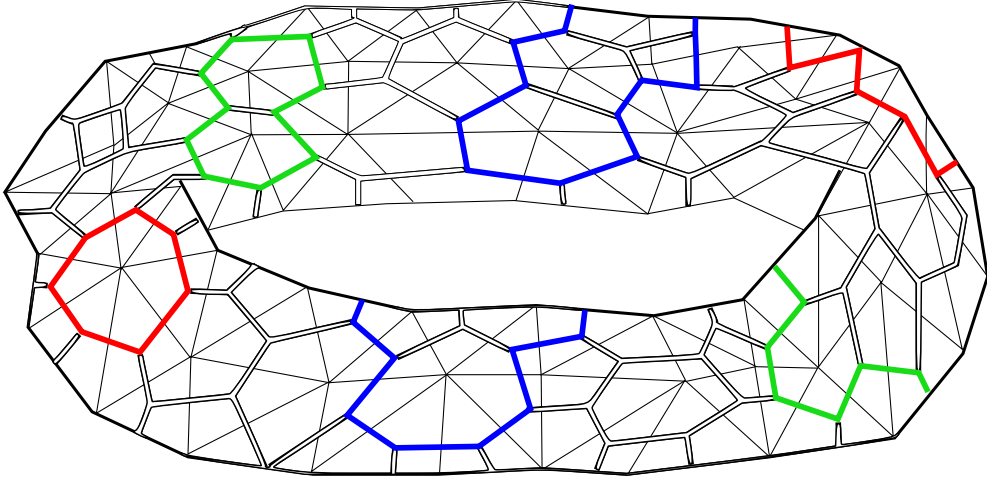


Figure 1.4: A configuration of self-avoiding loops on a random triangulated surface of genus 1 in the  $\mathcal{O}(n)$  loop-gas model on random lattices.

### 1.3.2 Potts model on random lattices

Another important model that can be easily defined on random graphs using the method of this section, is the Potts model. Given a graph  $\mathcal{G}$ , consider the spin variables  $\sigma$ , maps from the set of vertices  $V(\mathcal{G})$  to  $\mathbb{Z}_q$ . We associate to an edge  $e = (v, v')$  a factor  $1 + v_e \delta_{\sigma(v), \sigma(v')}$ , where we choose  $v_e = e^K - 1$ , corresponding to an energy of 0 if the spins in the two endpoints of  $e$  are unequal and  $K$  if they are equal. The  $q$ -state Potts model partition function on a graph  $\mathcal{G}$  is

$$Z_{\mathcal{G}}^{\text{Potts}}(q, K) = \sum_{\sigma: V(\mathcal{G}) \rightarrow \mathbb{Z}_q} \prod_{e \in E(\mathcal{G})} \left(1 + v_e \delta_{\sigma(v), \sigma(v')}\right). \quad (1.30)$$

When we let the lattice fluctuate into arbitrary cubic graphs, the partition function of the model becomes [26]:

$$Z_N^{\text{Potts}}(g, K, q) = \sum_{\mathcal{G}} \frac{1}{|\text{Aut}(\mathcal{G})|} g^{A(\mathcal{G})} N^{2-2h(\mathcal{G})} Z_{\mathcal{G}}^{\text{Potts}}(q, K). \quad (1.31)$$

We want to construct a matrix model that generates all connected cubic graphs with  $q$  different types of vertices, according to the values of the spin at each vertex. For this purpose we introduce  $q$  Hermitian matrices  $M_1, \dots, M_q$ . A vertex of type  $a$ ,  $a = 1, \dots, q$  will be produced by a term  $g/3 \text{Tr} M_a^3$ . Then we consider a Gaussian potential  $\sum_{a,b=1}^q M_a Q_{ab} M_b$  such that the propagator between vertices of the same type is  $e^K$ , and between vertices of different type is 1. This is achieved by using an inverse quadratic form  $(Q^{-1})_{ab} = 1 + (e^K - 1)\delta_{ab}$ ,  $a, b = 1, \dots, q$ , that is easily inverted to give

$$Q_{ab} = \frac{1}{e^K - 1} \left( \delta_{ab} - \frac{1}{e^K - 1 + q} \right). \quad (1.32)$$

Then the partition function will be:

$$Z_N^{\text{Potts}}(g, K, q) = \log \frac{\int \mathcal{D}M_1 \dots \mathcal{D}M_q e^{-N\text{Tr}V(M_1, \dots, M_q)}}{\int \mathcal{D}M_1 \dots \mathcal{D}M_q e^{-N\text{Tr}V_0(M_1, \dots, M_q)}} \quad (1.33)$$

$$V(M_1, \dots, M_q) = \frac{1}{2} \sum_{a,b=1}^q Q_{ab} M_a M_b - \frac{g}{3} \sum_{a=1}^q M_a^3 \quad (1.34)$$

$$V_0(M_1, \dots, M_q) = \frac{1}{2} \sum_{a,b=1}^q Q_{ab} M_a M_b$$

with  $Q_{ab}$  as in (1.32). This matrix integral will reproduce through the Wick's theorem the sum over lattices with a  $q$ -color spin on their vertices (figure 1.5), and each graph will receive an overall contribution  $N^{V-E+F} = N^{2-2h}$  as before, regardless of the value of the spin. When  $q = 2$  the model is the Ising model equivalent to the  $\mathcal{O}(n = 1)$  model above (by high-temperature expansion).

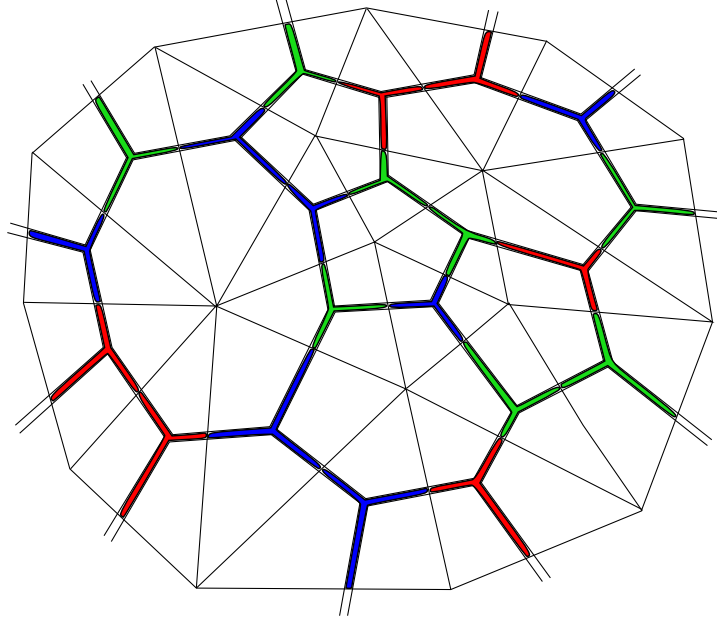


Figure 1.5: A configuration of the Potts model on random graphs. Edges colored in one color weight  $e^k$ , while edges that links vertices with different colors weight 1.

As a last remark we want to derive the matrix integral for the Fortuin-Kasteleyn representation of the Potts model. Given a graph  $\mathcal{G} = (V, E)$ , expand the product over  $e$  in (1.30) and let  $A \subseteq E$  be the set of edges for which  $v_e \delta_{\sigma(v), \sigma(v')}$  is not zero. Then the color in each component of  $(V, A)$  is constant and if we sum over  $\sigma : V(\mathcal{G}) \rightarrow \mathbb{Z}_q$ , we get the Fortuin-Kasteleyn expression of the partition function of the Potts model

$$Z_{\mathcal{G}}^{\text{FK}}(q, K) = \sum_{A \subseteq E} q^{k(A)} \prod_{e \in A} v_e \quad (1.35)$$

where  $k(A)$  is the number of connected components in the subgraph  $(V, A)$ . Equation (1.35) is related to the Tutte polynomial of the graph, as explained in section B.1.

The version of this model on random lattices is obtained as before by summing over cubic connected graphs  $\mathcal{G}$  the partition function (1.35):

$$Z_N^{\text{FK}}(g, q, K) = \sum_{\mathcal{G}} \frac{1}{|\text{Aut}(\mathcal{G})|} g^{A(\mathcal{G})} N^{2-2b(\mathcal{G})} Z_{\mathcal{G}}^{\text{FK}}(q, K). \quad (1.36)$$

For integer values of  $q$ , the configurations of the Potts model in the Fortuin-Kasteleyn representation can be produced by introducing the  $q + 1$  Hermitian matrices  $M_a$ ,  $a = 1, \dots, q$  and  $B$ . A potential that reproduces the sum over subgraphs in (1.35) with a correct factor of  $q$  for every component and  $e^K - 1$  for propagators of edges pertaining to the subgraph is:

$$V_{\text{FK}}(M_1, \dots, M_q, B) = \frac{1}{2} B^2 + \frac{1}{2} \frac{1}{e^K - 1} \sum_{a=1}^q M_a^2 + \frac{g}{3} \sum_{a=1}^q (M_a + B)^3. \quad (1.37)$$

Note that the interaction is such that also the components made of a single vertex, produced by the term  $g/3 \sum_{a=1}^q B^3$ , receive a factor  $q$ .

Then the partition function (1.36) can be specified by the matrix integral

$$Z_N^{\text{FK}}(g, q, K) = \log \frac{\int \mathcal{D}M_1 \dots \mathcal{D}M_q \mathcal{D}B e^{-N \text{Tr} V_{\text{FK}}(M_1, \dots, M_q, B)}}{\int \mathcal{D}M_1 \dots \mathcal{D}M_q \mathcal{D}B e^{-N \text{Tr} \left( \frac{1}{2} B^2 + \frac{1}{2} \frac{1}{e^K - 1} \sum_{a=1}^q M_a^2 \right)}}. \quad (1.38)$$

We can easily show that correctly (1.38) reduces to (1.33). Indeed if we perform the change of variable  $M_a \rightarrow M_a - B$  with Jacobian 1 the interaction for the fields  $B$  in (1.37) becomes trivial and we are left with a Gaussian integral for  $B$

$$V_{\text{FK}} \rightarrow \frac{1}{2} \left( 1 + \frac{q}{e^K - 1} \right) \left( \left( B - \frac{1}{e^K + 1 + q} \sum_{a=1}^q M_a \right)^2 - \left( \frac{1}{e^K + 1 + q} \sum_{a=1}^q M_a \right)^2 \right) + \frac{1}{2} \frac{1}{e^K - 1} \sum_{a=1}^q M_a^2 + \frac{g}{3} \sum_{a=1}^q M_a^3. \quad (1.39)$$

Performing the integral over  $B$  we have a matrix integral that corresponds exactly to (1.33).

## Chapter 2

# Solution of the $\mathcal{O}(n)$ loop-gas model for $n = 0, -2$

In chapter 1 we have established the combinatorial connection between matrix integrals and the sum over graphs and we showed how the integral (1.29) represents the  $\mathcal{O}(n)$  loop-gas model on cubic random lattices.

This model has received a lot of interest during the years [25, 27, 28, 18, 29, 30, 12] thanks to its appealing geometrical interpretation and for its rich critical structure. We are interested in the model with  $n = -2$  and a quartic potential, since this is connected with spanning forests on fluctuating lattices as we will show later. Before addressing our attention to it, we present the solution of the  $\mathcal{O}(0)$  loop-gas model for pedagogical purposes.

We start by considering a partition function more general than (1.29):

$$Z_N^{\mathcal{O}(n)}(\{g_i\}, b_0) = \log \frac{\int \mathcal{D}A_1 \dots \mathcal{D}A_n \mathcal{D}B e^{-N\text{Tr}W(A_1, \dots, A_n, B)}}{\int \mathcal{D}A_1 \dots \mathcal{D}A_n \mathcal{D}B e^{-N\text{Tr}W_0(A_1, \dots, A_n, B)}} \quad (2.1)$$
$$W(A_1, \dots, A_n, B) = V(B) + \frac{1}{2} \sum_{c=1}^n A_c^2 - \frac{1}{4b_0} B \sum_{c=1}^n A_c^2$$
$$W_0(A_1, \dots, A_n, B) = \frac{1}{2} B^2 + \frac{1}{2} \sum_{c=1}^n A_c^2.$$

Here we admit higher powers of  $B$  in the action to allow for arbitrary unoccupied vertices and we have defined the coupling that counts the number of occupied vertices  $1/4b_0$ . Note that if we consider  $V(B) = \frac{1}{2}B^2$  in (2.1), this corresponds to loops densely packed onto cubic graphs. Instead a quartic potential with weights  $g_1$  for cubic vertices and  $g_2$  for quartic vertices, makes the problem equivalent to the counting of self-avoiding loops and dimers configurations on a cubic lattice. This is because a quartic vertex can be viewed as obtained by shrinking a dimer on a cubic graph to a single vertex. If we give a weight  $\zeta$  to dimers, then the term in the potential of a matrix integral that produces dimers on cubic lattices is of the form  $1/2D^2 - \sqrt{\zeta}g_1DB^2$ . Performing Gaussian integration we are left with a quartic term  $g_1^2\zeta/2B^4$ .



To deal with the computation of this matrix integral, we first perform a change of variables that takes the matrix  $B$  to its diagonal form and is unitary on the matrices  $A_c$

$$B \longrightarrow UDU^{-1}, \quad A_c \longrightarrow UA_cU^{-1} \quad (2.2)$$

where  $U$  is a unitary matrix and  $D = \text{diag}(b_1, \dots, b_N)$ .  $\text{Tr}W$  in (2.1) becomes:

$$\text{Tr}W \longrightarrow \sum_{i=1}^N V(b_i) + \frac{1}{2} \sum_{c=1}^n \sum_{ijkl=1}^N (A_c)_{ij} \delta_{il} \delta_{kj} \left( 1 - \frac{1}{4b_0} (b_i + b_j) \right) (A_c)_{kl}. \quad (2.3)$$

From the invariance of the measure of the matrices  $A_c$  under a unitary transformation, the Jacobian of the transformation depends only on  $B$  and in particular on its eigenvalues. To see this, we compute the square of the line element and read the Jacobian as the square root of the metric tensor. Call  $\Omega_{ij}$  the skew symmetric matrix  $(U^{-1} dU)_{ij}$ , we have:

$$\text{Tr}(dB)^2 = \text{Tr} \left( U(dD + [\Omega, D])U^{-1} \right)^2. \quad (2.4)$$

The matrix  $L = dD + [\Omega, D]$  has diagonal entries  $L_{ii} = db_i$  and off diagonal entries  $L_{ij} = (b_i - b_j)(b_j - b_i)\Omega_{ij}\Omega_{ji}$ . Therefore we have

$$\text{Tr}(dB)^2 = \text{Tr}L^2 = \sum_{i,j=1}^N L_{ij}L_{ji} = \sum_k (db_k)^2 + \sum_{i \neq j} (b_i - b_j)^2 |d\Omega_{ij}|. \quad (2.5)$$

The determinant of the metric tensor is then  $g = \prod_{i \neq j} (b_i - b_j)^2$  and we get that the Jacobian is  $\prod_{i < j} (b_i - b_j)^2 = \Delta^2(\{b_i\})$ , which is the square of the Vandermonde determinant  $\Delta(\{b_i\}) = \det(b_i^{j-1})$ ,  $i, j = 1, \dots, N$ . Further, the ‘‘angular’’ integral over the  $U$  matrices factorizes in (2.1) and can be simplified.

We finally note that the integral over the  $A_c$  matrices is Gaussian<sup>1</sup> and can be immediately performed. Then (2.1) takes the form

$$Z_N^{\mathcal{O}(n)}(\{g_i\}, b_0) = \log \frac{\int \prod_{i=1}^N db_i \Delta^2(\{b_i\}) \prod_{ij} \left( 1 - \frac{1}{4b_0} (b_i + b_j) \right)^{-n/2} e^{-N \sum_i V(b_i)}}{\int \prod_{i=1}^N db_i \Delta^2(\{b_i\}) e^{-N/2 \sum_i b_i^2}}. \quad (2.6)$$

We are left with a matrix integral over only the eigenvalues of a single Hermitian matrix.

## 2.1 Saddle point equation

We now compute (2.6) in the ‘‘planar’’ (large  $N$ ) limit, applying the saddle point technique introduced by Brezin *et al.* in [2]. To do this we first write the partition function

<sup>1</sup> To make positive definite the Gaussian integration, from (2.3) we get that the eigenvalues  $b_i$  have to satisfy  $1 - \frac{1}{4b_0} (b_i + b_j) > 0$ .

in the form

$$\begin{aligned}
Z_N^{\mathcal{O}(n)}(\{g_i\}, b_0) &= \log \frac{\int \prod_{i=1}^N db_i e^{-N^2 S}}{\int \prod_{i=1}^N db_i e^{-N^2 S_0}} \quad (2.7) \\
S &= \frac{1}{N} \sum_i V(b_i) - \frac{1}{N^2} \sum_{i \neq j} \log |b_i - b_j| + \frac{n}{2N^2} \sum_{ij} \log |4b_0 - b_i - b_j| \\
S_0 &= \frac{1}{2N} \sum_i b_i^2 - \frac{1}{N^2} \sum_{i \neq j} \log |b_i - b_j|.
\end{aligned}$$

Then the saddle point method states that as  $N \rightarrow \infty$  the integral can be approximated by evaluating the integrand in the stationary point of the action. The method is applicable since the explicit powers of  $N$  present in (2.7) appears together with a sum over  $N$  terms. Note that if we had applied this method before going to eigenvalues, the stationary matrix  $B_0$ ,  $V'(B_0) = 0$ , would not be the dominant term. Indeed all the  $N^2 - N$  points related to  $B_0$  by the unitary transformation  $B = UB_0U^{-1}$  are stationary and they contribute as  $e^{N^2}$ , so not being sub-dominant.

In the form of equation (2.7) the problem is analogous to a unidimensional gas of eigenvalues. The equilibrium point is shifted from the minimum of the bulk potential  $V$  by the Vandermonde determinant which acts as a two-body Coulomb repulsion and by the additional two-body potential proportional to  $n$  that, depending on the sign of  $n$ , attracts or repels the particles to their mirror coordinates with respect to the origin. The saddle point equation is

$$\frac{\partial S}{\partial b_i} = 0 = \frac{1}{N} V'(b_i) - \frac{2}{N^2} \sum_{j \neq i} \frac{1}{b_i - b_j} - \frac{n}{N^2} \sum_j \frac{1}{4b_0 - b_i - b_j}. \quad (2.8)$$

To solve equation (2.8) for large  $N$ , we introduce the spectral density of eigenvalues

$$\rho(y) = \frac{1}{N} \sum_i \delta(y - b_i) \quad (2.9)$$

which is positive,  $\rho(y) \geq 0$ , and normalized

$$\int \rho(y) dy = 1. \quad (2.10)$$

In the limit  $N \rightarrow \infty$  the distribution of eigenvalues becomes continuous and the saddle point equation (2.8) can now be rewritten as an integral equation for the density:

$$\int dy \rho(y) \left( P \frac{1}{x - y} + \frac{n}{2} \frac{1}{4b_0 - x - y} \right) = \frac{1}{2} V'(x) \quad (2.11)$$

where  $P$  denotes the Cauchy principal value.

## 2.2 The $\mathcal{O}(0)$ loop-gas model, i.e. the one-matrix model

Setting  $n = 0$  in (2.6) leaves us with a one-matrix model

$$Z_N^{1M}(\{g_i\}) = \log \frac{\int \prod_{i=1}^N db_i \Delta^2(\{b_i\}) e^{-N \sum_i V(b_i)}}{\int \prod_{i=1}^N db_i \Delta^2(\{b_i\}) e^{-N/2 \sum_i b_i^2}} \quad (2.12)$$

and the saddle point equation is

$$P \int dy \rho(y) \frac{1}{x-y} = \frac{1}{2} V'(x). \quad (2.13)$$

Following [13], to solve this model it is convenient to introduce the discrete resolvent

$$\omega_N(x) = \frac{1}{N} \sum_{i=1}^N \frac{1}{x-b_i}, \quad (2.14)$$

where  $b_i$  are the values that makes the action stationary when  $n = 0$ . If we rewrite equation (2.8) with  $n = 0$  as:

$$\frac{1}{N} \sum_i \frac{V'(b_i) - V'(x) + V'(x)}{x-b_i} = \frac{1}{N^2} \sum_{i \neq j} \frac{1}{b_i - b_j} \left( \frac{1}{x-b_i} - \frac{1}{x-b_j} \right) \quad (2.15)$$

under the assumption that  $\omega_N$  tends in the limit  $N \rightarrow \infty$  to a differentiable function, the resolvent  $\omega(x)$ , (2.15) becomes a quadratic equation for  $\omega$ :

$$\omega(x)^2 - \omega(x)V'(x) + P(x) = 0 \quad (2.16)$$

whose solution is

$$\omega(z) = \frac{1}{2} \left( V'(z) - \sqrt{V'(z)^2 - 4P(z)} \right). \quad (2.17)$$

$P(x)$  is an unknown polynomial of degree  $k-2$ , given that  $V$  has degree  $k$ .

$\omega(x)$  is the Hilbert transform of the spectral density

$$\omega(x) = \int dy \frac{\rho(y)}{x-y} = \sum_{k=0}^{\infty} \frac{1}{x^{k+1}} \int dy \rho(y) y^k \quad (2.18)$$

and can be defined analytic in the whole complex plane except a cut located on the support of  $\rho$ . Equation (2.18) can be inverted into a discontinuity equation for  $\omega$  by means of the Sokhotsky-Weierstrass formula  $P \frac{1}{x \pm i\pi\delta(x)} = 1/(x \mp i0)$  :

$$\rho(x) = \frac{1}{2\pi i} (\omega(x-i0) - \omega(x+i0)), \quad x \in \text{supp}(\rho). \quad (2.19)$$

Equation (2.18) determines the resolvent in terms of the moments of  $\rho$  and this can be used to fix the coefficients of  $P(x)$  and determine  $\omega(x)$  from (2.17).

In particular the resolvent must behave as  $\omega(x) \sim 1/x$  for large  $x$ . In the simplest case the support of  $\rho$  is a connected subset of the real axis  $[a, b]$  (one-cut assumption), so  $\omega(x)$  has two branch points and  $V'(x)^2 - 4P(x)$  has  $k - 2$  double roots. This is all we need to determine  $P(x)$  and then  $\omega(x)$ . Knowing  $\omega$  or  $\rho$ , entirely solves the problem in the planar limit. The averages of  $\text{Tr} B^n$  will be given by the moments of  $\rho$

$$\frac{1}{N} \langle \text{Tr} B^n \rangle \sim \int dy \rho(y) y^n \quad (2.20)$$

and the partition function in the large  $N$  limit  $Z^{1M} \sim Z_N^{1M}/N^2$  will be:

$$\begin{aligned} Z^{1M} \sim -S + S_0 = & - \int dy \rho(y) V(y) + \int dy dx \rho(y) \rho(x) \log |y - x| + \\ & + \int dy \rho^0(y) V(y) - \int dy dx \rho^0(y) \rho^0(x) \log |y - x| \end{aligned} \quad (2.21)$$

where  $\rho^0$  is the density in the Gaussian case.

### 2.2.1 Wigner semicircle law and quartic potential

Here we apply the method developed above to the case of a Gaussian potential. This case is trivial:

$$\omega^0(x) = \frac{1}{2} \left( x - \sqrt{x^2 - 4} \right) \quad (2.22)$$

and we note that  $\omega^0$  has the appropriate large  $x$  behaviour. From (2.19) we obtain the celebrated *Wigner semicircle law* that describes the density of eigenvalues in the Gaussian unitary ensemble

$$\rho^0(x) = \frac{1}{2\pi} \sqrt{4 - x^2}. \quad (2.23)$$

Note that as  $x$  approaches the ends of the cut, the density has a square root edge. Further,  $1/N \langle \text{Tr} B^n \rangle$  corresponds to the  $n$ -th moment of the eigenvalue density and coincides with our previous result (1.14). Accordingly  $x^{-1} \omega^0(x^{-1})$  is the generating function of Catalan numbers (of argument  $x^2$ ).

Consider the quartic case  $V(x) = \frac{1}{2}x^2 - \frac{g}{4}x^4$ . Under the one-cut assumption, the support of  $\rho$  will be  $[-a, a]$  and:

$$\omega(x) = \frac{1}{2} \left( x - gx^3 - (c_1 + c_2x^2) \sqrt{x^2 - a^2} \right). \quad (2.24)$$

Imposing  $\omega(x) \sim 1/x$  fixes the unknowns  $c_1, c_2$  and the support of  $\rho$ . We end with:

$$\omega(x) = \frac{1}{2} \left( x - gx^3 - \left( 1 - \frac{ga^2}{2} - gx^2 \right) \sqrt{x^2 - a^2} \right) \quad (2.25)$$

$$\rho(x) = \frac{1}{2\pi} \left( 1 - \frac{ga^2}{2} - gx^2 \right) \sqrt{a^2 - x^2} \quad (2.26)$$

$$a^2 = 2 \frac{1 - \sqrt{1 - 12g}}{3g}. \quad (2.27)$$

The partition function can be calculated from (2.21) and the result is:

$$\begin{aligned} Z(g) &= \frac{1}{2} \log \frac{a^2}{4} + \frac{1}{384} (a^2 - 4)(a^2 - 36) \\ &= \sum_{n=1}^{+\infty} \frac{(2n-1)! 12^n (g/4)^n}{(n+2)! n!}. \end{aligned} \quad (2.28)$$

Equation (2.28) is an expansion over 4-valent graphs weighted by the inverse of the order of their automorphism, as shown in figure 2.1. In the language of quantum field theory (2.28) counts the vacuum planar bubbles in the theory  $\phi^4$  with coupling  $g/4$ .

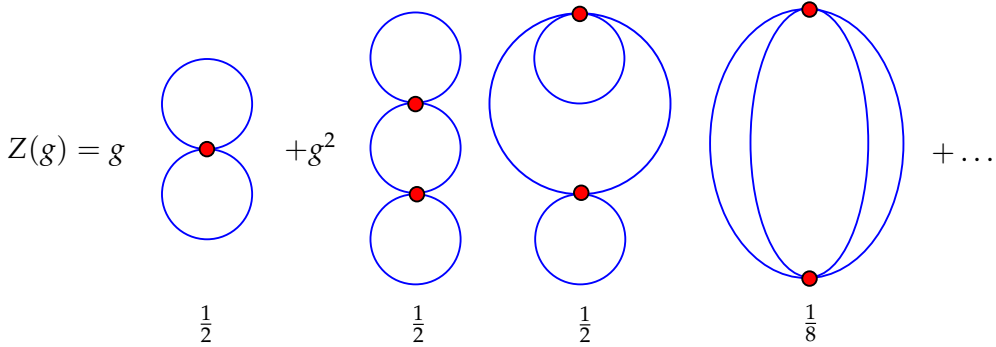


Figure 2.1: The terms in the expansion (2.28) up to  $n = 2$ . Under every graph there is its weight.

The partition function has an analytic continuation from  $g < 0$  to  $g > 0$  and the critical point is located at  $g_c = 1/12$ , where there is a square root branch point and the regime  $0 < g < g_c$  makes sense only in the large  $N$  limit. The analyticity near the origin means that the original path integral (2.12) has been drastically cut up when  $N \rightarrow \infty$ . When  $g \rightarrow g_c$ ,  $\rho(x) \sim (x - a)^{3/2}$  and the density has no more a square root edge. This is due to the fact that, in this class of models, at criticality a zero of the singular part of  $\omega(x)$  coalesces with an end point of the cut.

### 2.2.2 The continuum limit

The critical behaviour of the partition function in the large  $N$  limit  $Z(g) = \sum_n Z_n g^n$  is related to the asymptotic of the coefficients of its power series,  $Z_n$ , giving an estimate for the number of planar fat-graphs. Indeed, call  $1 - g/g_c = t$  and suppose that the behaviour of the partition function is described by the critical exponent  $\gamma$  called the string susceptibility exponent:

$$Z(g) \sim t^{2-\gamma}, \quad \text{for } g \nearrow g_c. \quad (2.29)$$

This dependence gives the asymptotic

$$Z_n \sim g_c^{-n} n^{-3+\gamma} \quad (2.30)$$

since if we sum  $Z_n$  over  $n$ , and approximate the summand with this large- $n$  behaviour, we obtain (2.29).

For the quartic model solved above, the expansion of (2.28) near  $g_c$  yields  $\gamma = -1/2$ , that is the critical exponent of *pure gravity*.

If instead we consider more general potentials  $V(x)$  of a one matrix model, fine tunings of the coupling constants can change the value of  $\gamma$ . The crucial fact in obtaining  $\gamma = -1/2$  for the quartic model was that at  $g = g_c$ , a zero of the singular part of the resolvent coincided with an end of the cut. If we now adjust the parameters of  $V(x)$  in order that the singular part of the resolvent behaves as  $w(x) \sim (x - a)^{m-1/2}$ , it can be shown that we have  $\gamma = -1/m$  (see for example [5]). This new critical point is called *m-th multicritical point*.

## 2.3 The $\mathcal{O}(-2)$ loop-gas model

For solving the  $\mathcal{O}(-2)$  loop-gas model, we will mainly follow the approach of Kostov and Staudacher [18], considering the specific case of a fourth-degree potential:

$$V(x) = \sum_{k=2}^4 \frac{g_{k-2}}{k} x^k, \quad g_0 = 1. \quad (2.31)$$

We will present an explicit solution of the integral equation and an analysis of the singularities.

### 2.3.1 Eigenvalue density

Set  $n = -2$  in (2.11). If we call  $[a, b]$  the support of  $\rho$ , the saddle point equation is

$$\int_a^b dy \rho(y) \left( P \frac{1}{x-y} - \frac{1}{4b_0 - x - y} \right) = \frac{1}{2} \sum_{k=1}^3 g_{k-1} x^k \quad (2.32)$$

From now on, the principal value is understood. It is convenient to perform the change of variables  $\lambda' = \frac{1}{2}(2b_0 - x)$ ,  $\mu' = \frac{1}{2}(2b_0 - y)$

$$\int_{a'}^{b'} d\mu' \rho(\mu') \left( \frac{1}{\lambda' - \mu'} + \frac{1}{\mu' + \lambda'} \right) = \frac{1}{2} \sum_{k=1}^3 g_{k-1} (-2)^k (\lambda' - b_0)^k \quad (2.33)$$

and redefine  $2\rho(y) \rightarrow \rho(\mu')$  and  $(-2)^k g_k \rightarrow g_k$  to obtain

$$\int_{a'}^{b'} d\mu' \rho(\mu') \frac{\lambda'}{\mu'^2 - \lambda'^2} = \sum_{k=1}^3 g_{k-1} (\lambda' - b_0)^k. \quad (2.34)$$

If we then perform another change of variables  $\lambda' = \sqrt{A + B\lambda}$ ,  $\mu' = \sqrt{A + B\mu}$  where  $A = (a'^2 + b'^2)/2$  and  $B = (a'^2 - b'^2)/2$ , we obtain the simplified form

$$\int_{-1}^1 \frac{d\mu \rho(\mu)}{\sqrt{A + B\mu}} \frac{1}{\lambda - \mu} = 2 \sum_{k=1}^3 \frac{g_{k-1}}{\sqrt{A + B\lambda}} \left( \sqrt{A + B\lambda} - b_0 \right)^k. \quad (2.35)$$

Using results from the theory of singular integral equations [31], equation (2.35) can be inverted and we have the explicit expression of the eigenvalues density of the  $\mathcal{O}(-2)$  loop-gas model

$$\rho(\lambda) = -\frac{2}{\pi} \sqrt{A+B\lambda} \sqrt{1-\lambda^2} \int_{-1}^1 d\mu \frac{1}{\lambda-\mu} \frac{1}{\sqrt{1-\mu^2}} \sum_{k=1}^3 \frac{g_{k-1}}{\sqrt{A+B\mu}} \left( \sqrt{A+B\mu} - b_0 \right)^k. \quad (2.36)$$

The normalization conditions is

$$\frac{B}{2} \int_{-1}^1 d\mu \frac{\rho(\mu)}{\sqrt{A+B\mu}} = 1 \quad (2.37)$$

and positivity is assured by:

$$\int_{-1}^1 d\mu \frac{1}{\sqrt{1-\mu^2}} \sum_{k=1}^3 \frac{g_{k-1}}{\sqrt{A+B\mu}} \left( \sqrt{A+B\mu} - b_0 \right)^k = 0. \quad (2.38)$$

(2.37) and (2.38) gives  $a'$  and  $b'$ , the extrema of the support of  $\rho$ , in terms of the couplings and fully determine the solutions of the model.

### 2.3.2 Singularity structure

We now study the singularity structure by first showing some general results regarding the critical exponents of the  $\mathcal{O}(n)$  loop-gas model. The structure now is richer than the one studied for the the one-matrix model in section 2.2. If we go back to (2.11) we see that in addition to the criticality coming from the divergence of the volume of the graph, a non-zero  $n$  poses the new singularity condition  $b' = 0$ . In this case the term proportional to  $n$  in the saddle point equation diverges and this affects the distribution of the eigenvalues near 0 (cf. to equation (2.33)). This kind of singularity sets the critical value of the coupling  $b_0$  to  $b_0^* = b/2$ , and corresponds to diverging length of the loops on the random graphs. Supposing that  $\rho(\lambda') \sim \lambda'^\theta$  as  $\lambda' \rightarrow 0$  and with the parametrization  $n = 2 \cos(\pi\nu)$ ,  $0 \leq \nu \leq 1$ , one can show [30] that the string susceptibility exponent is

$$\gamma = \frac{-2\nu}{\theta + 1 - \nu}. \quad (2.39)$$

Note that when  $n = 0$ , that is  $\nu = 1/2$ , we recover the  $m$ -th multicritical point of a one-matrix model for  $\theta = m - 1/2$  with  $\gamma = -1/m$ . If we then restrict to the case of interest  $\nu = 1$ , we have  $\gamma = -2/\theta$ .

Before setting  $b' = 0$  in (2.36), we rewrite  $\rho$  in a form more convenient to identify

the critical points:

$$\begin{aligned} \rho(\lambda) = & \frac{2}{\pi} \sqrt{1-\lambda^2} r_1 \sqrt{A+B\lambda} - \frac{2}{\pi^2} \sqrt{1-\lambda^2} t_0 \sqrt{A+B\lambda} \cdot \\ & \cdot \int_{-1}^1 d\mu \frac{1}{\lambda-\mu} \frac{1}{\sqrt{1-\mu^2}} \frac{1}{\sqrt{A+B\mu}} + \\ & - \frac{2}{\pi^2} \sqrt{1-\lambda^2} t_2 \sqrt{A+B\lambda} \int_{-1}^1 d\mu \frac{1}{\lambda-\mu} \frac{\sqrt{A+B\mu}}{\sqrt{1-\mu^2}} \end{aligned} \quad (2.40)$$

where  $r_1$ ,  $t_0$  and  $t_2$  are functions of the couplings:

$$\begin{cases} r_1 = Bg_2 \\ t_0 = -b_0 + b_0^2 g_1 - b_0^3 g_2 \\ t_2 = g_1 - 3b_0 g_2 \end{cases} \quad (2.41)$$

The remaining integrals in (2.40) can be expressed as complete elliptic integrals of the third kind, but if we set  $b' = 0$  those integrals become simple, since  $A = B = a'^2/2$ . We note that the integral multiplying  $t_0$  tends to infinity as  $b' \rightarrow 0$  and this gives the condition  $t_0 = 0$ .

At criticality the density of eigenvalues  $\rho_c(\lambda') = \rho(\lambda')|_{b'=0}$  becomes:

$$\rho_c(\lambda') = \frac{4}{\pi a'^2} \sqrt{a'^2 - \lambda'^2} r_1 \lambda'^2 - \frac{4}{\pi^2} t_2 \lambda'^2 \log \frac{\lambda'}{a' + \sqrt{a'^2 - \lambda'^2}}. \quad (2.42)$$

We note that if the potential were even, we would not have a logarithmic piece in the density. To understand this, consider the partition function of the  $\mathcal{O}(-2)$  loop-gas model (2.6) with  $n = -2$  and perform the change of variables  $b_i \rightarrow 2b_0 - \lambda_i$  to have

$$\begin{aligned} Z_N^{\mathcal{O}(-2)}(\{g_i\}, b_0) &= \frac{1}{N^2} \log \frac{\int \prod_{i=1}^N d\lambda_i \prod_{i<j} (\lambda_i - \lambda_j)^2 \prod_{i,j} (\lambda_i + \lambda_j) e^{-N \sum_i V(2b_0 - \lambda_i)}}{\int \prod_{i=1}^N d\lambda_i \Delta^2(\{\lambda_i\}) e^{-N/2 \sum_i \lambda_i^2}} \\ &= \frac{1}{N^2} \log \frac{\int \prod_{i=1}^N d\lambda_i 2\lambda_i \prod_{i<j} (\lambda_i^2 - \lambda_j^2)^2 e^{-N \sum_i V(2b_0 - \lambda_i)}}{\int \prod_{i=1}^N d\lambda_i \Delta^2(\{\lambda_i\}) e^{-N/2 \sum_i \lambda_i^2}}. \end{aligned}$$

If we now change again variables to  $x_i = \lambda_i^2$ , we obtain a one-matrix model with a potential not polynomial, function of the square root of the matrix (note that  $dx_i = d\lambda_i 2\lambda_i$ ). Then, with an even potential the problem is exactly a one-matrix model in the variables  $x_i$ . The critical exponent  $m - 1/2$  of the eigenvalue density  $\tilde{\rho}(x)$  derived from this matrix model, translates into an exponent  $2m$  for the original problem, since  $\rho(\lambda) = 2\lambda \tilde{\rho}(\lambda^2)$ . Because our potential is not even, we have in addition a singular behaviour of the kind  $\lambda'^{2m} \log \lambda'$ .

From (2.42) we also find the critical exponent of the density of eigenvalues  $\theta = 2$ . This corresponds to  $\gamma = -1$ .

We now want to find the critical points. There are two kinds of critical points that correspond to a behaviour  $\rho(\lambda') \sim \lambda'^2$ .



1. The potential is cubic<sup>2</sup> and the critical points are obtained by setting  $g_2 = 0$  in addition to  $t_0 = 0$ .
2. The potential is quartic and the couplings are tuned to reach  $t_2 = 0, t_0 = 0$ .

Imposing the first conditions sets  $g_1 = 1/b_0$  and the density contains a logarithmic term. The positivity and normalization conditions are respectively  $2a' = b_0\pi$  and  $a'^3 = 3b_0\pi$ . Remembering that at the beginning of this section we redefined the couplings, we find at criticality for the cubic potential:

$$b_0^* = \frac{2\sqrt{6}}{\pi} \quad g_1 = -\frac{\pi}{4\sqrt{6}} \quad g_2 = 0. \quad (2.43)$$

In the second case imposing  $t_2 = t_0 = 0$  gives  $g_2 = 1/2b_0$  and  $g_1 = 3/2b_0$ . The density does not have a logarithmic piece along a line in coupling space where the previous conditions are satisfied and is  $\rho(\lambda') = 1/(\pi b_0^2)\lambda' \sqrt{(a'^2 - \lambda'^2)(\lambda'^2 - b'^2)}$ . Positivity gives  $a'^2 = 2b_0^2$  and normalization  $a'^4 = 16b_0^2$ . Then the critical couplings in this case are

$$b_0^* = 2 \quad g_1 = -\frac{3}{8} \quad g_2 = \frac{1}{32}, \quad (2.44)$$

giving positive weights for the cubic vertices and negative for the quartic vertices.

Finally we mention that if we had considered a more general potential with higher degree, we could have encountered multicritical phases for the  $\mathcal{O}(-2)$  loop-gas model corresponding to higher values of  $\theta$ , that are organized in the phase diagram of the  $\mathcal{O}(n)$  model on random lattices as explained in [18].

---

<sup>2</sup>This is the original problem studied by Kostov in [25]

## Chapter 3

# Counting unicellular maps

In chapter 1, we showed how integrals over Hermitian matrices are connected with the enumeration of fat-graphs. Now we want to make precise statements about the counting of unicellular (one face) maps. Having seen that a statistical model on random lattices is defined by summing over arbitrary graphs its partition function on fixed graph, we understand the importance of map enumeration in statistical mechanics and the interplay between combinatorial methods and solutions of random matrix models. In this spirit, the results presented here will be the core of the solution of the spanning trees model on lattices of arbitrary genus presented in chapter 6.

The problem of map enumeration is important in the mathematical literature and has been addressed by several authors. The first result in the enumeration of unicellular maps in positive genus was obtained by Lehman and Walsh [19], and later extended by Goupil and Schaeffer [20]. We will discuss those results in section 3.2. Another approach has been pursued by Harer and Zagier [11], via matrix integrals techniques. They obtained a formula known as the Harer-Zagier theorem, that we will present in section 3.1. This result has been retrieved later by several authors, by various techniques. A combinatorial interpretation was given by Lass [32], and the first bijective proof was given by Goulden and Nica [33].

### 3.1 An exponential generating function from matrix integrals

We first recall the combinatorial interpretation of the Gaussian average of  $\text{Tr}M^n$ . For convenience we will remove the factor  $N$  in the Gaussian weight. Setting

$$Z_0 = (2\pi)^{N/2} 2^{(N-N^2)/2},$$

the quantity  $T_n(N)$  defined by

$$T_n(N) = \frac{1}{Z_0} \int \mathcal{D}M e^{-\frac{1}{2}\text{Tr}M^2} \text{Tr}M^{2n} \quad (3.1)$$

for  $n = 1, 2, \dots$ , is a polynomial in  $N$  where the coefficient of the term<sup>1</sup>  $N^{n+1-2\mathfrak{h}}$  is the number  $\epsilon_{\mathfrak{h}}(n)$  of one-vertex maps of genus  $\mathfrak{h}$  and  $n$  edges, or considering the dual graph, of unicellular maps of genus  $\mathfrak{h}$  and  $n$  edges. In the language of dual graphs we will talk about gluings of the sides of a  $2n$ -gon, dual to the contractions of the  $2n$  half-edges of a star diagram. Refer to section A.2.3 for the definition of duality and an example of the dual of a one-vertex map.

$T_n(N)$  can be written as

$$T_n(N) = \sum_{\mathfrak{h}=0}^{\infty} \epsilon_{\mathfrak{h}}(n) N^{n+1-2\mathfrak{h}} \quad (3.2)$$

and  $\epsilon_{\mathfrak{h}}(n) = 0$  for  $\mathfrak{h} > \lfloor n/2 \rfloor$ .

Our task is to compute the numbers  $\epsilon_{\mathfrak{h}}(n)$ . We already know their values in the case  $\mathfrak{h} = 0$ , since they are the number of planar contractions of a star diagram with  $2n$  half-edges, and according to our result (1.14) they are the Catalan numbers  $C_n = \frac{1}{n+1} \binom{2n}{n}$ . Then we know that  $T_n(1) = \sum_{\mathfrak{h}} \epsilon_{\mathfrak{h}}(n) = (2n-1)!!$ , since it is the number of contractions of  $2n$  half-edges, regardless the planarity.

Following [11, 34] we derive an expression for the exponential generating function for the sequence of polynomials  $T_n(N)$ . The derivation proceeds in two steps. Define  $t(n, N)$  as

$$t(n, N) = \frac{T_n(N)}{(2n-1)!!}. \quad (3.3)$$

The first step is demonstrating that this ratio is a polynomial in  $n$ . If we go to the eigenvalues coordinates in (3.1), and call the measure of the unitary matrices  $c_N$ , we have

$$T_n(N) = c_N \int \prod_i d\lambda_i \prod_{i<j} (\lambda_i - \lambda_j)^2 e^{-1/2 \sum_i \lambda_i^2} \sum_i \lambda_i^{2n}. \quad (3.4)$$

Since the integral is symmetric under permutations of the eigenvalue labels, we can substitute  $\sum_i \lambda_i^{2n}$  with  $N \lambda_1^{2n}$ . Then we expand the square of the Vandermonde determinant and integrate on all  $\lambda_i$  except  $\lambda_1$ . The resulting integrand is the Gaussian weight  $e^{-1/2 \lambda_1^2}$  times a polynomial in  $\lambda_1$  of degree  $2n + 2N - 2$ . In this way  $T_n(N)$  is a sum of integrals of monomials  $\lambda_1^{2n-2k}$  whose value is  $(2n + 2k - 1)!!$  and  $t(n, N)$  will be a sum of terms of the form  $(2n + 2k - 1)!! / (2n - 1)!!$ , each being a polynomial in  $n$  of degree  $k$ . Then  $t(n, N)$  is a polynomial in  $n$  of degree  $N - 1$ .

The next step in obtaining the expression for the generating function is purely combinatorial. Consider a coloring of the vertices of a graph obtained by gluing a  $2n$ -gon. The vertices of the polygon glued will be consequently colored and this gluing will agree with this coloring, that is, vertices of the same color are glued together. Since

---

<sup>1</sup> Since we are omitting  $N$  in the exponential with respect to what we did in section 1.1, propagators will not receive anymore a factor  $N$ . Then a general one-vertex graph  $\mathcal{G}$  will have a weight  $N^{F(\mathcal{G})} = N^{V(\mathcal{G}^*)}$ , that can be expressed in term of genus and number of edges with the Euler formula.  $\mathcal{G}^*$  is the dual unicellular graph.

there are  $N^V$  ways to color the vertices of the graph with  $N$  colors,  $T_n(N)$  can be regarded as the number of gluings of the  $2n$ -gon that agree with possible colorings of the vertices in no more than  $N$  colors. Then call  $\tilde{T}_n(L)$  the set of gluings of the  $2n$ -gon that agree with the colorings of its vertices in precisely  $L$  colors. We have:

$$T_n(N) = \sum_{L=1}^N \binom{N}{L} \tilde{T}_n(L). \quad (3.5)$$

The function

$$\tilde{t}(n, N) = \frac{\tilde{T}_n(N)}{(2n-1)!!} \quad (3.6)$$

is a polynomial in  $n$  of degree  $N-1$  according to our previous matrix integral result. We know  $N-1$  roots of this polynomial, because  $\tilde{T}_0(N) = \tilde{T}_1(N) = \dots = \tilde{T}_{N-2}(N) = 0$  since a graph with  $n$  edges has at most  $n+1$  vertices. Therefore we could write  $\tilde{t}(n, N)$  as

$$\tilde{t}(n, N) = A_N n(n-1) \dots (n-N+2) \quad (3.7)$$

where the factor  $A_N$  depends only on  $N$ . If we substitute this expression in formula (3.5), we have

$$T_n(N) = (2n-1)!! \sum_{L=1}^N A_L \binom{n}{L-1} \binom{N}{L} (L-1)!. \quad (3.8)$$

$A_L$  can be fixed by equating the coefficient of  $N^{n+1}$ ,  $(2n-1)!! A_{n+1} n! / (n+1)!$ , to the Catalan number  $C_n$ . It follows that  $A_{n+1} = 2^n / n!$  and

$$T_n(N) = (2n-1)!! \sum_{L=1}^N 2^{L-1} \binom{n}{L-1} \binom{N}{L}. \quad (3.9)$$

Then the exponential generating function  $T(N, s)$  for  $T_n(N)$  is

$$T(N, s) = 1 + 2s \sum_{n=0}^{\infty} \frac{T_n(N)}{(2n-1)!!} s^n, \quad (3.10)$$

where we used  $T_0(N) = N$ . Since the binomial  $\binom{n}{L-1}$  vanishes if  $n < L-1$ , we obtain the Harer-Zagier theorem:

$$T(N, s) = 1 + \sum_{L=1}^N 2^L \binom{N}{L} \sum_{n=L-1}^{\infty} \binom{n}{L-1} s^{n+1} = \sum_{L=0}^N \binom{N}{L} \left( \frac{2s}{1-s} \right)^L = \left( \frac{1+s}{1-s} \right)^N, \quad (3.11)$$

that can be written as

$$1 + 2 \sum_{n=0}^{\infty} t(n, N) s^{n+1} = \left( \frac{1+s}{1-s} \right)^N. \quad (3.12)$$

In this form the computation of the number of unicellular maps is not evident and we want to go further and obtain a more explicit formula for the numbers  $\epsilon_h(n)$ .

Our task now is to extract the coefficient of  $s^{n+1}$  in the l.h.s of equation (3.12). To do this is convenient to first differentiate (3.12) and expand the right member in power series around  $s = 0$  to have

$$(n+1)t(n, N) = \frac{N}{2\pi i} \oint \frac{ds}{s^{n+1}} \frac{1}{1-s^2} \left( \frac{1+s}{1-s} \right)^N. \quad (3.13)$$

Now indeed we can perform the change of variables  $s = \tanh \frac{t}{2}$  since the Jacobian of this transformation has been produced by deriving:

$$\begin{aligned} (n+1)t(n, N) &= \frac{N}{2\pi i} \oint \frac{dt}{2} \left( \frac{1}{\tanh \frac{t}{2}} \right)^{n+1} e^{tN} \\ &= \frac{N}{2} \text{Res} \left( \left( \frac{1}{\tanh \frac{t}{2}} \right)^{n+1} e^{tN}, 0 \right) = 2^n N [t^n] \left( e^{tN} \left( \frac{t/2}{\tanh \frac{t}{2}} \right)^{n+1} \right) \\ &= 2^n N \sum_{r=0}^n \frac{N^r}{r!} [t^{n-r}] \left( \left( \frac{t/2}{\tanh \frac{t}{2}} \right)^{n+1} \right) \end{aligned} \quad (3.14)$$

where we used the notation  $[z^n]f(z)$  for the operation of extracting the coefficient of  $z^n$  in the power series  $f(z) = \sum_n f_n z^n$ . The function  $t/(2 \tanh \frac{t}{2})$  is even and  $n-r$  is zero unless is an even number, say  $n-r = 2h$ . Finally we have:

$$T_n(N) = \frac{(2n)!}{(n+1)!} \sum_{h=0}^{\lfloor n/2 \rfloor} \frac{N^{n+1-2h}}{(n-2h)!} [t^{2h}] \left( \left( \frac{t/2}{\tanh \frac{t}{2}} \right)^{n+1} \right) \quad (3.15)$$

and from equation (3.2) we get an expression for the numbers  $\epsilon_h(n)$  as a corollary of the Harer-Zagier theorem:

$$\epsilon_h(n) = \frac{(2n)!}{(n+1)!(n-2h)!} [t^{2h}] \left( \left( \frac{t/2}{\tanh \frac{t}{2}} \right)^{n+1} \right). \quad (3.16)$$

Remark that in this expression we don't have anymore dependence on  $N$  as was in (3.12), and we have obtained a formula for computing directly  $\epsilon_h(n)$ . In table 3.1 we list the values of  $\epsilon_h(n)$  for  $1 \leq n \leq 8$  and  $0 \leq h \leq 4$ . Note that correctly the sum of the values in the  $n$ -th line is  $(2n-1)!!$ , and  $\epsilon_0(n) = C_n$ .

## 3.2 More facts about counting unicellular maps

In this section we will present the formula of Goupil and Schaeffer [20] for counting unicellular bicolored maps and its monochromatic version obtained by Walsh and Lehman several years before. We will not go into the details of the quite long derivations and just state the results needed for the analysis of chapter 6.

$n \setminus \mathfrak{h}$	0	1	2	3	4
1	1	0	0	0	0
2	2	1	0	0	0
3	5	10	0	0	0
4	14	70	21	0	0
5	42	420	483	0	0
6	132	2310	6468	1485	0
7	429	12012	66066	56628	0
8	1430	60060	570570	1169740	225225

Table 3.1: Values of  $\epsilon_{\mathfrak{h}}(n)$  for  $1 \leq n \leq 8$  and  $0 \leq \mathfrak{h} \leq 4$ .

We start with some definitions. A *partition*  $\lambda = (\lambda_1, \dots, \lambda_k)$  is a non-increasing finite sequence of positive integers  $\lambda_i$  called parts such that  $\lambda_1 \geq \lambda_2 \geq \dots \geq \lambda_k > 0$ . The number of parts is the length  $L(\lambda) = k$  and if  $\alpha_i$  parts of  $\lambda$  are equal to  $i$ , we will use the frequency representation  $\lambda = 1^{\alpha_1} \dots n^{\alpha_n}$ . The sum  $\sum_{i=1}^k \lambda_i = n$  is the weight and in this case  $\lambda$  is said to be a partition of  $n$ , and we will write  $\lambda \vdash n$ . A partition can be represented by a *Ferrers' diagram*, composed of rows positioned on top of each other from the shorter to the longer where if we start counting from top, in the  $i$ -th row there are  $\lambda_i$  elements. The total number of elements is the weight of the partition. For an example see figure 3.1.

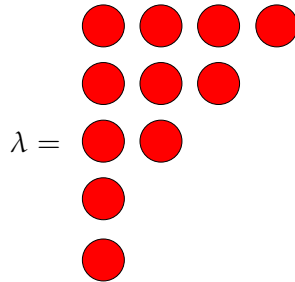


Figure 3.1: A representation of the partition  $\lambda = (4, 3, 2, 1, 1)$  of 11 by its Ferrers' diagram.

A *composition*  $p = (i_1, \dots, i_l)$  of  $n$  is a finite sequence of non-negative integers summing up to  $n$  and we will denote it by  $p \vDash n$ .

A bicolored map has a vertex set composed by two subsets corresponding to black or white vertices and each edge connects a black vertex to a white one. When not specified, by maps we will intend monochromatic maps, with only one type of vertices. Consider a bicolored unicellular map of genus  $\mathfrak{h}$  with  $n$  edges and the degree of the two types of vertices given respectively by the two partitions of  $n$ ,  $\lambda = 1^{\alpha_1} \dots n^{\alpha_n}$  and

$\mu = 1^{\beta_1} \dots n^{\beta_n}$ . The number of such maps according to Goupil and Schaeffer is<sup>2</sup>:

$$c_{\lambda\mu}^n = \frac{n}{\prod_i \alpha_i! i^{\alpha_i} \prod_i \beta_i! i^{\beta_i} 2^{2\mathfrak{h}}} \sum_{\mathfrak{h}_1 + \mathfrak{h}_2 = \mathfrak{h}} (l + 2\mathfrak{h}_1 - 1)!(m + 2\mathfrak{h}_2 - 1)! \cdot \sum_{\substack{(i_1, \dots, i_k) = \mathfrak{h}_1 \\ (j_1, \dots, j_m) = \mathfrak{h}_2}} \prod_k \binom{\lambda_k}{2i_k + 1} \prod_k \binom{\mu_k}{2j_k + 1}. \quad (3.17)$$

$L(\lambda) = l$  and  $L(\mu) = m$  are the parts of  $\lambda$  and  $\mu$ , which satisfy the formula  $l + m = n + 1 - 2\mathfrak{h}$ . The sets of  $i_k$  and  $j_k$  are compositions of the integers  $\mathfrak{h}_1$  and  $\mathfrak{h}_2$ .

The monochromatic version of this formula can be obtained by giving coordination 2 to one type of vertices. Taken as weight for the partitions  $2n$ , we set  $\lambda = 2^n$ . Then every  $i_k$  in (3.17) is equal to 0, otherwise the binomial coefficient is zero, and we have that the number of monochromatic maps with one face and  $n$  edges is

$$c_{2^n, \mu}^{2n} = \frac{2n(n-1)!}{\prod_i \beta_i! i^{\beta_i} 2^{2\mathfrak{h}}} \sum_{(i_1, \dots, i_m) = \mathfrak{h}} \prod_k \binom{\mu_k}{2i_k + 1}. \quad (3.18)$$

Here the length of  $\mu$  is the number of vertices of the map, or returning to the dual one-vertex graph, is its number of faces and  $\mu$  gives the number of sides of every face. As a first non-trivial example, and also for later purposes, we consider the case of triangulations, i.e. fixing all  $\mu$  equal to 3, to have faces with three sides in the one-vertex map. (An example of a one-vertex triangulation of the torus together with its dual map can be found in section A.2.3, figure A.5). The number of edges in a triangulation of a surface of genus  $\mathfrak{h}$ ,  $\mathfrak{h} \geq 1$ , is  $6\mathfrak{h} - 3$  and by Euler formula we get the number of triangles,  $4\mathfrak{h} - 2$ . We have thus a simple formula, coherent with the one derived in [35] with a different approach:

$$\begin{aligned} \sum_{T \in \mathcal{T}} \frac{1}{|\text{Aut}(T)|} &= \frac{c_{3^{4\mathfrak{h}-2}, 2^{6\mathfrak{h}-3}}^{12\mathfrak{h}-6}}{12\mathfrak{h} - 6} \\ &= \frac{2}{12^{\mathfrak{h}}} \frac{(6\mathfrak{h} - 5)!}{\mathfrak{h}!(3\mathfrak{h} - 3)!} \end{aligned} \quad (3.19)$$

where  $\mathcal{T}$  is the set of one-vertex triangulations of a genus  $\mathfrak{h}$  surface.

We checked with a direct computation the result (3.19) for  $n$  less than 7. This check was done with a Hermitian matrix model. Consider the following average

$$F_{\mathfrak{h}}(N) = \frac{1}{Z_0} \int \mathcal{D}M e^{-\frac{1}{2}M^2} \frac{(\text{Tr}M^3)^{4\mathfrak{h}-2}}{3^{4\mathfrak{h}-2}(4\mathfrak{h}-2)!}. \quad (3.20)$$

<sup>2</sup> This is a rather complicated and powerful formula and the authors derived it in the context of character theory and group algebra of the symmetric group. In this framework called  $C_\lambda$  and  $C_\mu$  two conjugacy classes of the symmetric group, (3.17) counts the number of pairs of permutation of  $n$  elements  $(\sigma, \tau) \in C_\lambda \times C_\mu$ , such that  $\sigma\tau = (1, 2, \dots, n)$ .

Using Wick's theorem we produce the ensemble of cubic graphs with  $4\mathfrak{h} - 2$  vertices.  $F_{\mathfrak{h}}(N)$  is a polynomial in  $N$  and its coefficients can be obtained by calculating explicitly the matrix integral for the first  $N$  and solving a linear system for the coefficients. Then, expanding the logarithm of  $F = \sum_k F_k(N)x^k$  and matching the expansion of  $f = \sum_k f_k(N)x^k$  gives  $f_k(N)$ , that is the polynomial that counts only connected graphs. The coefficient of the monomial  $N$  in  $f_{\mathfrak{h}}(N)$  is the sum over one-vertex triangulations of a genus  $\mathfrak{h}$  surface weighted by the inverse of their automorphism group. The values obtained with this method were in agreement with (3.19).

Now we can make contact with the results obtained in section 3.1, and if we sum (3.18) over all the possible partitions  $\mu \vdash 2n$  with fixed length  $m = n + 1 - 2\mathfrak{h}$ , we obtain a more tractable expression for  $\epsilon_{\mathfrak{h}}(n)$ . The result is:

$$\epsilon_{\mathfrak{h}}(n) = \frac{1}{2^{2\mathfrak{h}}} \frac{(2n)!}{n!(n+1)!} \sum_{\gamma \vdash \mathfrak{h}} \frac{(n+1) \cdots (n+2-2\mathfrak{h}-L(\gamma))}{\prod_i c_i! (2i+1)^{c_i}}. \quad (3.21)$$

As before  $\gamma = \prod_i i^{c_i}$  is a partition of  $\mathfrak{h}$  and  $L(\gamma)$  is the number of parts. We correctly have  $\epsilon_0(n) = C_n$ . (3.21) coincides with the formula of Walsh and Lehman obtained many years before (also before the work of Harer and Zagier) by means of a direct recursive method, relying on multivariate recurrence equations [19].

The asymptotic in  $n$  of (3.21) can be easily derived using Stirling formula. If we fix  $\mathfrak{h}$  and consider the limit of large  $n$ , only Ferrers' diagrams with every row made of one element contributes. So, in the large volume limit,  $\epsilon_{\mathfrak{h}}(n)$  becomes:

$$\epsilon_{\mathfrak{h}}(n) \sim \frac{n^{3(\mathfrak{h}-1/2)} 4^n}{\sqrt{\pi} \mathfrak{h}! 12^{\mathfrak{h}}}. \quad (3.22)$$



## Chapter 4

# Random matrix approach to spanning forests on random lattices

In this chapter we will discuss the spanning forests model on random lattices in connection with the Potts and  $\mathcal{O}(n)$  models and the results obtained on flat lattices. Then, we will follow the procedure outlined by Caracciolo and Sportiello in [21] to derive a matrix integral for spanning forests. Lastly we will present the contribution to this problem we did in this thesis, that is solving this integral thanks to its equivalence with the  $\mathcal{O}(-2)$  loop-gas model discussed in section 2.3, and interpret the results.

### 4.1 General background and motivations

A statistical system observed in the thermodynamic limit can exhibit critical points where some thermodynamic quantities diverge. At criticality the Hamiltonian of the system flows to a scale invariant fixed point since the correlation length becomes infinite and every local scale becomes negligible. Then, when we reach a critical point, the critical exponents become universal, they do not depend on the short-scale characteristics of the model and are determined only by the symmetry properties. Systems that share the same universal properties are in the same universality class. Critical phenomena on 2D flat lattices can be efficiently studied using conformal field theory (CFT). If we admit the larger invariance of the Hamiltonian under conformal transformations, the identification of the model under investigation with a conformal field theory is indeed very useful. A conformal field theory is specified by a central charge  $c$ , related to the scaling behaviour of the stress tensor of the theory, and its knowledge characterizes a given universality class and allows to derive the critical exponents (for a recent review of the topic, see [36]).

Both the Potts model (in the range  $0 \leq q \leq 4$ ) and the  $\mathcal{O}(n)$  loop-gas model (in the range  $-2 \leq n \leq 2$ ) on a large portion of a periodic two dimensional lattice  $\mathcal{G}$ , specified respectively by the partition functions (1.30) and (1.27), can be identified with conformal field theories. This can be done from known exact results on these models.

Indeed the  $\mathcal{O}(n)$  loop-gas model can be mapped onto a Solid-On-Solid model [37] and the Potts model can be mapped onto an Ice model [38] and subsequently transformed again to a Solid-On-Solid model. Then, the critical behaviour of the Solid-On-Solid model is found thanks to its connection to the Coulomb gas as explained by Nienhuis in [39].

On the other hand, starting from the work of Kazakov on the Ising model on dynamical planar lattices [3], a lot of statistical models on fluctuating surfaces were solved with random matrix techniques. Among these, there are the Potts model, studied in [26, 40, 41, 42], and the  $\mathcal{O}(n)$  loop-gas model, that we partially solved in chapter 2.

The critical behaviour of systems in the standard plane and in a random 2D metric can be related by the KPZ relations, obtained by Knizhnik, Polyakov and Zamolodchikov analyzing a conformal theory in presence of 2D quantum gravity [6]. In particular they were able to conjecture the relation between the string susceptibility exponent that accounts for the non analyticity of the partition function when we reach the continuum limit (see section 2.2.2), to the central charge of the model on flat space:

$$\gamma = 2 - \frac{1}{12} \left( 25 - c + \sqrt{(1-c)(25-c)} \right). \quad (4.1)$$

Despite the fact that explicit solutions of statistical models on random graphs and on flat lattices were a testing ground for KPZ relations and confirmed their previsions [43], these formulas as yet eluded a rigorous approach and are a current active research field [44, 45, 46]. Nonetheless they have been used as a powerful tool by Duplantier [47] to give insights about random walks on the plane from their random surface solution.

Now we want to address our attention to the spanning forests model on random lattices. A spanning forest over a graph is a spanning subgraph without cycles, made of components called trees.<sup>1</sup> The partition functions of spanning forests  $Z_G^{\text{forest}}(t, \vec{w})$  and spanning trees  $Z_G^{\text{tree}}(\vec{w})$  on a graph  $G$  are defined as

$$Z_G^{\text{tree}}(\vec{w}) = \sum_{T \prec G} \prod_{(ij) \in E(T)} w_{ij} \quad (4.2)$$

$$Z_G^{\text{forest}}(t, \vec{w}) = \sum_{F \prec G} t^{K(F)} \prod_{(ij) \in E(F)} w_{ij}. \quad (4.3)$$

where the sum on respectively  $F \prec G$  and  $T \prec G$  means on all spanning forests and trees over  $G$ , and  $K(F)$  is the number of connected components of the forest. These models have great combinatorial interest and arise in physics when we consider the limit  $q \rightarrow 0$  of the Potts model in the Fortuin-Kasteleyn representation as explained in section B.1.

Another connection between spanning forests and a statistical model of great interest was given by Caracciolo *et al.* in [17] when they introduced Grassman integrals to

---

<sup>1</sup>For a list of useful definitions from graph theory see section A.1.

generalize Kirchoff's matrix-tree theorem <sup>2</sup> to unrooted forests:

$$Z_G^{\text{tree}}(\vec{w}) = \int \mathcal{D}(\psi, \bar{\psi}) \exp(\bar{\psi} L_G(\vec{w}) \psi) \bar{\psi}_i \psi_i \quad (4.6)$$

$$Z_G^{\text{forest}}(t, \vec{w}) = \int \mathcal{D}(\psi, \bar{\psi}) \exp\left[\bar{\psi} L_G(\vec{w}) \psi + t \left( \sum_i \bar{\psi}_i \psi_i - \sum_{(ij) \in E(G)} w_{ij} \bar{\psi}_i \psi_i \bar{\psi}_j \psi_j \right)\right]. \quad (4.7)$$

We see how the complex free fermion representation of spanning trees is extended in the case of forests to a Gaussian term and a local four fermions interaction.

In this form, the partition function of spanning forests can be mapped to all orders in perturbation theory to an  $\mathcal{O}(n)$  invariant  $\sigma$ -model at  $n = -1$ <sup>3</sup> defined on the lattice  $G$  by the following Hamiltonian  $\mathcal{H}_G$

$$\mathcal{H}_G = -T^{-1} \sum_{(ij) \in E(G)} w_{ij} (\vec{\sigma}_i \cdot \vec{\sigma}_j - 1) \quad (4.8)$$

where  $\vec{\sigma}_i \in \mathbb{R}^N$ ,  $|\vec{\sigma}_i| = 1$ , located at the sites  $i \in V(G)$  and  $T =$  temperature. The coupling constant of the continuum formulation of the model is identified with the temperature. The correspondence of this model with spanning forests is such that the coupling constant of the  $\sigma$ -model is interpreted as minus the fugacity of the trees  $t$ . So this approach sheds light also on an unexpected connection between the Potts and the  $\mathcal{O}(n)$   $\sigma$ -model.

Studying spanning trees is simple and a lot of results have been achieved in this case. But these results can be no more than useful checks of an eventual solution of spanning forests, since to study forests we need information at finite values of the coupling constant  $t$  and trees correspond only to the critical limit  $t \rightarrow 0$ . We want to address the study of general values of the coupling and we then wonder how far we

---

<sup>2</sup> Kirchoff's matrix-tree theorem is a result proved by Kirchoff in 1848 and states that the generating function of spanning trees is given by the determinant of a minor of the Laplacian matrix. The Laplacian matrix of a graph  $G$  is defined as

$$L_G(\vec{w}) = \begin{cases} -w_{ij} & \text{if } (ij) \in E(G) \\ 0 & \text{if } (ij) \notin E(G) \\ \sum_{k \sim i} w_{ik} & \text{if } i = j \end{cases} \quad (4.4)$$

where  $k \sim i$  denotes the vertices  $k$  connected to  $i$  and  $\vec{w} = \{w_{ij}\}_{(ij) \in E(G)}$ . The Laplacian matrix can be generalized to the case of graphs with an infinite number of vertices and edges; this generalization is known as the discrete Laplace operator. Kirchoff's theorem is

$$Z^{\text{tree}}(G; \vec{w}) = \det L_G(\vec{w})_{\setminus i} \quad (4.5)$$

where  $L_G(\vec{w})_{\setminus i}$  is the minor of the  $L_G(\vec{w})$  with the column and row  $i$  deleted and this result is independent from the choice of  $i$ .

<sup>3</sup> But the  $\mathcal{O}(n)$  loop-gas model at  $n = -1$  has a central charge  $c(-1) = -3/5$  and does not describe spanning forests. Instead  $c(-2) = -2$ . This puzzling issue is maybe pertinent to considering different realizations of the  $\mathcal{O}(n)$  symmetry: in the loop-gas model, whose random-matrix variant is discussed in chapter 2, we have the "logarithmic" realization, while in [17] we have a purely quadratic, although projective, realization of the symmetry. We will show that on random planar graphs spanning forests are exactly the  $\mathcal{O}(-2)$  loop-gas model solved in section 2.3.

can go in this way on both 2D flat regular lattices (for example the square lattice) and the ensemble of random graphs described in chapter 1.

Given this perspective, we want to derive results directly for spanning trees and forests on random lattices in order to understand as much as we can about these and related models on random graphs, having then the possibility of inferring about their flat lattice counterpart using the KPZ relations. We will use basically two methods to investigate the models. One is a purely combinatorial approach, based on the fact that on random lattices, degrees of freedom of the lattice and of the matter fields cooperate to simplify the counting of the configurations. With this combinatorial method we will show how to easily obtain some partially known results, but with a greater control of the finite size and the possibility of directly investigate the all genus partition function of spanning trees. Having understood the procedure for trees, immediately gives us the possibility of solving other models that present the same combinatorial formulation, such as *spanning hypertrees on spanning hypergraphs* and *Hamiltonian cycles*. This will give more information about the universality class corresponding to the KPZ mapping of the  $c = -2$  theory. Apart from this approach, we will also establish the equality of the spanning forests matrix integral to the  $\mathcal{O}(-2)$  loop-gas model and use the results for that model to have information about the critical structure of spanning forests. This will be the topic of the present chapter and we refer to the next chapters for an explanation of the combinatorial methods.

## 4.2 The model

Given a graph  $\mathcal{G}$  and a spanning forest  $\mathcal{F}$  over it, define the *contraction*  $\mathcal{G}/\mathcal{F}$  as the graph in which the components of the forest are shrunk to points, by identifying vertices pertaining to edges of the same tree. Then, we define the partition function for spanning forests over a fixed graph  $\mathcal{G}$  as

$$Z_{\mathcal{G}}(t) = \sum_{\mathcal{F} \prec \mathcal{G}} t^{K(\mathcal{F})} \frac{|\text{Aut}(\mathcal{G})|}{|\text{Aut}(\mathcal{G}/\mathcal{F})|} \quad (4.9)$$

This corresponds to the partition function  $Z_{\mathcal{G}}^{\text{forest}}(t, 1)$  where we introduce the additional ratio  $|\text{Aut}(\mathcal{G})|/|\text{Aut}(\mathcal{G}/\mathcal{F})|$  for later convenience.

In chapter 1 we saw that the random matrix prescription to define a model on random lattices is summing over graphs  $\mathcal{G}$  weighting by <sup>4</sup>

$$\frac{N^{-2h(\mathcal{G})} g^{|\mathcal{V}(\mathcal{G})|}}{|\text{Aut}(\mathcal{G})|}.$$

---

<sup>4</sup>With respect to our former definition, here for convenience we substitute  $\chi$  with  $-2h$  in the exponent of  $N$ , since  $Z/N^2$  is the sensible quantity that has a non trivial limit  $N \rightarrow \infty$ .

Then the partition function for spanning forests on random lattices is

$$\begin{aligned} Z(t, g, N) &= \sum_{\mathcal{G}} N^{-2\mathfrak{h}(\mathcal{G})} g^{V(\mathcal{G})} \sum_{\mathcal{F} \prec \mathcal{G}} t^{K(\mathcal{F})} \frac{1}{|\text{Aut}(\mathcal{G}/\mathcal{F})|} \\ &= \sum_{\mathcal{F}} t^{K(\mathcal{F})} g^{|V(\mathcal{F})|} \sum_{\mathcal{G} \succ \mathcal{F}} \frac{N^{-2\mathfrak{h}(\mathcal{G}/\mathcal{F})}}{|\text{Aut}(\mathcal{G}/\mathcal{F})|} \end{aligned} \quad (4.10)$$

where  $\mathcal{G}$  are connected graphs with fixed coordination  $k = h + 2$ . In this formula we exchange the two sums because this form simplifies the analysis, and we can do this since  $V(\mathcal{G}) = V(\mathcal{F})$  and  $\mathfrak{h}(\mathcal{G}) = \mathfrak{h}(\mathcal{G}/\mathcal{F})$  (a tree is homotopic to a point).

Note that the partition function (4.10) is a triple series in  $N$ ,  $g$  and  $t$ . We will mainly be interested in the thermodynamic limit that occur for large size of the graph, when  $g$  tends to its critical value, and we will investigate directly the planar limit  $N \rightarrow \infty$  and the limit of trees,  $t \rightarrow 0$ .

### 4.3 Useful counting problems

Before explaining how to derive a random matrix representation for the partition function (4.10), we will give combinatorial results regarding the enumeration of trees rooted on the plane and on the disk that are important in the following discussions. Call  $\mathbb{H}$  the upper half plane, and  $\mathbb{D}$  the unit disk.

#### 4.3.1 Counting non-intersecting trees in $\mathbb{H}$

We want to solve the problem of counting the configurations of non-intersecting trees of degree  $k = h + 2$  with  $n$  vertices in  $\mathbb{H}$  and  $hn + 2$  leaves on the boundary of the plane  $\partial\mathbb{H}$ . Call this number  $A_{h,n}$ . We set  $A_{h,0} = 1$ , since there is only one empty configuration. Then, we start by considering the case of trees with  $h = 1$  (for a typical configuration see top of figure 4.1) because is easier and the result well-known. Given a configuration with  $n > 0$ , we remove the rightmost leaf in such a way that the two edges connected to the vertex to which this leaf is attached, become themselves new rightmost leaves for the two remaining components (bottom of figure 4.1).

We can then write the following convolutional formula for the coefficient  $A_{1,n}$ :

$$A_{1,n} = \sum_{n_1=0}^{n-1} A_{1,n_1} A_{1,n-1-n_1}. \quad (4.11)$$

We recognize the convolutional relation of Catalan numbers (1.9) that lead to the quadratic equation (1.10) for the generating function  $A_1(q) = \sum_{n=0}^{\infty} A_{1,n} q^n = C(q)$ . So we have:

$$A_{1,n} = \frac{1}{n+1} \binom{2n}{n}; \quad A_1(q) = \frac{1 - \sqrt{1 - 4q}}{2q}. \quad (4.12)$$

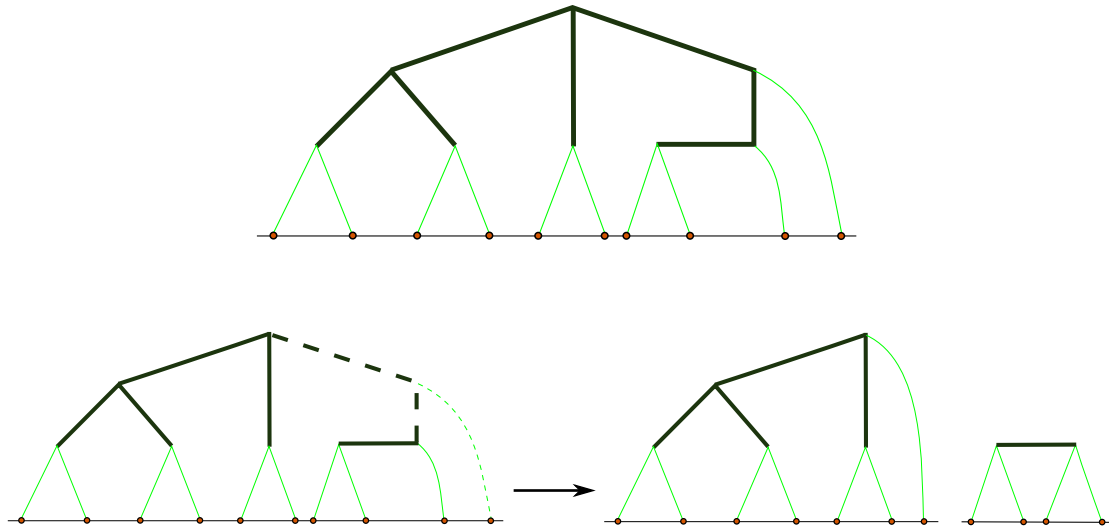


Figure 4.1: On top, there is a cubic tree ( $h = 1$ ) with  $n = 8$  vertices and 10 leaves on  $\partial\mathbb{H}$ . On bottom, we depicted the procedure of removal of the rightmost leaf and the resulting trees that remains.

One can convince himself that when  $h = 1$  this problem is solved by Catalan numbers also by direct enumeration of the first terms.

The derivation in the case of generic  $h$  is analog to the  $h = 1$  case. Upon removing the rightmost leaf, this time we have  $h + 1$  remaining components and accordingly, the equation satisfied by the generating function  $A_h(q) = \sum_n A_{h,n} q^n$  generalizes to:

$$A_h(q) = 1 + q(A_h(q))^{h+1}. \quad (4.13)$$

The coefficients of  $A_h(q)$  are a generalization of the Catalan numbers<sup>5</sup>

$$A_{h,n} = \frac{1}{hn+1} \binom{(h+1)n}{n}. \quad (4.14)$$

The large  $n$  behaviour of  $A_{h,n}$  is easily obtained performing a Stirling expansion:

$$A_{h,n} \sim \left( \frac{(h+1)^{h+1}}{h^h} \right)^n n^{-\frac{3}{2}} \sqrt{\frac{h+1}{2\pi h^3}}. \quad (4.15)$$

The radius of convergence of  $A_h(q)$  can be obtained from the condition that the ratio of two successive terms in the expansion tends to 1 and it is

$$|q| < \frac{h^h}{(h+1)^{h+1}}. \quad (4.16)$$

<sup>5</sup>In [24],  $A_{2,n}$ : [A0001764](#);  $A_{3,n} \cdots A_{6,n}$ : [A0002293](#)  $\cdots$  [A0002296](#).

Despite equation (4.13) does not have an easy solution except at  $h = 1$  or  $2$ , where  $A_1$  is the generating function of Catalan numbers and  $A_2$  can be written as  $A_2\left(\frac{4x^2}{27}\right) = \frac{3}{x} \sin\left(\frac{1}{3} \arcsin x\right)$ , it admits a parametric solution in algebraic form

$$\begin{cases} q^{1/h} = x(1 - x^h) \\ A_h = (1 - x^h)^{-1} \end{cases} .$$

This generalizes to

$$\begin{cases} z = x(1 - gx^h) \\ z(A_h(gz^h) - 1) = gx^{h+1} \end{cases} . \quad (4.17)$$

### 4.3.2 Counting non-intersecting trees in $\mathbb{D}$

The number of non-intersecting trees on the disk  $\mathbb{D}$  with  $n$  vertices of fixed coordination  $k = h + 2$  and  $hn + 2$  leaves on  $\partial\mathbb{D}$  is immediately computed by dividing  $A_{h,n}$  by the number of border legs, which accounts for the cyclic symmetry among the leaves on a disk. If we call these numbers  $A'_{h,n}$ ,

$$A'_{h,n} = \frac{A_{h,n}}{hn + 2} = \frac{((h + 1)n)!}{n!(hn + 2)!} . \quad (4.18)$$

Their generating function  $A'_h(q) = \sum_{n \geq 1} A'_{h,n} q^n$ , where now the summation starts from 1, is related to  $A_h$  by the relation

$$z(A_h(gz^h) - 1) = \frac{d}{dz} \left( z^2 A'_h(gz^h) \right) . \quad (4.19)$$

From the parametric formula (4.17), the above relation becomes

$$z^2 A'_h(gz^h) = \frac{x^2}{2} \left( \frac{2}{h+2} gx^h - (gx^h)^2 \right) . \quad (4.20)$$

## 4.4 A matrix integral for the partition function

In this section we will write a matrix integral to represent the partition function (4.10). That formula suggests to first contract the trees to points and then represent the combinatorics of the resulting effective vertices by a suitable integral. The procedure is explained in [21] and works as follows.

Given a connected graph  $\mathcal{G}$  with coordination  $k = h + 2$  and a spanning forest  $\mathcal{F}$  over it, mark the edges of the forest and all the vertices, and leave the remaining edges unmarked. Then  $K(\mathcal{F})$  coincides with the number of marked components. Now insert in every unmarked edge two intermediate vertices such that every unmarked edge can be considered as the contraction of three auxiliary edges, two attached to trees a middle one. For every component of the forest, regard the tree with the auxiliary edges attached to its terminations as a new tree  $T_\alpha$ ,  $\alpha = 1, \dots, K(\mathcal{F})$  with its leaves on the

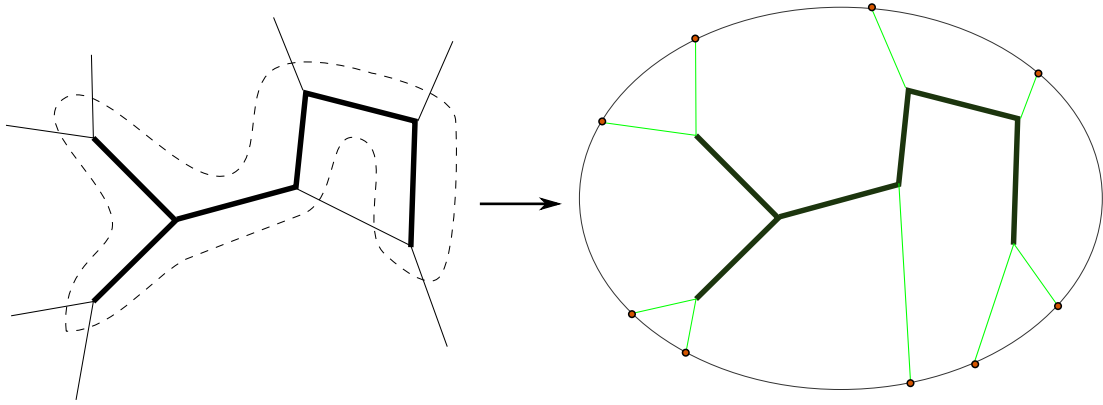


Figure 4.2: The identification of a component of a forest on a random cubic graph with a tree on the disk. The edges of the tree are marked in bold and the region enclosed by the shaded line is the tree with its border legs.

disk, as depicted in figure 4.2. From section 4.3.2 we know that the number of such trees with  $n$  vertices is  $A'_{h,n}$ .

Now contract every  $T_\alpha$  to single vertices respecting the ordering of the the border legs, as in figure 4.3. The resulting graph is  $\mathcal{G}/\mathcal{F}$ , whose vertices are linked by the middle auxiliary edges, what remains of the unmarked edges of the original graph.

To keep track of this shrinking procedure, we assign to every tree with  $n$  vertices an effective coupling  $g_n = t g^n A'_{h,n}$ , since we have to add a factor  $t$  for every component, a power of  $g$  for every vertex and count all the possible trees with  $n$  vertices and coordination  $h + 2$ .

Then, the coordination of vertices of  $\mathcal{G}/\mathcal{F}$  is  $hn + 2$ ,  $n \geq 1$ , and at every vertex there is a corresponding coupling  $g_n$ . In this form, thanks to the language of Wick's contraction and Feynman diagrams developed in section 1.1, the problem can be represented by a one-Hermitian matrix integral:

$$Z(t, g, N) = \frac{1}{N^2} \log \frac{\int \mathcal{D}M e^{-N \text{Tr} V(M)}}{\int \mathcal{D}M e^{-\frac{N}{2} \text{Tr} M^2}} \quad (4.21)$$

where the potential is

$$\begin{aligned} V(z) &= \frac{1}{2} z^2 - \sum_{n \geq 1} g_n z^{hn+2} \\ &= \frac{1}{2} z^2 (1 - t A'_h(gz^h)). \end{aligned} \quad (4.22)$$

Note that despite we have only one matrix, the potential is not polynomial in the fields, in analogy with what occurred in section 2.3 for the  $\mathcal{O}(-2)$  loop-gas, and we will show later that this is more than a mere coincidence.



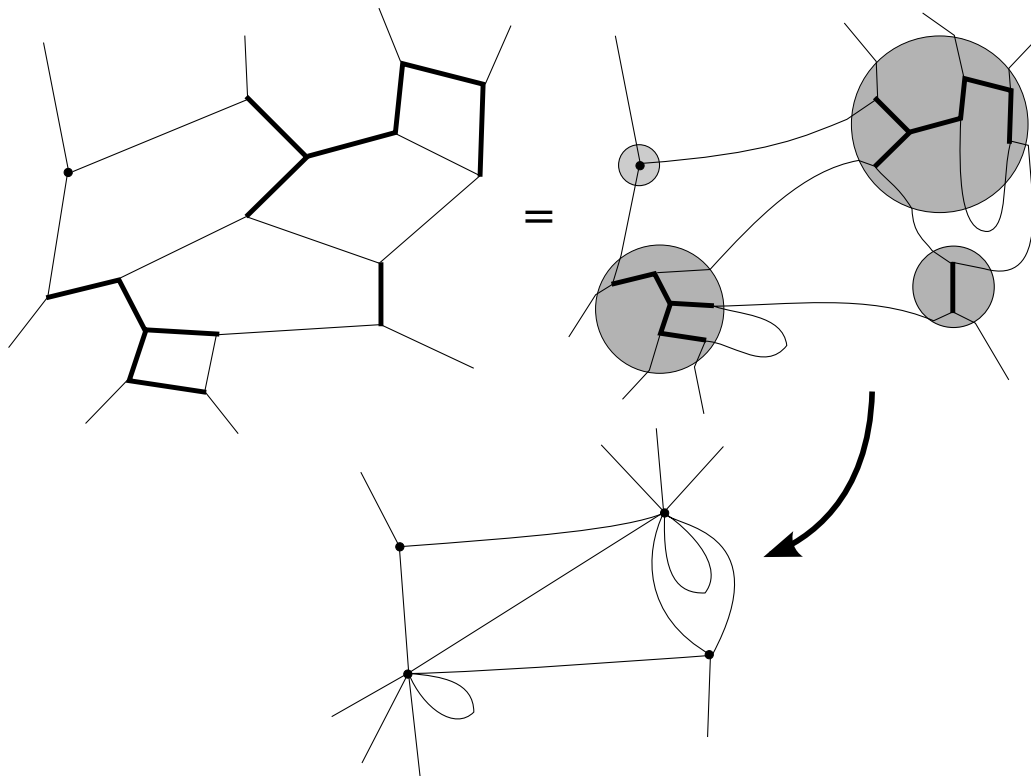


Figure 4.3: The procedure for shrinking the trees. Given a spanning forest  $\mathcal{F}$  over a graph  $\mathcal{G}$ , we mark the components of the forest (here in bold), and we shrink the trees with their leaves to single vertices respecting the ordering of the border legs. Then we obtain  $\mathcal{G}/\mathcal{F}$  (graph on the bottom). The figure on top right is an intermediate step, where we deform the graph and color in gray the region to be shrunk, to better visualize the procedure.

Nonetheless there is a suitable change of coordinates that will give a polynomial potential at the price of an additional term in the integrand. First of all we go to the eigenvalues basis,  $M \rightarrow (\Lambda, U)$ , as done in chapter 2 for the solution of the  $\mathcal{O}(n)$  loop-gas model. Remember that the Jacobian of this transformation is the square of the Vandermonde determinant  $\Delta^2(\{\lambda_i\}) = \prod_{i < j} (\lambda_i - \lambda_j)^2$ . (4.21) becomes:

$$Z(t, g, N) = \frac{1}{N^2} \log \frac{\int \prod_{i=1}^N d\lambda_i \Delta^2(\{\lambda_i\}) e^{-N \sum_i V(\lambda_i)}}{\int \prod_{i=1}^N d\lambda_i \Delta^2(\{\lambda_i\}) e^{-\frac{N}{2} \sum_i \lambda_i^2}} \quad (4.23)$$

and from the expression of the potential  $V$  in equation (4.22), we note that we have to integrate inside the analyticity region of  $A'_h(q)$ , according to (4.16).

In section 4.3 we gave a parametric formula for  $A'_h(gz^h)$ , equation (4.20). This suggests the right change of variables to obtain a polynomial potential:

$$\lambda_i(x_i) = x_i(1 - gx_i^h). \quad (4.24)$$

Upon this transformation in (4.23), we end with the following expression for the partition function of spanning forests<sup>6</sup>:

$$Z(t, g, N) = \frac{1}{N^2} \log \frac{\int \prod_{i=1}^N dx_i \Delta^2(\{x_i\}) \hat{\Delta}_g(\{x_i\}) e^{-N \sum_i \tilde{V}(x_i)}}{\int \prod_{i=1}^N dx_i \Delta^2(\{x_i\}) e^{-\frac{N}{2} \sum_i x_i^2}} \quad (4.25)$$

where the potential  $\tilde{V}$  is now polynomial

$$\tilde{V}(z) = \frac{z^2}{2} \left( 1 - 2g \left( 1 + \frac{t}{h+2} \right) z^h + g^2 (1+t) z^{2h} \right) \quad (4.26)$$

and the new factor  $\hat{\Delta}_g(\{x_i\})$  comes from the combination of the Jacobian and the change of the Vandermonde determinant in the new coordinates, and is

$$\hat{\Delta}_g(\{x_i\}) = \prod_{i,j} (1 - g(x_i^h + x_i^{h-1}x_j + \dots + x_j^h)). \quad (4.27)$$

## 4.5 Critical structure of spanning forests

### 4.5.1 Equivalence with the $\mathcal{O}(-2)$ loop-gas model

We now want to solve the matrix integral (4.25) exploiting the equality with the partition function of the  $\mathcal{O}(-2)$  loop-gas model, upon identification of the parameters. This is actually the original work with respect to the rest of the chapter. To make easier seeing the correspondence let us rewrite here the matrix integral for the  $\mathcal{O}(-2)$  loop-gas

<sup>6</sup> At the denominator we simply call the integration variables  $x_i$

model with a quartic potential that can be interpreted as a model of self-avoiding loops and dimers on the cubic lattice,

$$Z_N^{\mathcal{O}(-2)}(\{g_i\}, b_0) = \frac{1}{N^2} \log \frac{1}{\int \prod_{i=1}^N db_i \Delta^2(\{b_i\}) \exp\left(-\frac{N}{2} \sum_i b_i^2\right)} \cdot \int \prod_{i=1}^N db_i \Delta^2(\{b_i\}) \prod_{i,j} \left(1 - \frac{1}{4b_0}(b_i + b_j)\right) \exp\left(-N \sum_i \left(\frac{1}{2}b_i^2 + \frac{g_1}{3}b_i^3 + \frac{g_2}{4}b_i^4\right)\right), \quad (4.28)$$

and that for spanning forests on cubic lattices ( $h = 1$ )

$$Z(t, g, N) = \frac{1}{N^2} \log \frac{1}{\int \prod_{i=1}^N dx_i \Delta^2(\{x_i\}) \exp\left(-\frac{N}{2} \sum_i x_i^2\right)} \cdot \int \prod_i d^N x_i \Delta^2(\{x_i\}) \prod_{i,j} (1 - g(x_i + x_j)) \cdot \exp\left(-N \sum_i \frac{x_i^2}{2} \left(1 - 2g \left(1 + \frac{t}{3}\right) x_i + g^2(1+t)x_i^2\right)\right). \quad (4.29)$$

The two expressions are the same if we match the parameters in the following way:

$$\begin{cases} \frac{1}{4b_0} = g \\ g_1 = -g(3+t) \\ g_2 = 2g^2(1+t) \end{cases}. \quad (4.30)$$

Further, also the integration region are the same for these two models. The analyticity condition on  $x_i$  that restricts the region of integration in (4.29) coincide with the condition of positivity of the Gaussian weight in (2.3) on  $b_i$ .

Having established the correspondence of spanning forests on random lattices with the  $\mathcal{O}(-2)$  loop-gas model previously discussed, we can use the study of the critical behaviour of the latter, pursued in section (2.3.2). There we studied exactly (4.28) with the saddle point technique and found two kinds of critical points: (2.43) and (2.44), both corresponding to a string susceptibility exponent  $\gamma = -1$ . The first set of critical points translates into

$$t^* = -1 \quad g^* = \frac{\pi}{8\sqrt{6}}, \quad (4.31)$$

while the second set into

$$t^* = 0 \quad g^* = \frac{1}{8}. \quad (4.32)$$

## 4.5.2 Mapping to flat lattice

So far we obtained that spanning forests on cubic graphs possess two critical values for the fugacity of the trees,  $t = 0$  and  $t = -1$ . Both these points correspond to a string susceptibility exponent  $\gamma = -1$ . Our interest now is to map this results to flat two dimensional lattices using the KPZ relations. From formula (4.1) we have that the central charge corresponding to  $\gamma = -1$  is  $c = -2$ .

## Critical behaviour of spanning forests on flat lattice

The critical values of the fugacity can be understood in light of what is known in the literature about spanning forests on fixed graphs. The correspondence established in [17] permitted the authors to derive the continuum limit of spanning forests on flat lattices from the renormalization group analysis of the  $\mathcal{O}(n)$   $\sigma$ -model. The beta function of the  $\mathcal{O}(n)$   $\sigma$ -model is such that this model is *asymptotically free* for  $N > 2$ , that is, at small distances the coupling constant  $u$  becomes small, and it grows at large distances, and the point of zero coupling  $u = 0$  is an ultraviolet-stable fixed point. However if  $N < 2$  the model can be again asymptotically free if we approach  $u = 0$  from the region where the coupling is negative, and  $u = 0$  is still an ultraviolet-stable fixed point. Then, the identification of spanning forests with the  $\mathcal{O}(n)$   $\sigma$ -model allows to conclude that at least perturbatively, spanning forests are asymptotically free. Further, since the fugacity of the trees  $t$  is minus the coupling of the  $\mathcal{O}(n)$   $\sigma$ -model, spanning forests do not possess any critical point in the region  $t > 0$  and the model is attracted to the trivial infinite temperature fixed point at  $t = +\infty$  that corresponds to a massive theory. If instead we are in the region  $t_c < t < 0$ , we are attracted to the spanning trees point  $t = 0$  with  $c = -2$  described by free fermions. This phase is massless and has  $c = -2$ , while for  $t < t_c$  the model is again massive.

Other insights into the critical behaviour can be derived from the analysis of the Potts model in the limit  $q \rightarrow 0$ , with  $w = v/q$  fixed, where  $v$  is the uniform weight of edges. For the square lattice, the ferromagnetic and antiferromagnetic critical curves where Baxter solved the model [48], define near the point  $(q, v) = (0, 0)$  two regions corresponding to a high temperature non-critical phase and a massless low temperature phase with central charge  $c = -2$ . The phase diagram of the Potts model according to [49] is depicted in figure 4.4 where we enlarge the region near the origin and highlight the critical behaviour. This is consistent with our previous discussion of spanning forests derived from the  $\mathcal{O}(n)$   $\sigma$ -model since the slope of the curves  $w = v/q$  corresponds to the inverse of the fugacity of the trees  $t$ , if in the fermionic model we assign a weight 1 to edges (formula (B.12)). In particular we can fix  $t_c$ , interpreted as the  $q \rightarrow 0$  limit on the antiferromagnetic critical curve, to  $t_c = -4$ . This point corresponds to a critical theory with  $c = -1$  [50, 51].

On the triangular lattice the picture is similar, but the ferromagnetic curve is not known exactly. There is numerical evidence [49] that the massless universal phase with  $c = -2$  is still present but the value of  $t_c$  is different from the square lattice result and it appears to be difficult to detect if the critical behaviour at  $t_c$  changes.

Asymptotic freedom of spanning forests is a characteristic pertaining only to 2D. It has been shown numerically in three, four and five dimensions in the  $q \rightarrow 0$  limit of Potts model [52] and analytically in infinite dimension (complete graph case) [53], that there is a finite nonzero critical value  $t^*$  at which a *percolation* transition can occur. This means that for  $t < t^*$  emerges a gigantic component, a tree which occupies a fraction of order one of the volume of the forest, while for  $t > t^*$  all trees have a characteristic size depending on  $t$ . In 2D asymptotic freedom should emerge because  $t^*$  coincides with the criticality of trees,  $t = 0$ .

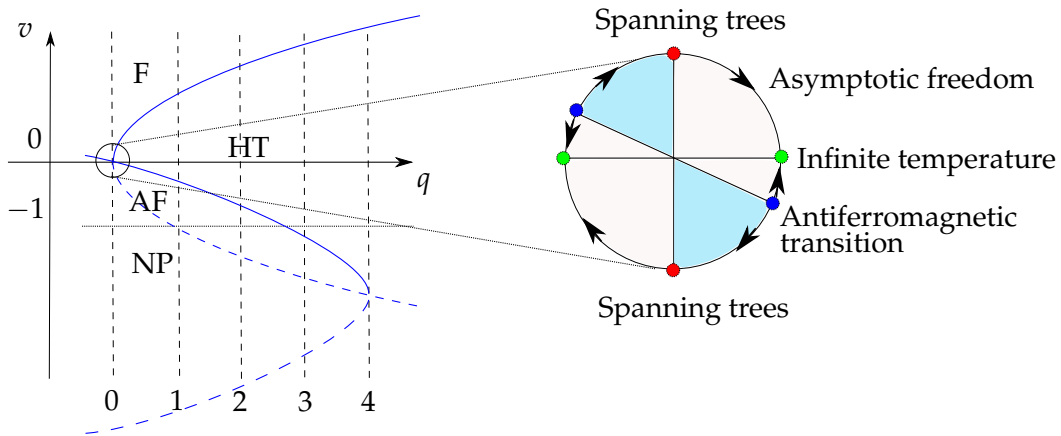


Figure 4.4: The phase diagram of the Potts model on the square lattice. There are four regions, corresponding to a ferromagnetic phase (F), a high temperature phase (HT), an antiferromagnetic phase (AF), and a non physical region (NP) where  $v < -1$ . The blue solid curve are the ferromagnetic and antiferromagnetic transition curves of the Baxter solution. We enlarge the phase diagram near the origin related to spanning forests. The two regions corresponding to a high temperature phase and a massless low temperature phase, are colored respectively in light red and light blue. Note that there are not critical points between  $w = +\infty$  (spanning trees,  $c = -2$ ) and  $w = -1/4$  (antiferromagnetic transition,  $c = -1$ ), beside the trivial point  $w = 0$ , thus confirming asymptotic freedom. The point  $v = e^K - 1 = 0$  ( $w = 0$ ) is the infinite temperature point, and the arrows determine the stability of critical points according to the renormalization group analysis of the  $\mathcal{O}(n)$   $\sigma$ -model.

$t = 0$

Our results obtained on random planar graphs predict no critical points in the region  $t > 0$ , coherently with asymptotic freedom, and state that the spanning trees limit  $t = 0$  is described on flat lattices by a central charge  $c = -2$ , in agreement with what obtained directly on flat lattices. Moreover we have also agreement with the solution of the Potts model on random graphs by Eynard and Bonnet [42], that predicts for  $q = 0$ ,  $\gamma = -1$ .

$t = -1$

The critical point  $t = -1$  instead is harder to interpret. The presence of another point with  $c = -2$  at a negative value of the fugacity, could be related to  $t_c$  on flat lattice and so to the antiferromagnetic critical line of the Potts model. But, if the critical point  $t = 0$  is an universal feature for spanning forests on flat lattices, as already mentioned the antiferromagnetic curve is lattice-dependent and its critical behaviour is understood only for the square lattice. We could then speculate that  $t = -1$  is indeed the critical value corresponding to the transition from high to low temperature in the Potts model with  $q \rightarrow 0$  on the triangular lattice, also if on the square lattice it corresponds to  $c = -1$ .

A computation that could help us in interpreting the presence of  $t = -1$  is solving the integral (4.25) for random graphs with coordination  $k = 4$ . In that case we could check the consistency with the prevision for the square lattice, in particular with the presence of a critical point with  $c = -1$  at a negative value of  $t$ . Unfortunately this computation is not as immediate as the one for the cubic graphs, since we have to deal with a saddle point equation that cannot be directly solved using the results for the  $\mathcal{O}(-2)$  loop-gas model, where the loops are built from cubic vertices, and so deserves a more complicated treatment.

We note also that a central charge  $c = -1$  corresponds, via KPZ, to a the unnatural value of the string susceptibility  $\gamma = -(1 + \sqrt{13})/6$ , when for every minimal models  $(p, q)$ ,  $p > q$ , the string susceptibility is rational,  $\gamma = 1 - p/q$ .

Lastly we remark that at the point  $t = -1$  the partition function of spanning forests (4.3) has a non positive definite Boltzmann weight. However we can still give to this point a probabilistic interpretation in the sense of a positive weight of configurations if we describe the partition function (4.3) no more in terms of spanning forests, but as a sum over spanning trees weighted according to their activities. This form of the partition function is discussed in section B.2 where we introduced also the new notion of activity due to Bernardi that is natural for embedded graphs, and then for random planar graphs. We recall here the formula for the partition function of spanning forests in terms of activities (B.18):

$$Z_G^{\text{forest}}(t, 1) = t \sum_{T \prec G} (1 + t)^{\mathcal{I}(T)}$$

where  $\mathcal{I}(T)$  is the number of internal embedding-active edges. Given a rooted embedding of  $G$  and a spanning tree  $T$  over it, starting from the root draw a line that walks around the tree and label the edges in order according to their appearance. Then an

internal (resp. external) edge is an internal (resp. external) embedding-active edge if minimal in its fundamental cocycle (resp. cycle). This partition function is probabilistic for  $t \in [-1, +\infty)$ , and at the special point  $t = -1$  is given by the number of spanning trees over the graph  $G$  that possess no internal embedding-active edges. A rooted graph with a spanning tree that have no internal embedding-active edge must have at least one external embedding-active edge in the fundamental cocycle of every internal edge. In terms of random planar graphs, the partition function of spanning forests at  $t = -1$  is obtained by considering the ensemble of graphs and spanning trees that satisfies  $\mathcal{I}(T) = 0$ , as the one in figure 4.5.2.

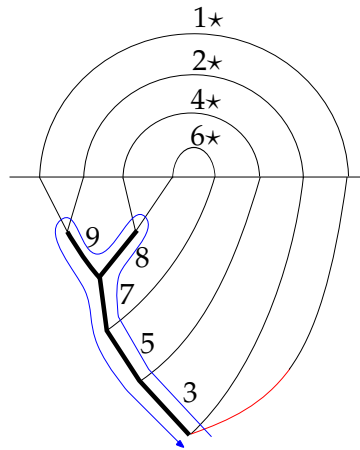


Figure 4.5: A rooted cubic random planar graph with 6 vertices and a spanning tree over it that has no internal embedding-active edges and then contributes to the partition function of spanning forests on random planar graphs at  $t = -1$ . External embedded-active edges are marked with a star. The blue line starting at the root (red half-edge) is the walk that defines the ordering and consequently the activity.

Then our random matrix solution of the spanning forests model predicts that this point is critical and corresponds to a CFT of central charge  $c = -2$ .

## Chapter 5

# Exploring the universality class

$$\gamma = -1$$

In chapter 4 we explained how to study spanning forests on random lattices representing the partition function as a matrix integral and we obtained that spanning trees corresponds to a criticality described by the exponent  $\gamma = -1$ . In this chapter we will solve spanning trees on random planar graphs by a direct enumeration of the possible configurations, following what is done in [21]. This approach is simple and efficient and can be applied to other statistical models. Indeed slight modifications of the procedure outlined in section 5.1 for spanning trees will give us the possibility of exhibit the exact solutions of spanning hypertrees and Hamiltonian cycles. These models share the feature to possess  $\gamma = -1$  and this approach allows us to explore this universality class. The study of spanning hypertrees and Hamiltonian cycles is the original work we describe in this chapter.

### 5.1 Spanning trees on random planar graphs

We start by considering spanning trees, whose partition function  $Z_0^{\text{tree}}(g, N)$  corresponds to the limit  $t \rightarrow 0$  of the one for spanning forests  $Z(t, g, N)$  defined in equation (4.10). If we restrict to the ensemble of random planar graphs ( $N \rightarrow \infty$ ), it is

$$Z_0^{\text{tree}}(g) = \lim_{N \rightarrow \infty} \lim_{t \rightarrow 0} \frac{Z(t, g, N)}{t} \quad (5.1)$$

and from (4.10):

$$Z_0^{\text{tree}}(g) = \sum_{\mathcal{T}} g^{V(\mathcal{T})} \sum_{\mathcal{G} \supset \mathcal{T}} \frac{1}{|\text{Aut}(\mathcal{G}/\mathcal{T})|}. \quad (5.2)$$

The first sum is over trees  $\mathcal{T}$  of coordination  $k = h + 2$ , the second over connected planar graphs  $\mathcal{G}$  that have  $\mathcal{T}$  as a spanning tree over them. To compute this partition function we actually have a simple task: count all the possible pairs  $(\mathcal{G}, \mathcal{T})$ . This is indeed easy if we apply the idea exposed in section 4.4 of shrinking trees with their



leaves to points. This can be done if we keep track of the shrinking by counting all the possible configurations of a tree with its leaves on a disk, a problem solved by  $A'_{h,n}$  (see section 4.3.2) If we do so, we are left with planar one-vertex graphs with  $(hV + 2)/2$  edges (see picture 5.1), which are enumerated by the Catalan numbers, as shown in section 1.1.1.

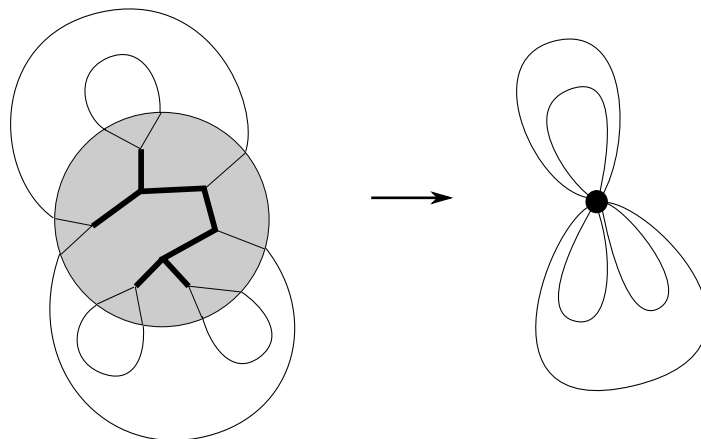


Figure 5.1: On the left a spanning tree (with edges in bold) on a random cubic planar graph. The gray region becomes a point when the tree is shrunk. Then we are left with a planar one-vertex diagram with petals juxtaposed or included into one-another.

In this way 5.2 can then be written as

$$\begin{aligned} Z_0^{\text{tree}}(g) &= \sum_{V>0} A'_{h,V} C_{\frac{hV+2}{2}} g^V \\ &= \sum_{V>0} \frac{((h+1)V)!}{V!(\frac{1}{2}hV+1)!(\frac{1}{2}hV+2)!} g^V. \end{aligned} \quad (5.3)$$

Notice that using  $A'_{h,V}$  we are considering the cyclic symmetry of the  $hV + 2$  legs of the tree and correctly reproducing the inverse of the order of the automorphism group as a weight for the configurations. The sum over  $V$  is intended over the values such that the ensemble of trees with  $V$  vertices and coordination  $k$  is not empty. So, if the coordination is odd the sum is over even number of vertices, while if it is even, every integer value of  $V$  has to be considered.

### 5.1.1 Critical coupling and string susceptibility exponent

If we fix  $h$  the sum 5.3 is a Hypergeometric function  ${}_pF_q$  of the type  $p = q + 1$ <sup>1</sup> and from its argument we can identify the critical coupling  $g_c$ .

<sup>1</sup>A hypergeometric function  ${}_pF_q(a_1, \dots, a_p; b_1, \dots, b_q; x)$  is a function that can be defined from a hypergeometric series, that is a series  $\sum_{n=0}^{\infty} c_n x^n$  for which the ratio of successive terms can be written as

$$\frac{c_{n+1}}{c_n} = \frac{(n+a_1)(n+a_2)\cdots(n+a_p)}{(n+b_1)(n+b_2)\cdots(n+b_q)(n+1)}.$$

Anyway a large volume limit is sufficient to obtain the critical value of the coupling and the string susceptibility exponent, as can be read from equation (2.30). Distinguishing the case of  $h$  odd and even, we can approximate equation 5.3 using Stirling formula on the summand:

$$Z_{0,\text{even}}^{\text{tree}}(g) \sim \sum_V \left( \frac{g}{g_c} \right)^V V^{-4} \quad (5.4)$$

$$Z_{0,\text{odd}}^{\text{tree}}(g) \sim \sum_V \left( \frac{g}{g_c} \right)^{2V} V^{-4}. \quad (5.5)$$

The critical value of the coupling

$$g_c = 2^{-h} \frac{h^h}{(h+1)^{h+1}}, \quad (5.6)$$

and the string susceptibility exponent  $\gamma = -1$  are as expected universal.

Here we have directly showed that spanning trees correspond to a critical theory that is mapped through the KPZ relation to a CFT with  $c = -2$ , in agreement with the discussion pursued in section 4.5.2.

We can analyze further the critical structure of the partition function if we sum the large limit approximation and look at the result that we obtain. For fixing ideas choose  $h = 1$ , then parametrizing  $g/g_c = e^{-\epsilon}$  and keeping the constant factors, in the thermodynamic limit we have to perform the following sum:

$$Z_0^{\text{tree}}(g) = c_1 \sum_{n \geq 1} e^{-2n\epsilon} n^{-4} \quad (5.7)$$

where  $c_1 = \sqrt{2}/(2\pi)$ . The sum is a polylogarithmic function, and if we expand (5.7) in  $\epsilon$ , we get

$$\frac{Z_0^{\text{tree}}(g)}{c_1} = \left( \frac{8192}{315} - \frac{16\sqrt{2}\pi}{3} \right) + \left( \frac{14848}{315} - \frac{32\sqrt{2}\pi}{3} \right) \epsilon + \dots + \frac{4}{3} \epsilon^3 \log \epsilon + \dots \quad (5.8)$$

This expansion is affected by the large volume approximation that we used, but nonetheless it has the correct dependence on the non-analytic term  $\frac{4}{3} \epsilon^3 \log \epsilon$ , as can be checked from the direct expansion of the Hypergeometric function that corresponds to the exact sum of the partition function. This is consistent with the fact that the critical behaviour can be studied in the thermodynamic limit.

## 5.2 Spanning hypertrees on random planar hypergraphs

Having shown how to deal with spanning trees on random planar lattices, it is a natural generalization to turn our attention to studying spanning hypertrees on random planar hypergraphs.

---

Note that when  $p = q + 1$  the ratio  $c_{n+1}/c_n \rightarrow 1$  so in this case the radius of convergence of the series is 1.

Studying the ensemble of spanning hypertrees is particularly interesting because no matrix integral can generate it and so random matrix techniques are not applicable. It will turn out that  $\gamma = -1$ , then they are in the same universality class of spanning trees, as one could expect. We start with the definition of hypergraphs.

A hypergraph  $\mathcal{K} = (V, E)$  is defined by its vertex set  $V$  and the set of hyperedges  $E$  which consists of subsets of  $V$  of cardinality at least 2. A sub-hypergraph  $\mathcal{H} \subseteq \mathcal{K}$  has  $V(\mathcal{H}) \subseteq V(\mathcal{K})$  and  $E(\mathcal{H}) \subseteq E(\mathcal{K})$ , and is spanning if  $V(\mathcal{H}) = V(\mathcal{K})$ .  $\mathcal{H}$  is a hypertree if it is connected and there are no cyclic sequences of vertices and hyperedges

$$v_1, e_1, v_2, e_2, \dots, v_\ell, e_\ell, v_{\ell+1} \quad (v_{\ell+1} = v_1)$$

such that  $\ell \geq 2$ ,  $v_i \neq v_{i+1}$  and  $v_i, v_{i+1} \in e_i$ .

For embedding a hypergraph in a Riemann surface  $\mathbb{S}$ , we first consider a bipartite graph  $G = (V \cup V_E, L)$  on  $\mathbb{S}$ .  $G$  can be seen as an incidence graph of a hypergraph if for each  $v_e \in V_E$  we merge  $v_e$  and its incident edges into a hyperedge  $e$  with  $v_e$  as its center. Calling  $E$  the set of hyperedges, a hypergraph on  $\mathbb{S}$  is  $\mathcal{K} = (V, E)$ . In this way the notions of 2-dimensional cell complexes are extended to hypergraphs and the genus of a hypergraph is well defined.

In the following we will consider connected planar hypergraphs with fixed coordination of vertices  $k$  and  $l$ -uniform, that is with all hyperedges of cardinality  $l$ . The case  $l = 2$  corresponds to ordinary graphs. Inspired by (5.2), we define the partition function for spanning hypertrees  $\mathcal{H}$  over hypergraphs  $\mathcal{K}$  as:

$$Z^{\text{h-tree}}(g) = \sum_{\mathcal{H}} g^{V(\mathcal{H})} \sum_{\mathcal{K} \supseteq \mathcal{H}} \frac{1}{|\text{Aut}(\mathcal{K}/\mathcal{H})|}. \quad (5.9)$$

See figure 5.2 for an example of a spanning hypertree over a random planar hypergraph.

As before, we want to shrink hypertrees and count the remaining configurations. To do this, we first have to do some preliminary combinatorics.

### 5.2.1 Two combinatorial results for spanning hypertrees

In this section we will solve two counting problems. First we count the number of hyperlink patterns and then the number of hypertrees with border legs on the boundary of the upper half plane. As in 4.3 we call  $\mathbb{H}$  the upper half plane and  $\partial\mathbb{H}$  its boundary.

#### Counting hyperlink patterns

Define a  $l$ -hyperarc as a generalization of an arc, where its  $l$  endpoints on  $\partial\mathbb{H}$  are joined together with a hyperedge of cardinality  $l$ . An arc is a 2-hyperarc. Now we will count the configurations of  $m$  non-intersecting  $l$ -hyperarcs in  $\mathbb{H}$ , with endpoints in  $\partial\mathbb{H}$ . Call such configurations hyperlink patterns (for a typical hyperlink pattern, see top of figure 5.3) and their number  $C_{l,m}$ . This section has the purpose of generalizing the enumeration of link patterns and Catalan numbers that correspond to the case of graphs,  $l = 2$ .

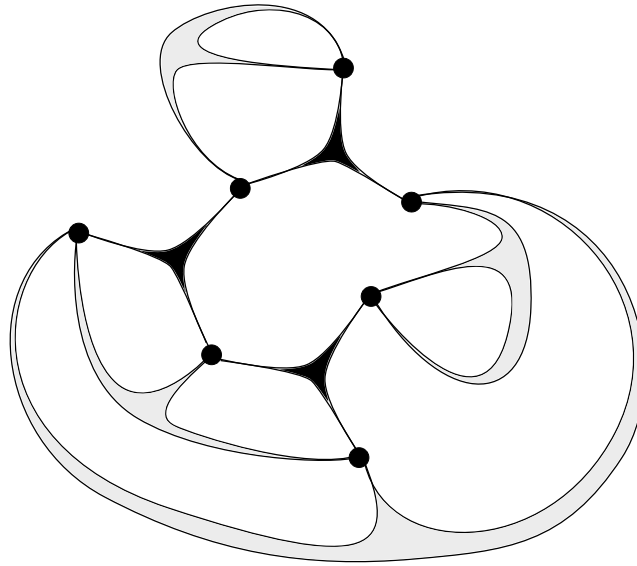


Figure 5.2: A spanning hypertree on a 3-uniform cubic random hypergraph. Hyperedges of the spanning tree are in black.

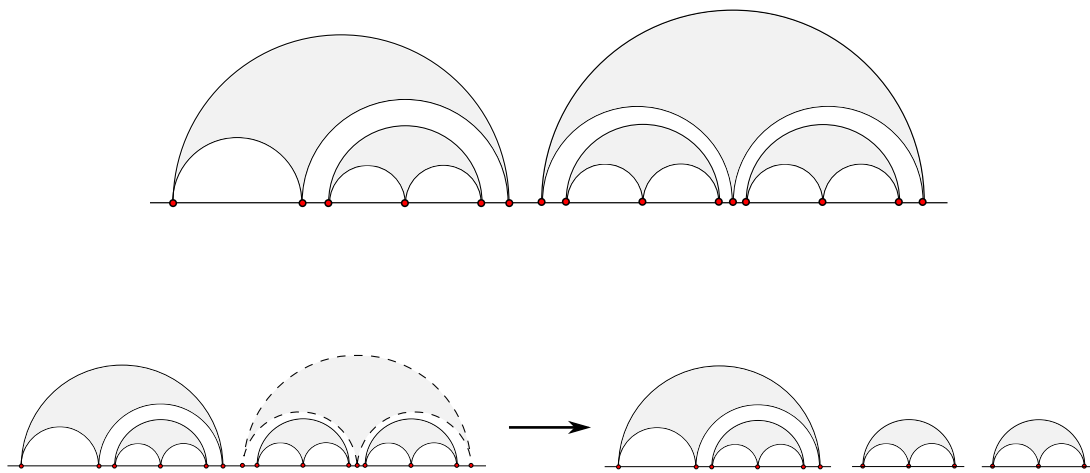


Figure 5.3: On top a hyperlink pattern with  $m = 5$  3-hyperarcs. On bottom the removal procedure of the rightmost hyperarc that leaves  $l = 3$  remaining component.

Given a configuration, upon removing the right-most hyperarc, we are left with  $l$  remaining components as at the bottom of figure 5.3, and we have the familiar convolutional relation:

$$C_{l,m} = \sum_{m_1, \dots, m_l} \prod_{\alpha=1}^l C_{l, m_\alpha} \quad (5.10)$$

where the  $m_\alpha$ 's satisfies  $m_1 + \dots + m_l = m - 1$ .

This is exactly the same problem of counting trees of coordination  $l + 1$  with border legs on  $\partial\mathbb{H}$  solved in 4.3.1. So once again we introduce the generating function  $C_l(x) = \sum_m C_{l,m} x^m$  and relation (5.10) turns into the non linear equation  $C_l(x) = 1 + x(C_l(x))^l$  leading us to the hyper-Catalan numbers:

$$C_{l,m} = \frac{1}{(l-1)m+1} \binom{lm}{m}. \quad (5.11)$$

### Counting non-intersecting hypertrees with leaves in $\partial\mathbb{H}$

Now we turn our attention to the enumeration of the configurations of non-intersecting  $l$ -uniform hypertrees of degree  $k$ , with leaves in  $\partial\mathbb{H}$ .

Define the generating function  $F_{k,l}(z)$ :

$$F_{k,l}(z) = \sum_{m>0} \sum_{\sigma(m)} z^m \quad (5.12)$$

where  $\sigma(m)$  are the configurations of non-intersecting  $l$ -uniform hypertrees of degree  $k$ , with  $m$  border legs rooted (we distinguish the rightmost leg) on  $\partial\mathbb{H}$  (see top of figure 5.4). The coefficients of  $z^m$  are the number we want to compute.

Next, define an auxiliary generating function

$$F_{k,l}^*(z) = \sum_{m>0} \sum_{\sigma'(m)} z^m \quad (5.13)$$

where  $\sigma'(m)$  are the configurations of hypertrees which in addition to  $m$  border legs rooted on  $\partial\mathbb{H}$  have a vertex as the rightmost point on the boundary of the plane (see bottom of figure 5.4). While the sum in (5.12) contains the configurations with no hyperedges, of course the one in (5.13) does not.

$F_{k,l}(z)$  satisfies the following equation:

$$F_{k,l}(z) = z(z + F_{k,l}^*(z))^{k-1}. \quad (5.14)$$

Indeed, given a configuration in  $F_{k,l}(z)$ , associate a factor  $z$  to the rightmost leg and this account for the first factor  $z$  on the r.h.s. of (5.14). Then, the remaining  $k - 1$  objects attached to the vertex of the rightmost leg can be a border leg or part of a hyperedge, and this choice brings the term  $(z + F_{k,l}^*(z))^{k-1}$ . This is illustrated at the top of figure (5.5).

Instead, if we start from a configuration in  $F_{k,l}^*(z)$ , we can remove the hyperedge containing the rightmost vertex and attach a border leg to the  $l - 1$  vertices pertaining

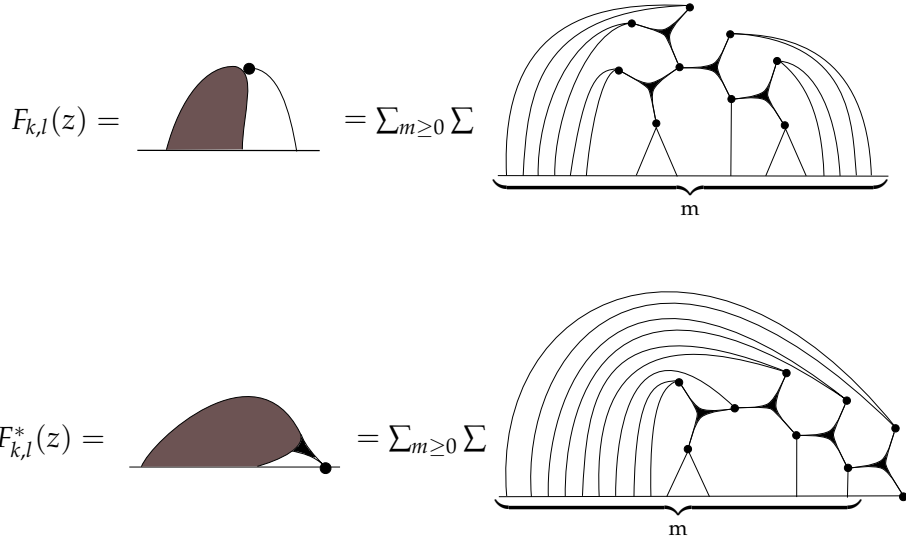


Figure 5.4: On top the generating function  $F_{k,l}(z)$ . It is a sum over  $m$  of the configurations of hypertrees with  $m$  border legs rooted on  $\partial\mathbb{H}$ . On bottom the auxiliary generating function  $F_{k,l}^*(z)$ . Here the sum is over configurations constrained to have a vertex as the rightmost point in  $\partial\mathbb{H}$ .

to this hyperedge. This brings a corrective term  $1/z$  for every leg that was not rooted and the equation satisfied by  $F_{k,l}^*(z)$  is:

$$F_{k,l}^*(z) = \left(\frac{1}{z}\right)^{l-1} F_{k,l}(z)^{l-1}. \quad (5.15)$$

The graphical explanation is given at the bottom of figure 5.5.

Putting together these two relations, we obtain:

$$\frac{F_{k,l}(z)}{z^k} = \left(1 + z^{l(k-1)-k} \left(\frac{F_{k,l}(z)}{z^k}\right)^{l-1}\right)^{k-1}. \quad (5.16)$$

Calling  $n$  the number of hyperedges in a hypertree, the number of border legs in terms on  $n$  is  $k + n(l(k-1) - k)$ , so not every monomial appears in (5.12):

$$F_{k,l}(z) = \sum_{n > 0} \sum_{\sigma(k+n(l(k-1)-k))} z^{k+n(l(k-1)-k)}. \quad (5.17)$$

It is then natural to consider

$$f^{(k,l)}(x) = \frac{F_{k,l}(z)}{z^k} \Big|_{x=z^{l(k-1)-k}} = \sum_{n \geq 0} f_n^{(k,l)} x^n \quad (5.18)$$

so that  $f_n^{(k,l)}$  coincides exactly with the number we want to compute. Expressing (5.16) in terms of  $f^{(k,l)}(x)$  we have to solve the following non linear equation

$$f^{(k,l)}(x) = (1 + x(f^{(k,l)}(x))^{l-1})^{k-1}. \quad (5.19)$$

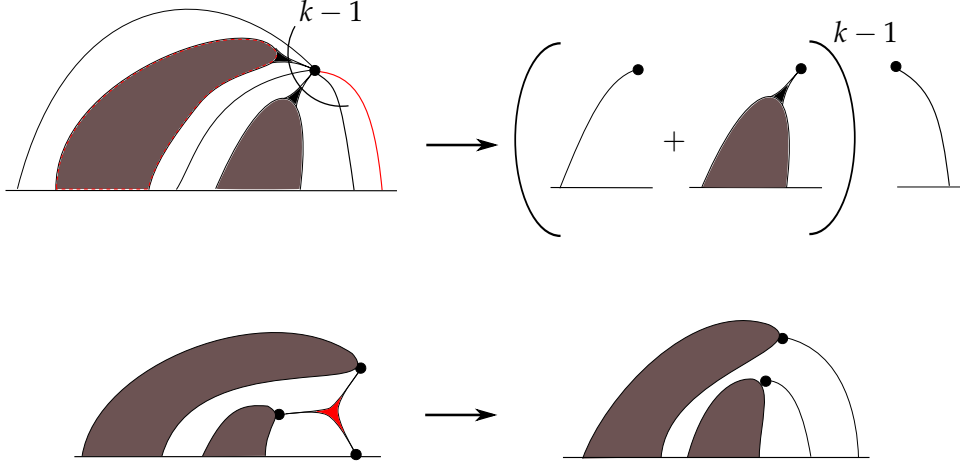


Figure 5.5: On top the graphical explanation of equation (5.14). The  $k - 1$  objects attached to the vertex of the rightmost leg (in red) can be part of a hyperedge or a border leg. This binary choice produces the factor  $(z + F_{k,l}^*(z))^{k-1}$  on the right hand side of the equation. On bottom the illustration of equation (5.15). We remove the hyperedge (in red) containing the rightmost vertex and substitute the hyperedge with  $l - 1$  border legs (here  $l = 3$ ). This operation brings the term  $1/z$  for every leg that was not rooted.

The values of  $f_n^{(k,l)}$  that solve (5.19) are

$$f_n^{(k,l)} = \frac{((k-1)(l-1)n + k - 2)!(k-1)}{n!((k-1)(l-1)n + k - n - 1)!}, \quad (5.20)$$

and before demonstrating that it is the solution, we can easily check the agreement with already known results that appear as particular cases.  $f_n^{(k,l)}$  reduces to the enumeration of trees with coordination  $k$  if  $l = 2$ . To make contact with our previous results, define  $k = h + 2$ . We have:

$$f_n^{(h+2,2)} = \frac{((h+1)n + h)!(h+1)}{n!((h+1)(n+1) - n)!} \quad (5.21)$$

that expressed in terms of the number of vertices  $V = n + 1$  coincides with the generalized Catalan number  $A_{h,n}$  discussed in section 4.3.1, the properly combinatorial factor to count non-intersecting trees with border legs on the plane. The series of factorial  $k = 2$  instead is the enumeration of hypertrees with vertices of coordination 2. The dual of a hypergraph is simply obtained by swapping the roles of hyperedges and vertices, and the dual of a  $l$ -uniform hypertree with coordination 2 is a tree with vertices of coordination  $l$ . Correctly we have

$$f_n^{(2,l)} = \frac{1}{(l-2)n + 1} \binom{(l-1)n}{n}. \quad (5.22)$$

Now we will prove that  $f^{(k,l)}(x) = \sum_{n \geq 0} f_n^{(k,l)} x^n$  with  $f_n^{(k,l)}$  as in (5.20) satisfies (5.19) by direct substitution. Note that  $f^{(k+1,l+1)}(x)$  depends on  $l$  only through the product  $kl = s$ . So we introduce  $\tilde{f}^{((k-1)(l-1),k-1)}(x)$  as a synonym of  $f^{(k,l)}(x)$ , that is

$$\tilde{f}^{(s,k)}(x) = \sum_{n \geq 0} \tilde{f}_n^{(s,k)} x^n = \sum_{n \geq 0} \frac{(sn+k-1)!k}{n!(sn+k-n)!} x^n \quad (5.23)$$

and (5.19) turns into

$$\tilde{f}^{(s,k)}(x) = (1 + x(\tilde{f}^{(s,k)}(x))^{s/k})^k. \quad (5.24)$$

In this form the problem is easier. We recognize that  $\tilde{f}^{(s,k)}(x) = (B_s(x))^k$ , where  $B_s(x)$  is the generalized binomial series

$$B_s(x) = \sum_{n \geq 0} \binom{sn+1}{n} \frac{1}{sn+1} x^n, \quad (5.25)$$

and  $B_s(x)$  has the remarkable property that

$$(B_s(x))^k = \sum_{n \geq 0} \binom{sn+k}{n} \frac{k}{sn+k} x^n. \quad (5.26)$$

For a proof see chapter 7 of [54]. Thus  $\tilde{f}^{(s,k)}(x) = \tilde{f}^{(s,h)}(x)\tilde{f}^{(s,k-h)}(x)$  and in particular  $(\tilde{f}^{(s,k)}(x))^{1/k} = \tilde{f}^{(s,1)}(x)$ . Thanks to this property, equation (5.24) for generic  $s$  and  $k$  is equivalent to its specialization  $k = 1$ :

$$\tilde{f}^{(s,1)}(x) = 1 + x(\tilde{f}^{(s,1)}(x))^s. \quad (5.27)$$

There are now two ways to conclude. Either we recognize that  $\tilde{f}^{(s,1)}(x) = f^{(2s+1)}(x)$ , that is, the ‘‘hyper-Catalan’’ numbers of equation (5.22), which we already know solving equation (5.27). Alternatively, remark that from the explicit expression for  $\tilde{f}_n^{(s,k)}$  we have  $\tilde{f}_{n+1}^{(s,1)} = \tilde{f}_n^{(s,s)}$ . With this relation, equation (5.27) reduces to an identity. In either ways, we have proved that (5.20) is the expression for the number of  $l$ -hypertrees of degree  $k$  with border legs on the boundary of the upper plane.

## 5.2.2 Computation of the partition function and critical behaviour

With the combinatorial results of section 5.2.1, we know how to keep track of the shrinking of the hypertrees and how to count the hyperlink patterns left after the shrinking. An example of the shrinking procedure and the resulting one-vertex planar hypergraph is depicted in figure 5.6.

The partition function (5.9) then is:

$$Z^{\text{h-tree}}(g) = \sum_{n \geq 0} g^{n(l-1)+1} \frac{f_n^{(k,l)}}{k+n(l(k-1)-k)} C_{l, \frac{k+n(l(k-1)-k)}{l}}. \quad (5.28)$$



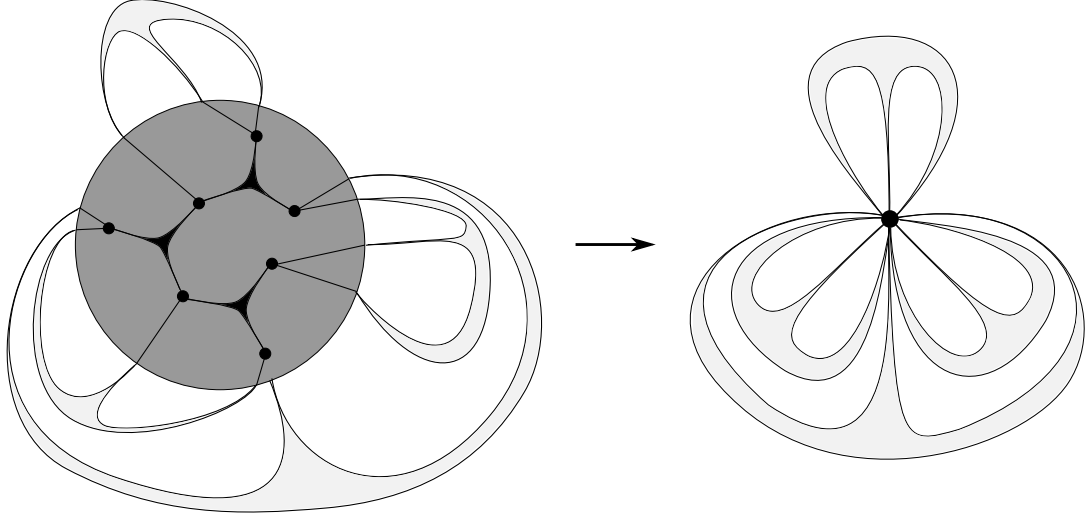


Figure 5.6: The shrinking procedure and the resulting one-vertex planar hypergraph. In dark gray the region to be shrunk.

The factor  $k + n(l(k-1) - k)$  at the denominator is introduced for accounting for the cyclic symmetry of the border legs of the hypertree on a disk and  $n(l-1) + 1$  is the number of vertices of the hypergraph.

The sum in (5.28) is restricted to  $n$  such that  $k + n(l(k-1) - k)$  is a multiple of  $l$ , or equivalently

$$n(k-1) + k/l(1-n) \in \mathbb{Z}_+,$$

since otherwise the legs of the hypertree cannot be contracted together to form hyperlink patterns, and the ensemble is empty. We first notice that  $n = 0$  can be achieved only if  $k/l$  is integer, and this respects the fact that we can contract together the legs attached to a single vertex only if the number of legs is a multiple of  $l$ . Then the allowed values of  $n$  can be parametrized as

$$n = \beta(i-1) + 1, \quad \begin{cases} i = 0, 1, 2, 3, \dots & \text{if } \beta = 1 \\ i = 1, 2, 3, \dots & \text{otherwise} \end{cases} \quad (5.29)$$

where  $\beta = l / \gcd(k, l)$ , the denominator of  $k/l$ . Trading the sum over  $n$  for the sum over  $i$  with the convention of equation (5.29) for the values of  $i$ , (5.28) becomes:

$$Z^{\text{h-tree}}(g) = \sum_i g^{(\beta(i-1)+1)(l-1)+1} \frac{f_{\beta(i-1)+1}^{(k,l)}}{k + (\beta(i-1) + 1)(l(k-1) - k)} \cdot C_{l, k+(\beta(i-1)+1)(l(k-1)-k)} \quad (5.30)$$

As in the case of spanning trees, for a given value of  $k$  and  $l$  this sum organizes into a hypergeometric series  ${}_pF_q$  with  $p = q + 1$  and from the argument of this function, we read the radius of convergence.

We checked that formula (5.30) reduces to the partition function of spanning trees (5.3) for  $l = 2$ , and the cases  $\beta = 1$ ,  $\beta \neq 1$  corresponds respectively to  $k$  even and odd.

As above, we compute the critical coupling and the string susceptibility exponent in the thermodynamic limit of large  $n$ .  $C_{l,m}$  and  $f_n^{(k,l)}$  have the following asymptotic:

$$C_{l,m} \sim \left( \frac{l^l}{(l-1)^{l-1}} \right)^m m^{-3/2} \sqrt{\frac{l}{2\pi(l-1)^3}} \quad (5.31)$$

$$f_n^{(k,l)} \sim \left( \frac{(k-1)(l-1)^{(k-1)(l-1)}}{((k-1)(l-1)-1)^{(k-1)(l-1)-1}} \right)^n n^{-5/2} \frac{(k-1)((k-1)(l-1))^{k-3/2}}{((k-1)(l-1)-1)^{k-1/2}(l(k-1)-k)}. \quad (5.32)$$

If  $n$  is large we can sum the asymptotic of the summand in (5.28) over  $n$  without restrictions. Omitting irrelevant numerical factors we end with:

$$Z^{\text{h-tree}}(g) \sim \sum_n \left( \frac{g}{g_c} \right)^{(l-1)n} n^{-4}. \quad (5.33)$$

where the critical coupling is

$$g_c = \frac{(l-1)^{(l(k-1)-k)/l}}{((k-1)(l-1))^{k-1}} \left( \frac{((k-1)(l-1)-1)^{(k-1)(l-1)-1}}{l^{l(k-1)-k}} \right)^{\frac{1}{l-1}}. \quad (5.34)$$

From (5.33) we get that spanning hypertrees on random hypergraphs have a critical exponent  $\gamma = -1$ , so being in the same universality class of spanning trees.

### 5.3 Hamiltonian cycles

A Hamiltonian cycle through a graph is a cycle that visits each node exactly once. In this section we will consider the statistical model of Hamiltonian cycles over random planar graphs.

Using the prescription of random matrix theory, we define the partition function for this model as:

$$Z_{\text{HC}}(g) = \sum_{\mathcal{G}} g^{V(\mathcal{G})} \frac{1}{|\text{Aut}(\mathcal{G})|} \sum_{\mathcal{H} \in \mathfrak{H}(\mathcal{G})} \quad (5.35)$$

where  $\mathcal{G}$  is the ensemble of cubic planar graphs and  $\mathfrak{H}(\mathcal{G})$  is the set of Hamiltonian cycles over  $\mathcal{G}$ . According to our purposes, the important remark is that a Hamiltonian cycle, being a cycle, divides a planar graph in two components, an inner and an outer one. This is done in such a way that a planar graph that admits a Hamiltonian cycle is nothing but the intertwining of two link patterns, one in the region enclosed by the space-filling cycle, and one out of it (see figure 5.7).

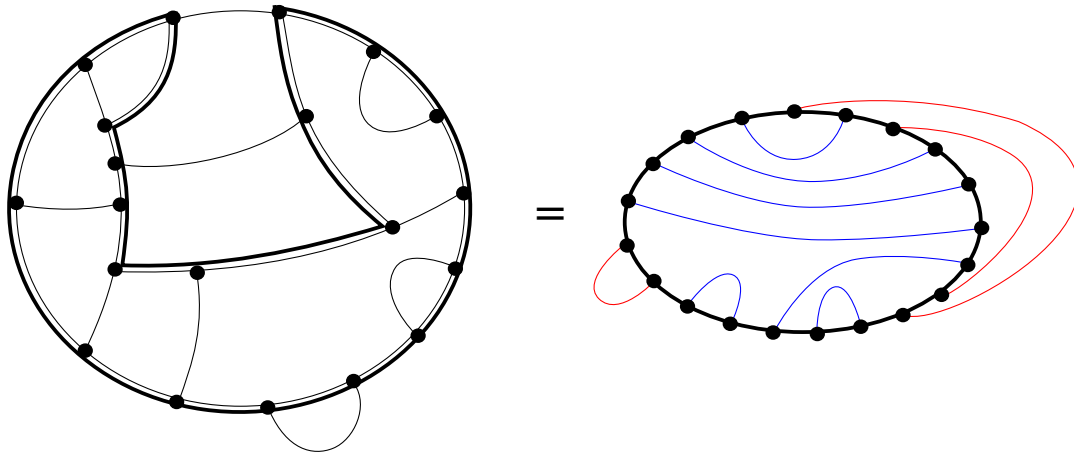


Figure 5.7: A cubic random planar graph with  $2n = 20$  vertices that possesses a Hamiltonian cycle over it (marked in bold), is equal to two sequences of link patterns defined as the inner (marked in blue) and outer (marked in red) configurations of the cycle.

Remember from section 1.1.1 that the enumeration of link patterns is done by Catalan numbers. Then, calling  $2n$  the number of vertices and  $m$  the number of internal link patterns enclosed by the Hamiltonian cycle, (5.35) can be written as:

$$Z_{\text{HC}}(g) = \sum_{n \geq 0} g^{2n} \sum_{m=0}^n \binom{2n}{2m} \frac{C_m C_{n-m}}{2n}. \quad (5.36)$$

By convention the trivial graph with a single node has one Hamiltonian cycle.  $C_m$  and  $C_{n-m}$  in (5.36) corresponds respectively to the enumeration of all possible configurations in and out of the Hamiltonian cycle, while the binomial coefficient derives from the possibility of choosing the  $2m$  vertices among the total  $2n$  to produce the same link pattern. In the large volume limit, equation (5.36) becomes

$$Z_{\text{HC}}(g) \sim \sum_n \sum_m g^{2n} \frac{(2n-1)!}{m!(m+1)!(n-m)!(n-m+1)!} \quad (5.37)$$

$$= \frac{4}{\sqrt{\pi}} \sum_n (2g^{2n}) \frac{(2n-1)! \Gamma(\frac{1}{2}(3+2n))}{n!(n+1)!(n+2)!} \quad (5.38)$$

Now we perform a Stirling approximation of the factorials and obtain:

$$Z_{\text{HC}}(g) \sim \sum_n (4g)^{2n} n^{-4}, \quad (5.39)$$

from which we read the critical coupling  $g_c$  and the string susceptibility exponent  $\gamma$ :

$$g_c = \frac{1}{4}; \quad \gamma = -1. \quad (5.40)$$

We conclude that this model is in the same universality class of spanning trees.

## 5.4 Discussions

In the present chapter we showed how some statistical models can be easily solved when defined on random planar graphs. Indeed simple combinatorics is all we need to compute exactly their partition function and obtain the critical coupling and the critical exponent  $\gamma$ . First we showed directly that spanning trees have  $\gamma = -1$ , as argued from the random matrix solution of section 4.5.2. Then we found that also spanning hypertrees and Hamiltonian cycles have both  $\gamma = -1$ . Using KPZ relation this value of the string susceptibility is related to a conformal field theory on flat 2D space with a central charge  $c = -2$ . This is an example of how the combined use of tools for studying models on random lattices and the KPZ relation allow to investigate the universality classes on flat space.

The field theory  $c = -2$  is an example of logarithmic CFTs, a CFT with logarithmic singularities in the correlation functions which lead to interesting consequences [55, 56], and is the continuum limit of a lot of discrete models. We have directly shown that spanning hypertrees and Hamiltonian cycles are among those. Other important models on random lattices that can be mapped by KPZ to  $c = -2$ , are dense polymers and the bosonic string in minus two dimensions. Indeed dense polymers are solved on random planar lattices in [27] using a mixture of random matrix and combinatorial techniques, and the authors find coherently with KPZ prediction,  $\gamma = -1$ . The bosonic string embedded in a space with dimension  $d = -2$  possesses  $\gamma = -1$  too [57]. We remark that if the belonging of trees and Hamiltonian cycles to  $c = -2$  is already known<sup>2</sup>, the general result for hypertrees is not, and our computation is an important evidence for their critical behaviour.

We have been able to solve the models presented here with the same combinatorial approach, thanks to some common features shared by these models. The key point in the solution was the possibility of separating an inner and an outer region in a given configuration, in a way that the patterns had cyclic symmetry. For spanning trees and their generalization to hypertrees this division was made by the cycle along the tree, while in Hamiltonian cycles it was made by the space-filling cycle. Then, a model that possesses the feature of having an inner and an outer region, whose configurations are respectively enumerated by  $\psi_{\text{in}}(n)$  and  $\psi_{\text{out}}(n)$ , functions of the size  $n$  of the graph, can be described by

$$Z(g) \simeq \sum_n \frac{\psi_{\text{in}}(n) \psi_{\text{out}}(n)}{n} g^n. \quad (5.41)$$

Further, if both  $\psi_{\text{in}}(n)$  and  $\psi_{\text{out}}(n)$  behave as  $n^{-3/2}$  in the large volume limit, it will be in the universality class of spanning trees.

---

<sup>2</sup>For a discussion on Hamiltonian cycles see [58]

## Chapter 6

# Spanning trees on random lattices of arbitrary genus

The purpose of this chapter is to extend the analysis done for trees on random planar lattices to lattices of arbitrary genus. Considering ensembles of graphs of positive genus in addition to the planar ones arises very naturally in the context of random matrix theory. Indeed we showed in section 1.15 that matrix integrals organize the partition function as a topological expansion, equation (1.18).

After having solved the model on random lattices of arbitrary genera, and exposed a method to visualize the graphs that constitute the leading contribution to the partition function, we will discuss the problem of studying the all-genus partition function for spanning trees, that is the sum over genus of the partition function for fixed genus. The work presented in this chapter is entirely original, and relies on the results about the enumeration of maps presented in chapter 3 and on the methods to simplify the diagrammatics exposed in [21].

### 6.1 Analysis at fixed genus

The extension of the partition function (5.2) for spanning trees on random planar graphs to arbitrary genus  $h$  is simply

$$Z_h^{\text{tree}}(g, N) = \sum_{\mathcal{T}} g^{V(\mathcal{T})} \sum_{\substack{\mathcal{G} \succ_{\mathcal{T}} \\ h(\mathcal{G})=h}} \frac{N^{-2h}}{|\text{Aut}(\mathcal{G}/\mathcal{T})|} \quad (6.1)$$

where  $\mathcal{T}$  is a tree of coordination  $k = h + 2$ , and now  $\mathcal{G}$  are connected graphs of genus  $h$  that have  $\mathcal{T}$  as a spanning tree over them.

This partition function can be computed by means of a combinatorial method similar to the one exposed in section 5.1 for planar lattices. Following the procedure of shrinking as in the planar case, the generalization to arbitrary genus will be simply obtained by replacing  $C_n$  in (5.3) with the number of all possible pairings of the half-edges

of a one-vertex graph respecting the topology of the surface (see figure 6.1). Turning to the dual graph, this corresponds to the number  $\epsilon_{\mathfrak{h}}(n)$  of unicellular maps of genus  $\mathfrak{h}$  introduced in chapter 3.

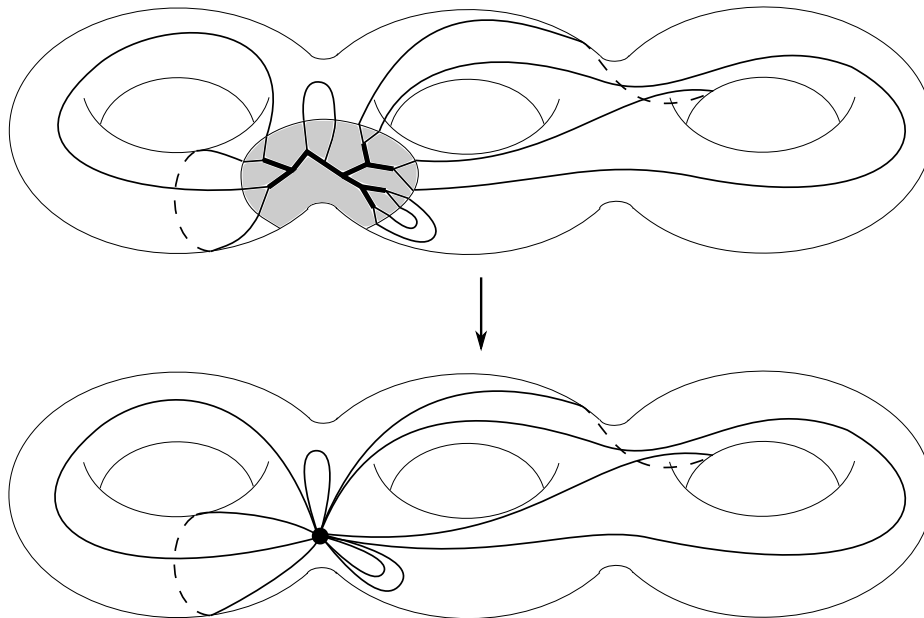


Figure 6.1: A spanning tree over a graph embedded in a surface of genus 3. The gray region encloses the tree with its leaves to be shrunk. After the shrinking we have a one-vertex graph on that surface.

Then equation (6.1) can be written in terms of the number  $n$  of edges of the one-vertex graph  $\mathcal{G}/\mathcal{T}$ , that corresponds to half the number of border legs of the tree in  $\mathcal{G}$ . We have

$$Z_{\mathfrak{h}}^{\text{tree}}(g, N) = \sum_{n>0} A'_{\mathfrak{h}, \frac{2n-2}{\mathfrak{h}}} \epsilon_{\mathfrak{h}}(n) N^{-2\mathfrak{h}} g^{\frac{2n-2}{\mathfrak{h}}}. \quad (6.2)$$

$\epsilon_{\mathfrak{h}}(n)$  can be written as a sum over integer partitions of  $\mathfrak{h}$  that can be evaluated easily for the first values of  $\mathfrak{h}$ , formula (3.21). For example in the case of spanning trees on random graphs embedded in the torus and in the surface with two handles, the partition function results

$$Z_1^{\text{tree}}(g, N) = \frac{(1 - 16g^2)K\left(\frac{16g}{8g+1}\right) - (8g+1)E\left(\frac{16g}{8g+1}\right)}{288\pi g^2 \sqrt{8g+1} N^2} \quad (6.3)$$

$$Z_2^{\text{tree}}(g, N) = \frac{1}{2880\pi g^2 (8g-1)^3 (8g+1)^{5/2} N^4} \left( (102144g^6 - 9276g^4 + 174g^2 - 1) \cdot E\left(\frac{16g}{8g+1}\right) - (8g-1)(6(4480g^4 + 618g^2 - 21)g^2 + 1)K\left(\frac{16g}{8g+1}\right) \right) \quad (6.4)$$

where  $E$  and  $K$  are the complete elliptic integral of the second and of the first kind.

### 6.1.1 Thermodynamic limit

We can easily obtain the thermodynamic limit of (6.2) by approximating the summand with Stirling formula and using the asymptotic of  $\epsilon_{\mathfrak{h}}(n)$ , equation (3.22). We have

$$Z_{\mathfrak{h}}^{\text{tree}}(g, N) \sim \sum_V \left( \frac{g}{g_c} \right)^V V^{-4+3\mathfrak{h}} \quad (6.5)$$

where  $V$  is the area of the graph. The value of the critical coupling  $g_c$  is the same found for spanning trees on planar graphs, equation (5.6). The fact that  $g_c$  does not depend on the topology is coherent with the general behaviour of the partition function. Indeed define  $\gamma_{\text{str}}(\mathfrak{h}) = \gamma + \mathfrak{h}(2 - \gamma)$ , then general results from the continuum Liouville theories of matter models coupled to 2D gravity state that the partition function should behave for non trivial genus as [5]:

$$Z_{\mathfrak{h}} \sim (g_c - g)^{2-\gamma_{\text{str}}(\mathfrak{h})}. \quad (6.6)$$

This implies

$$Z_{\mathfrak{h}} \sim \sum_V V^{-3+\gamma_{\text{str}}(\mathfrak{h})} \left( \frac{g}{g_c} \right)^V. \quad (6.7)$$

Given the value of the string susceptibility computed on random planar graphs, equation (6.7) in our case predicts that the exponent of the volume is  $-4 + 3\mathfrak{h}$ , in agreement with (6.5). This is also consistent with the KPZ relation (4.1) generalized in the case of arbitrary genus [59, 44]:

$$\gamma_{\text{str}}(\mathfrak{h}) = 2 - \frac{1-\mathfrak{h}}{12} \left( 25 - c + \sqrt{(1-c)(25-c)} \right). \quad (6.8)$$

for  $\gamma = -1$  and  $c = -2$ . We can also directly check that for  $\mathfrak{h} = 1, 2$  the explicit expressions (6.3) and (6.4) for  $g$  near  $g_c$  behaves respectively as  $\log(g - g_c)$  and  $(g - g_c)^{-3}$ .

Furthermore our procedure is validated also by comparison with known results for other models related to spanning trees when the topology is not trivial. Indeed, the bosonic string in a space of dimension  $d = -2$  [57], and those for the gravitational  $\mathcal{O}(n = -2)$  loop-gas model [27] are in agreement with our results.

### 6.1.2 Partition function as sum over triangulations

We now present another method to compute the thermodynamic limit of the partition function at fixed genus. This second approach, despite being more complicated, has the advantage of isolating the class of diagrams that contributes to the partition function. The idea underlying the method presented here is that the diagrammatics can be considerably simplified if we omit link patterns and parallel edges in a one-vertex graph. We will now explain how to make these simplifications using the tools to reduce the diagrammatics described in [21].

Given a graph  $\mathcal{G}$  on a surface of genus  $h$  and a spanning tree  $\mathcal{T}$  over it, call  $\mathcal{G}'$  the graph  $\mathcal{G}/\mathcal{T}$  in which we contract the tree.  $\mathcal{G}'$  is a one-vertex graph built with non contractible arcs and link patterns. The former are elements of the non trivial part of the homotopy group based on the vertex, while the latter can be contracted to points. Next remove link patterns from  $\mathcal{G}'$  and call  $\mathcal{G}''$  the resulting graph. Then call  $\mathcal{G}'''$  the graph obtained from  $\mathcal{G}''$  by removing parallel edges (by parallel edges we mean edges with the same winding number and no other non contractible arc in between).

Our task now is to replace the sum over  $\mathcal{G}$  in the partition function of spanning trees with a sum over  $\mathcal{G}'''$ . To explain how to do so, we first introduce a representation of  $Z_h^{\text{tree}}$  as a Cauchy integral. The function  $A_h(z)$ , defined in section 4.3.1 as the generating function of the generalized Catalan numbers  $A_{h,n}$ , is such that the substitution  $z^{-2n} \rightarrow A_{h, \frac{2n-2}{h}} g^{\frac{2n-2}{h}}$  can be implemented by the following Cauchy integral:

$$\oint \frac{dz}{2\pi iz} z^2 (A_h(gz^h) - 1) z^{-2n} = A_{h, \frac{2n-2}{h}} (1 - \delta_{\frac{2n-2}{h}, 0}) g^{\frac{2n-2}{h}}. \quad (6.9)$$

If we do not introduce the numbers  $\epsilon_h(n)$ , the partition function  $Z_h^{\text{tree}}$  can be written as:

$$Z_h^{\text{tree}}(g, N) = N^{-2h} \sum_{\mathcal{G}'} \frac{1}{|\text{Aut}(\mathcal{G}')|} A_{h, \frac{2E(\mathcal{G}')-2}{h}} g^{\frac{2E(\mathcal{G}')-2}{h}}, \quad (6.10)$$

where  $\mathcal{G}'$  are one-vertex graphs of genus  $h$ . If we then call  $a(z) = z(A_h(gz^h) - 1)$ ,  $Z_h^{\text{tree}}$  can be written also as a Cauchy integral:

$$Z_h^{\text{tree}}(g, N) = N^{-2h} \oint \frac{dz}{2\pi i} a(z) \sum_{\mathcal{G}'} \frac{1}{|\text{Aut}(\mathcal{G}')|} \left(\frac{1}{z}\right)^{2E(\mathcal{G}')}. \quad (6.11)$$

In this form the partition function is suitable for being written as a sum over the graphs  $\mathcal{G}''$  in which we have removed link patterns (for an example of the removal of link patterns in a one-vertex graph embedded in the torus, see figure 6.2(a)).

We can trade the sum over  $\mathcal{G}'$  for a sum over  $\mathcal{G}''$ , if we replace also the term  $z^{-1}$  in the integrand of (6.11) with  $q(z)$ , defined as

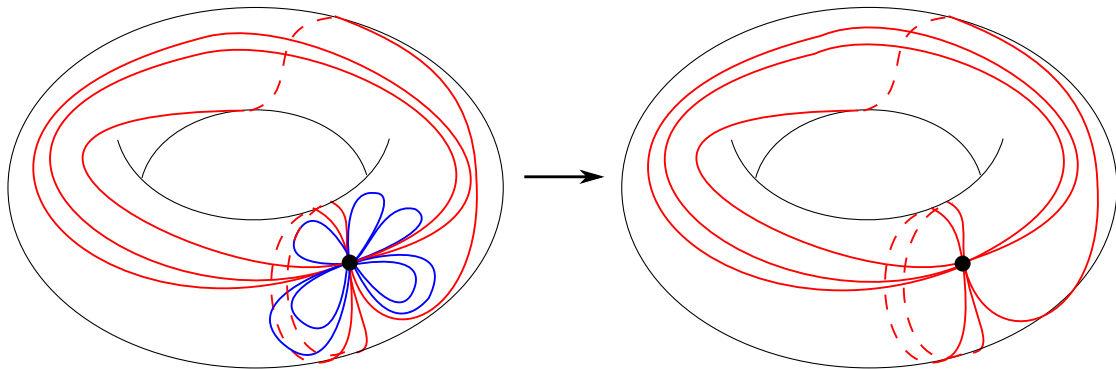
$$q(z) := z^{-1} C(z^{-2}), \quad (6.12)$$

where  $C(x)$  is the generating function of Catalan numbers, equation (1.11). This corresponds to dress each half-edge of a diagrams  $\mathcal{G}''$  with a link pattern of arbitrary size (possibly zero). Note that the cyclic symmetry of the edges is crucial for this operation. At this intermediate step the partition function looks like

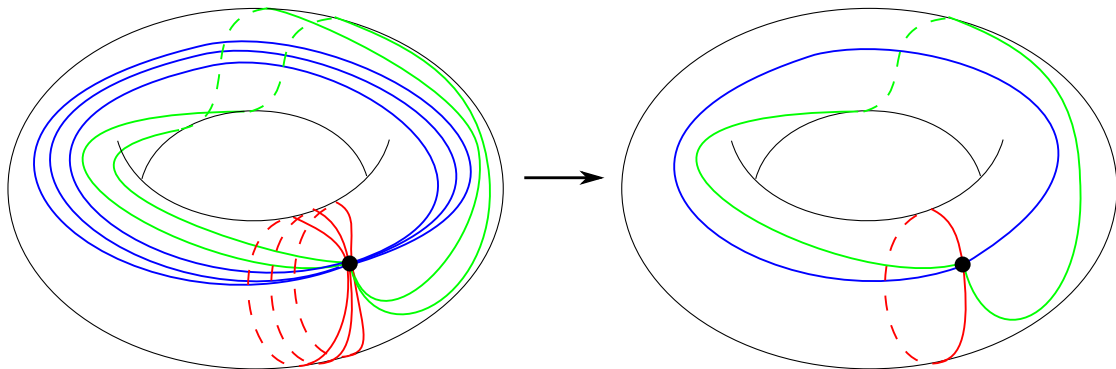
$$Z_h^{\text{tree}}(g, N) = N^{-2h} \oint \frac{dz}{2\pi i} a(z) \sum_{\mathcal{G}''} \frac{1}{|\text{Aut}(\mathcal{G}'')|} q(z)^{2E(\mathcal{G}'')}. \quad (6.13)$$

Next, replacing the sum over  $\mathcal{G}''$  with the sum over  $\mathcal{G}'''$  amounts to a resummation of parallel edges, since  $\mathcal{G}'''$  are generated from  $\mathcal{G}''$  by shrinking multiple edges to single





(a) The removal of link patterns (in blue) from a graph  $\mathcal{G}'$  embedded in the torus. This leaves us with its correspondent graph  $\mathcal{G}''$  with only non contractible arcs (in red).



(b) The procedure of removing parallel edges from a graph in  $\mathcal{G}''$  that lead to a graph in  $\mathcal{G}'''$ . Parallel edges are colored with the same shade.

Figure 6.2: The two steps for replacing  $G'$  with  $G'''$ .

ones. The resummation consists in replacing the integrand  $q^2(z)$  in (6.13) with  $Q_-(z)$ ,

$$\begin{aligned} Q_-(z) &:= \sum_{l \geq 1} q^{2l} = \frac{q^2(z)}{1 - q^2(z)} \\ &= \frac{1}{2} \left( \frac{1}{\sqrt{1 - \frac{4}{z^2}}} - 1 \right). \end{aligned} \quad (6.14)$$

The trading of multiple edges for single ones is illustrated in figure 6.2(b).

Our final formula for the partition function then is

$$Z_{\mathfrak{h}}^{\text{tree}}(g, N) = N^{-2\mathfrak{h}} \oint \frac{dz}{2\pi i} a(z) \sum_{\mathcal{G}'''} \frac{1}{|\text{Aut}(\mathcal{G}''')|} Q_-(z)^{E(\mathcal{G}''')}. \quad (6.15)$$

The integral now is over a circle between the two branch cuts of the integrand (figure 6.3). Indeed  $Q_-(z)$  has a branch cut in  $(-2, 2)$ , while  $a(z)$  in the region of the real line that depends on  $h$  and  $g$   $((hg)^{-1/h} / (h+1)^{(h+1)/h}, +\infty)$ , according to (4.16).

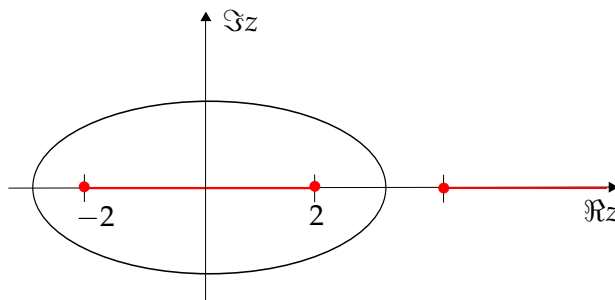


Figure 6.3: The circle over which the integral in equation 6.15 is performed. It is between the branch cuts of  $Q_-(z)$  and  $a(z)$ .

Note that diagrams in  $\mathcal{G}'''$  have only faces with at least three sides, because a face with one side is contractible and is a link pattern, while faces with two sides correspond to parallel edges, and both of these structures have been removed.

We now want to investigate the thermodynamic limit of (6.15). When  $g \rightarrow g_c$  the two branch cuts of the integrand merge together and  $Q_-(z)$  becomes singular. Then in this limit, the leading term in the sum (6.15) will be produced by the class of graphs that maximize the number of edges, that is triangulations<sup>1</sup>. Recall that we have already computed the sum over one-vertex triangulations of a genus  $\mathfrak{h}$  surface weighted by the inverse of the order of their automorphism, formula (3.19). Remember also that the number of edges in these triangulations is fixed to  $6\mathfrak{h} - 3$ . So when  $g$  approaches its critical value, the partition function can be written as:

$$Z_{\mathfrak{h}}^{\text{tree}}(g, N) \sim \frac{1}{N^{2\mathfrak{h}}} \frac{2}{12^{\mathfrak{h}}} \frac{(6\mathfrak{h} - 5)!}{\mathfrak{h}!(3\mathfrak{h} - 3)!} \oint \frac{dz}{2\pi i} a(z) Q_-(z)^{6\mathfrak{h} - 3}. \quad (6.16)$$

<sup>1</sup>In section 6.2.3 we will give a systematic perturbative expansion in the variable  $1/V$ , summing over polygons of increasing sides.

To compute this quantity we expand the integrand:  $a(z)$  is related to the generating function of the generalized Catalan numbers and thus can be expanded as a sum over  $A_{h,n}$ . Near the critical point, by removing a non-singular term, we can substitute the propagator  $Q_-(z)$  with

$$Q_0(z) = \frac{1}{2} \left( \frac{1}{\sqrt{1 - \frac{4}{z^2}}} \right) \quad (6.17)$$

and express it as a binomial series in  $1/z$ .

Performing the Cauchy integral we are left with

$$\begin{aligned} Z_{\mathfrak{h}}^{\text{tree}}(g, N) &\sim \frac{2^6}{(N^2 \cdot 12 \cdot 2^6)^{\mathfrak{h}}} \frac{(6\mathfrak{h} - 5)!}{\mathfrak{h}!(3\mathfrak{h} - 3)!\Gamma(3\mathfrak{h} - 3/2)} \sum_{V \geq 1} \frac{(2^{\mathfrak{h}}g)^V ((h+1)V)!}{(hV+1)!V!(\frac{hV}{2}+1)!} \\ &\cdot \Gamma\left(3\mathfrak{h} - \frac{1}{2} + \frac{hV}{2}\right) \\ &= \frac{2}{\sqrt{\pi}} \left(\frac{1}{\sqrt{12N}}\right)^{2\mathfrak{h}} \frac{1}{\mathfrak{h}!} \sum_{V \geq 1} \frac{(2^{\mathfrak{h}}g)^V ((h+1)V)!}{(hV+1)!V!(\frac{hV}{2}+1)!} \Gamma\left(3\mathfrak{h} - \frac{1}{2} + \frac{hV}{2}\right). \end{aligned} \quad (6.18)$$

The sum over  $V$  is intended on values that satisfy  $hV$  even. Notice how the factorials combine to give a simple term in  $\mathfrak{h}$ .

Perform Stirling approximation in (6.18), we end with the same large volume limit obtained above using the asymptotic of  $\epsilon_{\mathfrak{h}}(n)$ , equation (6.5), giving a consistency check of the two approaches.

## 6.2 All genus partition function

Now we are interested in summing the partition function (6.2) over  $\mathfrak{h}$  to describe the contribution of all genus surfaces

$$Z(g, N) = \sum_{\mathfrak{h} \geq 0} Z_{\mathfrak{h}}(g, N). \quad (6.19)$$

Looking at the result in the large volume limit, equation (6.18), we note that summing over genus will produce a divergent series, since the summand doesn't go to zero for large  $\mathfrak{h}$ . The fact that perturbation theory leads to a divergent series is a common feature of the topological expansion of matrix models.

We start by reviewing some aspects of divergent series.

### 6.2.1 Divergent series and Borel summability

In this section we shall review briefly asymptotic series and Borel summability, and in the end discuss our case. A function  $f(x)$  analytic in a sector  $S = \{x \in \mathbb{C} : |\arg(x)| \leq \alpha/2, |x| < |x_0|\}$  possesses an asymptotic expansion in  $S$

$$f(x) \approx \sum_{k=0}^{\infty} f_k x^k \quad (6.20)$$

if to every order  $N$  there exists a bound of the form

$$\left| f(x) - \sum_{k=0}^N f_k x^k \right| \leq C_{N+1} |x|^{N+1} \quad \text{for all } N \in \mathbb{Z}_+. \quad (6.21)$$

This means that, though the series diverges, its partial sums can be made an arbitrarily good approximation to  $f$  for  $|x|$  small enough. But in general the function  $f(x)$  is not unique, since we can always add a function that is smaller than  $\min_N C_N |x|^n$  in  $S$ . For example we can add  $e^{-1/x}$  for  $\Re x > 0$ , which has a Taylor series that at the origin converges to the zero function. However under certain conditions of maximality of the sector of analiticity  $S$ , the function  $f$  is unique. Indeed if we consider for definiteness the following asymptotic

$$f_k \sim A^{-k} (\beta k)!, \quad (6.22)$$

that is the typical large order behaviour of perturbation theory leading to a divergent series in quantum mechanics and field theory, then under the condition  $\alpha > \beta\pi$  the function  $f(x) = \sum_k f_k x^k$  is unique [60]. In this case there are summation methods that allow to reconstruct the function from the expansion. One of these methods relies on the *Borel transform*  $B_f(x)$  of  $f(x)$  defined as

$$B_f(x) = \sum_{k=0}^{\infty} b_k x^k \quad \text{with } b_k = \frac{f_k}{(\beta k)!}. \quad (6.23)$$

Under the assumption (6.22), the series that defines  $B_f(x)$  has a finite radius of convergence  $|A|$  and the Borel transform possesses a pole in  $x = A$ . Using the integral representation of the Gamma function

$$\Gamma(x) = \int_0^{+\infty} ds e^{-s} s^{x-1}, \quad (6.24)$$

$f(x)$  can be expressed as

$$f(x) = \sum_{k=0}^{\infty} f_k x^k = \sum_{k=0}^{\infty} (\beta k)! b_k x^k = \sum_{k=0}^{\infty} \int_0^{+\infty} ds e^{-s} s^{\beta k} b_k x^k. \quad (6.25)$$

Now we formally interchange the order of summation and integration to obtain

$$f(x) = \int_0^{+\infty} ds e^{-s} B_f(x s^\beta). \quad (6.26)$$

For  $x > 0$  this integral is convergent if  $A < 0$  so that no singularity occur in the path from 0 to  $\infty$ . In this case (6.26) is used to define the sum of the divergent series  $\sum_k f_k x^k$ . More precisely this equation should be read from right to left: upon a change of variables, the integral is a Laplace transform and then we can use Laplace method for  $x \rightarrow 0^+$  to make an asymptotic expansion and obtain the series in (6.20) with  $f_k = A^{-k} (\beta k)!$ .

As an example consider for  $A < 0$  the case  $\beta = 1$ , that is

$$f(x) = \sum_{k=0}^{\infty} A^{-k} k! x^k. \quad (6.27)$$

The Borel transform of  $f$  is

$$B_f(x) = \sum_{k=0}^{\infty} \left(\frac{x}{A}\right)^k = \frac{A}{A-x}, \quad (6.28)$$

and the series converges only for  $|x| < |A|$ . Then according to (6.26) we have to integrate the Borel transform, thus formally extending its definition, to obtain the following expression for  $f(x)$

$$f(x) = \int_0^{+\infty} ds e^{-s} \frac{A}{A-xs} = \frac{e^{-A/x} \text{Ei}(A/x)}{x} \quad (6.29)$$

where Ei is the exponential integral function which has a branch point at the origin. We have in this way associated a value to the divergent series (6.27) for  $A < 0$  in a sense that if we perform the Taylor expansion of the function (6.29) we obtain a series whose coefficients are  $A^{-k} k!$ .

If instead we consider the case  $A > 0$  we cannot run the integral (6.26) along the real axis, so the non alternating series  $\sum_k f_k x^k$  is said to be not Borel summable. However we could use a Borel-inspired approach to compute  $f(x)$ , where we deform the path of integration in order to avoid the singularity  $s = (A/x)^{1/\beta}$ . If we call the integrals above and under the singularity  $f_+(x)$  and  $f_-(x)$ , then one can show that the discontinuity of  $f$  gives information about the large order behaviour of  $f_k$

$$f_k \sim \int_0^{\infty} \frac{ds}{s^{k+1}} (f_+(s) - f_-(s)). \quad (6.30)$$

The difference  $f_+(x) - f_-(x)$  is of exponential order and does not have an expansion in  $x$ , so the ambiguity of choosing the contour of integration from origin to infinity in the case  $A > 0$  is related to the presence of non-perturbative effects [5].

In random matrix theory it happens that the topological expansion of the most interesting models, such as pure gravity or the unitary minimal models, is not Borel summable. In that case formula (6.30) joint with the Painlevé differential equation<sup>2</sup> satisfied by the full partition function, allows to access to the large order behaviour. For a thorough discussion on this method, see [5], where it is proved that every minimal model  $(p, q)$  coupled to 2D quantum gravity has a topological expansion that behaves as  $(2\mathfrak{h})!$  for  $\mathfrak{h}$  large.

Coherently we find the same large order behaviour from our explicit expression for the genus  $\mathfrak{h}$  partition function, formula (6.18). Further we note that in our case the

---

<sup>2</sup> Painlevé equations arise in random matrix theory when one considers the solution of a matrix integral with the technique of orthogonal polynomials and  $N$  and  $g$  scale in an appropriate way (*double scaling limit*). We do not treat these aspects in this thesis and we refer to [22, 5] for a review.

summand is positive definite so the all genus partition function (6.19), like the one of pure gravity, is not Borel summable.

Remark that here we are in a privileged position with respect to the usual situation one can encounter for the topological expansion of matrix integrals. Indeed we have more than a general functional form of the partition function usually obtained from the Painlevé equation: our combinatorial approach has furnished us with directly the exact expression of the partition function at every genus. However the non summability of the series, makes dealing with it difficult. A possible prescription to compute equation (6.19) could be using the Borel regularization in a region where the series is Borel summable (imaginary values of  $N$ ) and then continue analytically the result to the region of interest. This procedure unfortunately is hard to follow, since we cannot make any approximation on the summand, because terms small in some region of the complex plane can become important when we use analytic continuation, and then we would have to handle very cumbersome expressions.

Instead we will study the exponential generating function for spanning trees at fixed genus, that, being regularized, does not share the problematic issues of the generating function. We will show how to compute it at leading order and to derive the phase diagram. Then we will also present a method to have control over the subleading orders.

## 6.2.2 Critical behaviour of the exponential generating function

The purpose of this section is to study the regularized series

$$Z_{\text{reg}}(g, N) = \sum_{\mathfrak{h} \geq 0} \frac{Z_{\mathfrak{h}}^{\text{tree}}}{(2\mathfrak{h})!}. \quad (6.31)$$

In the large volume limit, we can approximate the integrand using equation (6.18)

$$Z_{\text{reg}}(g, N) \sim \sum_{\mathfrak{h} \geq 1} \frac{2}{\sqrt{\pi}} \left( \frac{1}{\sqrt{12N}} \right)^{2\mathfrak{h}} \frac{1}{\mathfrak{h}!(2\mathfrak{h})!} \sum_{V \geq 1} \frac{(2^{\mathfrak{h}}g)^V ((\mathfrak{h}+1)V)!}{(hV+1)!V! \left(\frac{hV}{2}+1\right)!} \Gamma \left( 3\mathfrak{h} - \frac{1}{2} + \frac{hV}{2} \right). \quad (6.32)$$

The sum over  $\mathfrak{h}$  starts from 1 because the summand does not reproduce at  $h = 0$  the planar partition function, but this is not relevant in the interpretation of (6.32), since we are interested in the large order behaviour that lead to the critical structure. We remark that among the factors that regularize the series,  $(2\mathfrak{h})!$  is the most natural one, since in that case  $Z_{\text{reg}}$  can be considered as an exponential generating function for spanning trees at fixed genus, and is within the typical framework of Borel sums.

The computation of this partition function proceeds as follows. First we express the Gamma function which entangles  $\mathfrak{h}$  and  $V$  in (6.32), with its integral form (6.24). Note that this is actually the same trick used in Borel regularization in section 6.2.1, but applied to a different factor.

All remaining factors depend either only on  $V$  or only on  $\mathfrak{h}$ . Then, we use Stirling

formula to approximate both kinds of factors. We end with:

$$Z_{\text{reg}}(g, N) \sim \frac{3h\sqrt{h+1}}{4\pi^{3/2}} \int_0^\infty ds e^{-s} s^{-\frac{3}{2}} \sum_{h \geq 1} \left( \frac{9s^3}{16N^2} \right)^h \frac{1}{\Gamma(3h + \frac{3}{2})} \sum_{V \geq 1} (\tilde{g}s^{\frac{h}{2}})^V \frac{1}{\Gamma(\frac{hV}{2} + \frac{7}{2})} \quad (6.33)$$

where  $\tilde{g} = g/g_c$ .

The two series can be summed separately. For simplicity call  $x$  and  $y$  the terms raised to respectively the power  $3h$  and  $V$  in (6.33) and call the sum over genus and vertices  $\phi_1(x)$  and  $\phi_2(x)$ :

$$\phi_1(x) = \sum_{h \geq 1} \frac{x^{3h}}{\Gamma(3h + \frac{3}{2})}; \quad \phi_2(y) = \sum_{V \geq 1} \frac{y^V}{\Gamma(V + \frac{7}{2})}. \quad (6.34)$$

$\phi_1(x)$  is a Hypergeometric function, but if we write this sum as

$$\phi_1(x) = \frac{1}{3} \sum_{h \geq 0} \left( \frac{x^h}{\Gamma(h + \frac{3}{2})} + \frac{(x\omega)^h}{\Gamma(h + \frac{3}{2})} + \frac{(x\omega^2)^h}{\Gamma(h + \frac{3}{2})} \right) - \frac{2}{\pi} \quad (6.35)$$

with  $\omega = e^{\frac{2\pi i}{3}}$  being a cubic root of the unit, we can exploit the simpler series

$$\sum_{h \geq 0} \frac{x^h}{\Gamma(h + \frac{3}{2})} = \frac{e^x \text{erf}(\sqrt{x})}{\sqrt{x}}$$

to have an expression easier to handle. When  $x$  is large, the Error Function approaches 1, so in this regime we can approximate  $\phi_1(x)$  with  $e^x/(3\sqrt{x})$ . Conversely when  $x$  is small,  $\phi_1(x)$  can be approximated with its value near the origin,  $16x^3/(105\sqrt{\pi})$ .

An analogous treatment can be made for the series on  $V$ . For convenience we fix the value of the coordination to 4,  $h = 2$ . Other cases are easily related to this one by the same trick used for the sum over genus. We have:

$$\phi_2(y) = \frac{e^y \text{erf}(\sqrt{y})}{y^{\frac{5}{2}}} - \frac{8}{15\sqrt{y}} - \frac{2}{\sqrt{\pi}y^2} - \frac{4}{3\sqrt{\pi}y} \quad (6.36)$$

Again we can use the approximation of the Error Function and trade  $\phi_2(y)$  for  $e^y y^{-\frac{5}{2}}$  if  $y$  is large and for  $16y/(105\sqrt{\pi})$  if  $y$  is small. To compute the integral over  $s$ , we approximate the integrand properly and then just solve simple integrals. Being interested in finding the critical regime, we can forget about numerical coefficients and write this

approximation for equation (6.33):

$$\begin{aligned}
Z_{\text{reg}}(g, N) &\sim \int_0^\infty ds e^{-s} s^{-\frac{3}{2}} \phi_1\left(\frac{a}{N^{2/3}}s\right) \phi_2(\tilde{g}s) \\
&\sim \int_0^\infty ds e^{-s} s^{-\frac{3}{2}} \cdot \begin{cases} \frac{16}{105\sqrt{\pi}} \left(\frac{a}{N^{2/3}}s\right)^3 & \text{if } \frac{a}{N^{2/3}}s \ll 1 \\ \frac{e^{asN^{-2/3}}}{asN^{-2/3}} & \text{if } \frac{a}{N^{2/3}}s \gg 1 \end{cases} \\
&\quad \cdot \begin{cases} \frac{16}{105\sqrt{\pi}} (\tilde{g}s)^3 & \text{if } \tilde{g}s \ll 1 \\ \frac{e^{\tilde{g}s}}{\sqrt{\tilde{g}s}} & \text{if } \tilde{g}s \gg 1 \end{cases} \quad (6.37)
\end{aligned}$$

where we call  $a$  the combination  $(3/4)^{2/3}$ .

Since we consider  $N \sim O(1)$  or large,  $\tilde{g} \sim O(1)$ , we actually have only three possible regimes:

1. small  $s$ :  $\frac{a}{N^{2/3}}s \ll 1$  and  $\tilde{g}s \ll 1$
2. large  $s$ :  $\frac{a}{N^{2/3}}s \gg 1$  and  $\tilde{g}s \gg 1$
3. quasi planar:  $\frac{a}{N^{2/3}}s \ll 1$  and  $\tilde{g}s \gg 1$

These three regimes correspond respectively to integration regions  $(0, 1)$ ,  $(1, \frac{N^{2/3}}{a})$ , and  $(\frac{N^{2/3}}{a}, \infty)$ .

The integral in the first region poses no problem, the one in the second is convergent for  $\tilde{g} \leq 1$ , and from the convergence of the third piece, we extract the critical curve:

$$1 - \tilde{g} - \frac{a}{N^{2/3}} = 0 \quad (6.38)$$

In figure 6.4 we depict the  $N^{2/3}$  vs.  $\tilde{g}$  phase diagram. The convergence region filled corresponds to  $1 - \tilde{g} - \frac{a}{N^{2/3}} \geq 0$ , and it includes also the boundary, the critical curve (6.38).

We have already mentioned that we choose to regularize with  $(2\mathfrak{h})!$  because we had not an indication of a preferable one and then the partition function could be seen as an exponential generating function. But this is not the only possible choice.

In fact we need a factor behaving like  $\mathfrak{h}^{2\mathfrak{h}}$  for large  $\mathfrak{h}$  to make the series convergent. So every term with this asymptotic, like  $(2\mathfrak{h} + c)!$  with arbitrary  $c$ , or like  $(\mathfrak{h}!)^2$ , could be equally used. The derivation makes clear that choosing a different regularization would not alter our picture of the critical behaviour.

As a last remark, we note that another good choice of regularization is dividing by  $\Gamma(\mathfrak{h} + \frac{1}{3})\Gamma(\mathfrak{h} + \frac{2}{3})$ . In this case we can perform the calculations without the need of using



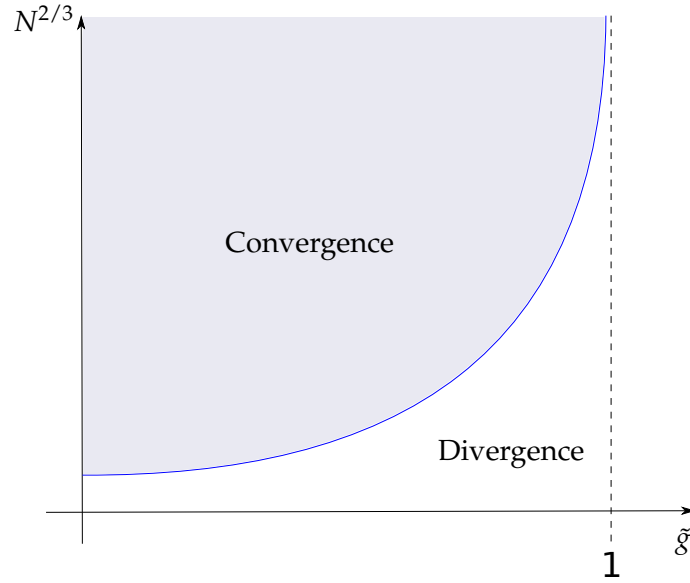


Figure 6.4: The  $N^{2/3}$  vs.  $\tilde{g}$  phase diagram. The region filled is where the integral converges. The boundary of this region is the critical curve, equation (6.38). Of course this analysis is not valid for values of  $N^{2/3}$  near the origin.

Stirling formula on the series on genus, since:

$$\Gamma\left(\mathfrak{h} + \frac{1}{3}\right) \Gamma\left(\mathfrak{h} + \frac{2}{3}\right) \Gamma(\mathfrak{h} + 1) = \frac{2\pi}{3^{3\mathfrak{h}+1/2}} \Gamma(3\mathfrak{h} + 1).$$

Using

$$\sum_{\mathfrak{h} \geq 0} \frac{\Gamma(3\mathfrak{h} + 1 + V - \frac{3}{2})}{\Gamma(3\mathfrak{h} + 1)} x^{\mathfrak{h}} = (1-x)^{1/2-V} \Gamma\left(V - \frac{3}{2}\right)$$

together with the trick of expressing the sum involving only  $\mathfrak{h}$  multiples of 3 with the cubic roots of the unity, we get for  $h = 2$ :

$$\begin{aligned} Z_{\text{reg}}(g, N) \sim \sqrt{\frac{3}{\pi^3}} \sum_{V \geq 1} (4g)^V \frac{(3V)! \Gamma(V - \frac{3}{2})}{(2V+1)! V! (V+1)!} \left( -1 + \frac{1}{3} \left( \left(1 - \frac{a}{N^{2/3}}\right)^{1/2-V} + \right. \right. \\ \left. \left. + \left(1 - \frac{a}{N^{2/3}} e^{-2\pi i/3}\right)^{1/2-V} + \left(1 - \frac{a}{N^{2/3}} e^{2\pi i/3}\right)^{1/2-V} \right) \right) \end{aligned} \quad (6.39)$$

Here we easily see how  $g$  and  $N$  combine. The sum on  $V$  is a combination of Hypergeometric functions and the convergence request leads us to the same critical behaviour discussed above.

### 6.2.3 Subleading corrections as sums over polygons

In section (6.1.2) we showed that when we are restricting to the class of diagrams with no parallel edges and link patterns, the thermodynamic limit (6.18) is obtained by considering only graphs with faces of degree 3. Using the method outlined in that section, it is clear that the subleading corrections in  $1/V$  to the partition function will be organized as a sum over graphs with polygonal faces of increasing number of sides. If for example we consider the case of a one-vertex graph with a pentagonal face and a triangular one embedded in a surface of genus  $h$ , we have that the entangling Gamma function in (6.18) changes from  $\Gamma(3h - \frac{1}{2} + \frac{hV}{2})$  to  $\Gamma(3h - \frac{3}{2} + \frac{hV}{2})$ , reducing by one the power of  $V$ , as can be easily understood using Stirling formula.

In section 6.2.2 we considered the leading order of the exponential generating function (6.31). The purpose of this section is showing how to perform a systematic expansion of this partition function in the size of the graphs.

Let us start from the expression of the partition function at fixed genus represented as a Cauchy integral, equation (6.15), and introduce the shortcut  $I_-^k$  for:

$$I_-^k = \oint \frac{dz}{2\pi i} a(z) Q_-(z)^k. \quad (6.40)$$

Then equation (6.15) looks like

$$Z_h^{\text{tree}}(g, N) = N^{-2h} \sum_{\mathcal{G}'''} \frac{1}{|\text{Aut}(\mathcal{G}''')|} I_-^{E(\mathcal{G}''')}. \quad (6.41)$$

In section 6.1.2 we noted that when the size of the graph is large we can trade  $Q_-$  for  $Q_0$  or equivalently  $I_-$  for  $I_0$ ,  $I_0$  defined as (6.40) with  $Q_0$  in place of  $Q_-$ . That allowed us to use the binomial series and easily compute the partition function in this limit. Now we can't do this approximation since we want to have more control on the size, but without it the computation of the Cauchy integral of equation (6.40) would be difficult. Furthermore using  $I_0$  in place of  $I_-$  would help us to make contact with the analysis done in the thermodynamic limit. For these reasons, we will show first how to replace  $I_-$  for  $I_0$  also when we are not at the thermodynamic limit at the price of introduce an ad hoc weight for the graphs.

#### Weighting the diagrams

In this paragraph we would like to derive a method to replace  $I_-$  with  $I_0$ . More generally, define  $I_c$  as

$$I_c = \oint \frac{dz}{2\pi i} a(z) \left( Q_-(z) + \frac{1+c}{2} \right) \quad (6.42)$$

and the corresponding partition function as

$$Z_h^{\text{tree}}(c, \vec{\alpha}) = N^{-2h} \sum_{\mathcal{G}'''} \frac{1}{|\text{Aut}(\mathcal{G}''')|} \left( \prod_{f \in F(\mathcal{G}''')} \alpha_{|f|}(c) \right) I_c^{E(\mathcal{G}''')} \quad (6.43)$$

where  $|f|$  is the number of sides of face  $f \in F(G''')$  and the dependence on  $N$  and  $g$  is understood. Then we would like to use (6.43) in place of our former partition function (6.41), that corresponds to  $Z_{\mathfrak{h}}^{\text{tree}}(-1, \vec{e})$  where  $\vec{e}$  is the vector with every component equal to 1. This can be done if we ask that for a given value of  $c$ ,  $\vec{\alpha}$  satisfies the consistency requirement

$$Z_{\mathfrak{h}}^{\text{tree}}(c, \vec{\alpha}) = Z_{\mathfrak{h}}^{\text{tree}}(-1, \vec{e}). \quad (6.44)$$

Once  $\vec{\alpha}$  has been determined, we can use (6.43) as the partition function of spanning trees at fixed genus. So trading  $I_-$  for  $I_c$  amounts to perform a weighted sum over graphs, with weights  $\vec{\alpha}$  that depend on the degree of the faces of the graph.

The computation of  $\vec{\alpha}$  proceeds as follows. Associate to the graphs of the sum in (6.43) two types of edges (say red and blue), one for  $Q_-$  and one for  $(1+c)/2$ . Graphs from the expansion of  $Z_{\mathfrak{h}}^{\text{tree}}(-1, \vec{e})$  will be built with only  $Q_-$  lines. Equation (6.44) states that the spurious contributions of  $(1+c)/2$  lines to graphs in  $Z_{\mathfrak{h}}^{\text{tree}}(c, \vec{\alpha})$  must sum up to zero.

As an example we show how the consistency requirement looks like for  $\mathfrak{h} = 1$ , where the diagrammatics is very simple, since we only have a graph with one face of four sides and one with two faces of three sides. For  $c = 0$ , equation (6.44) turns into



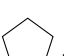
$$\frac{1}{4}\alpha_4 \left( I_-^2 + 2I_- \frac{1}{2} \right) + \frac{1}{6}\alpha_3^2 \left( I_-^3 + 3I_-^2 \frac{1}{2} + 3I_- \frac{1}{4} \right) = \frac{1}{4}I_-^2 + \frac{1}{6}I_-^3, \quad (6.45)$$

that gives  $\alpha_3 = 1, \alpha_4 = 0$ . This means that we can use  $I_0$  at genus 1 if we omit squares in the diagrammatics.

To generalize this example and compute  $\vec{\alpha}$ , fix a graph from  $Z_{\mathfrak{h}}^{\text{tree}}(-1, \vec{e})$  expansion with triangles and one polygon  $\mathcal{P}$ , built with only  $Q_-$  lines. The same graph in  $Z_{\mathfrak{h}}^{\text{tree}}(c, \vec{\alpha})$  can be decorated with  $(1+c)/2$  lines. Grouping their contribution together means that we can form arbitrary subpolygons of  $\mathcal{P}$ , each cut being weighted by  $(1+c)/2$ , and each face by the corresponding  $\alpha_k$ . Of course, the number of cuts equals the number of faces minus one. Call  $(p_1, \dots, p_k)$  the set of subpolygons and  $l_j$  is the number of sides of  $p_j$ , then we can write the following equation for  $\vec{\alpha}$ :

$$\sum_{(p_1, \dots, p_k)} \left( \prod_{j=1}^k \alpha_{l_j} \right) \left( \frac{c+1}{2} \right)^{k-1} = 1 \quad (6.46)$$

This equation can be solved easily if the number of sides of  $\mathcal{P}$  is small. The first cases are

-  :  $\alpha_3 = 1$
-  :  $\alpha_4 + 2\alpha_3^2 \frac{1+c}{2} = 1 \Rightarrow \alpha_4 = -c$
-  :  $\alpha_5 + 5\alpha_3\alpha_4 \frac{1+c}{2} + 5\alpha_3^3 \left( \frac{1+c}{2} \right)^2 = 1 \Rightarrow \alpha_5 = 1 - 5\frac{1+c}{2} \left( \frac{1+c}{2} - c \right)$

and these equations can be represented graphically as

- $\alpha_3 \triangle = \triangle$
- $\alpha_4 \square + 2\alpha_3^2 \square = \square$
- $\alpha_5 \text{pentagon} + 5\alpha_3\alpha_4 \text{pentagon} + 5\alpha_3^3 \text{pentagon} = \text{pentagon}$

Red lines correspond to  $Q_-$  lines, while blue lines are the spurious decorations and bring a factor  $(1+c)/2$  raised to their number. The general expression of the  $k$ -th element of  $\vec{\alpha}$  for  $c = 0$  is found to be, for  $k \geq 0$ ,

$$\begin{cases} \alpha_{2k+3} &= C_k \left(-\frac{1}{4}\right)^k \\ \alpha_{2k+4} &= 0 \end{cases} \quad (6.47)$$

where  $C_n$  are the Catalan numbers (see section 1.1.1), encountered many times in this thesis.  $\alpha_k$  is nonvanishing for odd  $k$  only, stating that polygons with even number of sides don't contribute when we use  $I_0$ .

### First terms of the expansion

Now that we have the formula for  $\vec{\alpha}(c = 0)$ , we can use the partition function (6.43) with  $I_0$  in place of  $I_-$ .

We can directly sum over genus and compute the corrections to the leading order of the regularized partition function studied in section 6.2.2. Since the approximation as a sum over triangulations is valid only in positive genus, we will sum only over  $\mathfrak{h} > 0$ .

Using formula (3.18) for the number of monochromatic unicellular maps, we can write the partition function a sum over partitions  $\mu = \prod_l l^{n_l}$  of the number of half-edges  $2n$ . Indeed recall that a partition  $\mu = \prod_l l^{n_l}$  corresponds to a graph with  $n_l$  faces of degree  $l$ , and from Euler formula satisfies  $L(\mu) = \sum_l n_l = E + 1 - 2\mathfrak{h}$ . So the number of edges and the genus can be written in terms of the parts of  $\mu$  as  $n = (\sum_l l n_l)/2$  and  $\mathfrak{h} = (\sum_l (l/2 - 1)n_l + 1)/2$ . We then have

$$\begin{aligned} Z_{\text{reg}}^{\mathfrak{h} > 0}(g, N) &= \sum_{\mathfrak{h} \geq 1} \frac{1}{N^{2\mathfrak{h}} (2\mathfrak{h})!} \sum_{n \geq 3} \sum_{\mu \vdash 2n} \frac{c_{2n, \mu}^{2n}}{2n} \left( \prod_l \alpha_l^{n_l} \right) I_0^n \\ &= \sum_{\mu} \frac{1}{2N} \prod_l \left( \frac{I_0^{\frac{l}{2}} \alpha_l}{(2N)^{\frac{l}{2} - 1} l} \right)^{n_l} \frac{1}{n_l!} \frac{\left( \frac{\sum_l l n_l}{2} - 1 \right)!}{\left( \sum_l \left( \frac{l}{2} - 1 \right) n_l + 1 \right)!} \sum_{(i_1, \dots, i_{L(\mu)}) = \mathfrak{h}} \prod_{k=1}^{L(\mu)} \binom{\mu_k}{2i_k + 1} \end{aligned} \quad (6.48)$$

If we restrict the sum in (6.48) over partitions  $\mu = 3^{n_3}$  by setting  $l = 3$  and summing over  $n_3$ , we have a sum over triangulations. Since  $\alpha_3 = 1$  this is:

$$Z_{\text{triang}}(g, N) = \sum_{n_3 \geq 1} \frac{1}{2N} \left( \frac{I_0^{3/2}}{3\sqrt{2N}} \right)^{n_3} \frac{1}{n_3!} \frac{\Gamma\left(\frac{3}{2}n_3\right)}{\Gamma\left(\frac{n_3}{2} + 2\right)} \binom{n_3}{\frac{2+n_3}{4}} 3^{3n_3/4 - 1/2}, \quad (6.49)$$

and rewriting this formula as a sum over the genus  $\mathfrak{h} = (2 + n_3)/4$ , we end with

$$Z_{\text{triang}}(g, N) = \sum_{\mathfrak{h}} \frac{2 I_0^{6\mathfrak{h}-3}}{12^{\mathfrak{h}} N^{2\mathfrak{h}}} \frac{(6\mathfrak{h} - 5)!}{(2\mathfrak{h})! \mathfrak{h}! (3\mathfrak{h} - 3)!}. \quad (6.50)$$

Expanding  $I_0$  and simplifying, we recognise exactly the thermodynamic limit of the partition function, formula (6.32).

The expansion in  $1/V$  will be achieved by considering partitions which have triangles and an increasing number of polygons with a higher number of sides. Indeed a  $k$ -gone in addition to triangles brings a factor of  $I_0^{k-3}$  in the denominator. We can compute explicitly an expansion in terms of  $1/I_0^2$

$$Z_{\text{reg}}^{\mathfrak{h}>0}(g, N) = Z_{\text{triang}} \sum_{l \geq 0} \frac{\mathcal{K}_l}{I_0^{2l}}. \quad (6.51)$$

Note that if we use the integral representation of the Gamma function in equation (6.51), the term containing  $V$  factorizes and the series on  $V$  does not depend on  $l$ . The coefficient  $\mathcal{K}_l$  can be easily computed by considering (6.48) with an increasing number of polygons with odd number of sides greater than 3 and dividing the result by  $Z_{\text{triang}}$ . In table 6.1 we present the first terms. We insert also  $\theta$  functions which ensure that certain series of polygons cannot be embedded in every surface. The denominator of every  $\mathcal{K}_l$  is  $(6\mathfrak{h} - 5)(6\mathfrak{h} - 7) \cdots (6\mathfrak{h} - 3 - 2l)$  and is precisely what we have in the numerator if we expand the corresponding term  $I_0^{6\mathfrak{h}-3-2l}$ , so the subleading corrections to the partition function are polynomials in  $\mathfrak{h}$  with the degree increasing with  $l$ , multiplied by  $\theta$  functions. Unfortunately we don't see any emerging general structure.

### 6.3 Discussions

Spanning trees on random lattices are easy to solve, even when the topology is not trivial. Indeed as we showed in this chapter the counting of their configurations can be done by enumerating unicellular maps, and this is all we need to compute the partition function exactly with a full control on the size. In this sense spanning trees are also easier to solve than the empty model, pure gravity, since the general procedure in random matrix theory to solve models on positive genus is using techniques from orthogonal polynomials or loop equations, both considerably harder than our approach. The solution at fixed genus we presented is validated by comparison of the critical exponents with already known results in literature and our previous work.

In this chapter we tried also to address the computation of the all genus partition function, but the difficulty of studying this non Borel summable series, led us to study its regularized version first, the exponential generating function. In this case we have been able to compute the phase diagram in the thermodynamic limit and thanks to our procedure of simplification of the diagrammatics, we could also give a recipe to have control over the subleading orders.



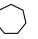
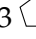
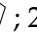
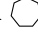

$\mathcal{K}_1$		$\frac{3(5 - 12h)(-1 + n)\theta(h - 2)}{10(-5 + 6h)}$
$\mathcal{K}_2$	2  ; 	$\frac{1}{2800(-7 + 6h)(-5 + 6h)} 3(3625 + 2h(-12179 + 6h \cdot (3449 + 12h(-187 + 42h))))\theta(h - 2)$
$\mathcal{K}_3$	3  ; 2  +  ; 	$-\frac{1}{1008000(2h - 3)(6h - 7)(6h - 5)} (h - 2)(9h(3h(4h(864h \cdot (28h - 199) + 455263) - 2160181) + 3117815) - 2712500)\theta(h - 3)$

Table 6.1: First values of the coefficient of the perturbative expansion in  $\frac{1}{l_0^2}$ . In the second column there are the polygons (beside triangles) one has to consider to increase the power of  $1/l_0^2$ .  $\mathcal{K}_1$  correspond to the first subleading order and is obtained considering all triangles but one pentagon (partition of length 5) in the sum over partitions in equation (6.48).  $\mathcal{K}_2$  corresponds to the sum of two contributions, one from the addition of two pentagons and one from the presence of a heptagon.  $\mathcal{K}_3$  is the sum of three contributions, one where we add three pentagons, one with a pentagon and a heptagon, and one with a nonagon.

We remark however that a study of the generating function for spanning trees at fixed genus could be interesting in the context of non perturbative 2D quantum gravity. Indeed it is a debated issue if non perturbative matrix models coincide with non perturbative 2D quantum gravity. This amounts to ask if we can trust the resummation of the topological expansion as non perturbative quantum gravity. In the non Borel summable case, it has been conjectured that since perturbation series does not define a unique function, the matrix model does not define the sum over topologies beyond perturbation series. For example it has been shown in the case of pure gravity that the real solution of the Painlevé equation has unphysical properties, in disagreement with what obtained by other methods [5]. Then our explicit expression of every order in perturbation theory can help to understand better this question, that usually is addressed only by considerations on the solutions of the Painlevé equations. This could be an interesting development of our work.

# Conclusion and outlook

In this thesis we studied spanning trees and forests on random lattices. We first reviewed some aspects of random matrix theory, a modern set of tools to deal with models on fluctuating surfaces. Despite nowadays there is not so much enthusiasm on 2D quantum gravity and random matrices as when this study started, statistical models on random lattices are still worth to study in the light of their connection with combinatorics and models on flat lattices. Both these connections are elucidated in this thesis and the conclusions we can guess from them are the motivations of our work.

The original contribution we developed is the study of the singularities of spanning forests on random lattices pursued in chapter 4. It is based on the random matrix approach derived in [21] and the solution of the  $\mathcal{O}(-2)$  loop-gas model [18]. We obtained two critical values for the fugacity of the trees  $t = 0$  and  $t = -1$ , both corresponding to a central charge  $c = -2$  on flat space. The statement at  $t = 0$  is consistent with asymptotic freedom and with the criticality of trees, while the interpretation of the point  $t = -1$  is not clear.

The rest of our results relies on combinatorics, following a recent trend in statistical mechanics of fluctuating surfaces, that have seen an increasing number of combinatorial methods entering the field of 2D quantum gravity, witnessing a combined work of mathematicians and physicists in this research area. In chapter 5 we directly studied spanning trees, spanning hypertrees and Hamiltonian cycles by enumerating their configurations, and we obtained that all these models have a central charge  $c = -2$  on flat space. The results obtained for trees are a review of what obtained in [21], while Hamiltonian cycles and spanning hypertrees are original contributions. We remark that our derivation is easy and self-contained, giving the possibility of a refined control of the finite size. The analysis of spanning hypertrees is of particular interest since no matrix integral can represent hypergraphs. Spanning trees on random lattices of arbitrary genus are treated for the first time in this thesis with our combinatorial model. Our derivation confirms that spanning trees are intrinsically easier than pure gravity, reducing the problem to the enumeration of unicellular maps. Our methods then allow a full analysis of the exponential generating function of spanning trees at given genus.

Spanning trees and forests are a vast topic with both combinatorial and physical interest, and our work is only a modest contribution toward their comprehension. There are indeed a lot of possible developments that can naturally follow what is done in this

thesis.

First, our analysis of the singularities of spanning forests done in chapter 4 needs more evidences to be properly understood. It would be interesting solving the model on random lattices of coordination four, and confront the results with what obtained on the fixed square lattice. This could help us in interpreting the role of the critical point  $t = -1$  and give more insights in the antiferromagnetic phase of the Potts model. Another helpful computation would be directly solving the model at  $t = -1$ . This task could be done using the form of the partition function in terms of embedding-activities. Indeed the problem posed in this way is equivalent to count planar graphs without any embedding-active internal edge and could be addressed with a combinatorial model.

The combinatorial method presented here for spanning trees has been derived in [21] and there generalised in the case of forests, but some open questions remain. In chapter 5 we stressed that the form of the functions that enumerates the inner and outer configurations of the models presented had the general feature of having the asymptotic  $n^{-3/2}$  when the size of the graph  $n$  is large. This suggests that the thermodynamic limit could be investigated approximating this functions with the Lèvy distribution, and then tools of Lèvy calculus could be used to address the general problem of solving spanning forests.

Our study of spanning trees on lattices of arbitrary genus is still incomplete for what concerns the computation of the exact non Borel-regularized all genus partition function. This solution can be interesting in the context of non perturbative 2D quantum gravity.

Another possible development of the work done for spanning trees on random planar graphs, could be investigating their connection with Stochastic Loewner Evolution (SLE). Uniform spanning trees on a regular 2D lattice with boundary, and a specific boundary condition, allow for the definition of stochastic curves, whose continuum limit is described by SLE. Then we could study the random planar graph variant of this model where we consider random triangulations, instead of the Riemann sphere, of a surface homotopic to a disk.



# Appendix A

## Basic notions about graphs and maps

In this thesis we have generally used the words graphs and maps as synonyms to indicate graphs embedded in a surface, but between these two words there is a subtle difference that we will explain here, after having recalled some notions about graphs.

### A.1 Graphs

A *graph* is a pair  $G = (V, E)$ , where  $V$  is a finite set whose elements are called vertices and  $E$  is a collection of subsets of  $V$  with two elements, called edges. Vertices  $v, w$  connected by  $e = \{v, w\}$  are said adjacent. A graph is complete if every pair of vertices is adjacent. In a graphical representation, vertices are points and edges are lines connecting two vertices. The number of edges incident to a vertex is called the coordination number (or degree) of  $v$ .

A graph  $G' = (V', E')$  is called a subgraph of  $G$  if  $V' \subseteq V$  and  $E' \subseteq E$ . When  $V' = V$ , the subgraph is said to be *spanning*.

A walk  $\omega$  connecting  $\omega_0$  with  $\omega_k$  in  $G$  is a sequence

$$(\omega_0, e_1, \omega_1, e_2, \dots, e_k, \omega_k) \quad \text{with } \omega_i \in V, e_i \in E$$

and  $\{\omega_{i-1}, \omega_i\} = e_i$  for  $1 \leq i \leq k$ . A walk is said a loop if  $\omega_0 \equiv \omega_k$ , a path if  $\omega_0, \dots, \omega_k$  are distinct vertices and  $e_1, \dots, e_k$  are distinct edges, a cycle if  $\omega_0, \dots, \omega_{k-1}$  with  $k \geq 2$  are distinct vertices,  $\omega_k \equiv \omega_0$ , and  $e_1, \dots, e_k$  are distinct edges. We allow graphs with multiple edges and loops (multi-graphs) as well as vertices of coordination 1 and 2. If  $e$  is an edge of  $G$ , we denote by  $G_{/e}$  the graph obtained by deleting  $e$  and by  $G_{\setminus e}$  the graph in which we contract  $e$ , i.e. we identify its two endpoints (see figure A.1).

A graph is connected if every pair of vertices is joined by at least one path on  $G$ . We will call the number of connected components  $K(G)$ .

A *forest* is a graph that contains no cycles. A *tree* is a connected forest and then connected components of forests are trees. In figure A.2 there are the graphical representations of a graph with a spanning tree and a spanning forest over it.

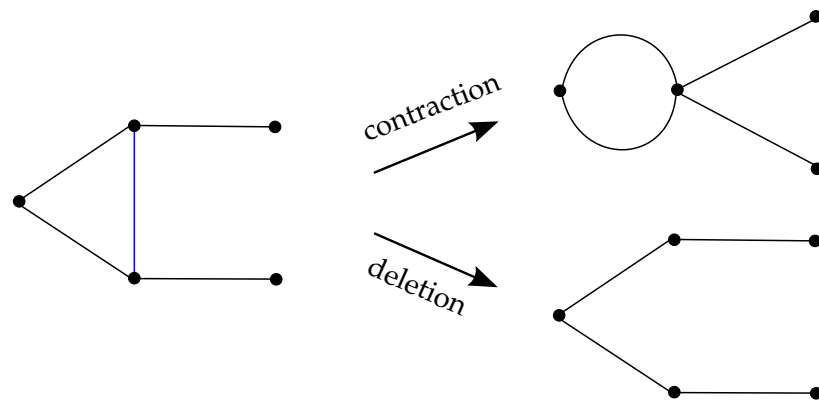


Figure A.1: Deletion and contraction of the edge marked in blue.

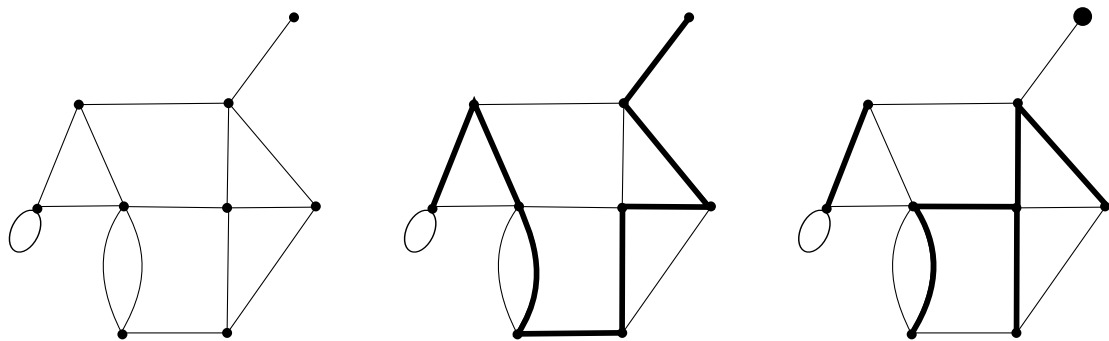


Figure A.2: A graph, together with a spanning tree (middle) and a spanning forest with three connected components (right) over it.

## A.2 Maps

Now we turn to the embedding of graphs. We will follow mainly the exposition presented in [61], and we refer to [34] for a rigorous and extensive treatment of the topics discussed in this section.

A combinatorial map, or map for short, is a graph drawn on a surface. By a surface we mean a compact oriented two-dimensional manifold without boundary. Surfaces are classified according to their genus, that is their number of handles or holes: a surface can only be homeomorphic to the sphere or to a connected sum of tori.

The difference between a graph and a map is difficult to catch since when we deal with graphs, we draw them. But the drawing provides graphs with an additional structure. To explain this fact, let us define precisely what is a map. A *map* is a graph drawn on (or embedded into) a surface in such a way that it has non intersecting edges and cutting along these edges produces a disjoint union of sets which are homeomorphic to open disks, called faces. Analogously to the degree of a vertex, we define the degree of a face as the number of its boundary edges.

Further, two maps are isomorphic if there exists an orientation preserving homeomorphism (a topological symmetry of the surface) which takes one map into the other<sup>1</sup>.

Maps can be viewed as two-dimensional cellular complexes, specified by 0-cell, vertices, 1-cell, edges, and 2-cell, faces. Then the Euler characteristic  $\chi$  of a map is defined as

$$\chi = 2 - 2\mathfrak{h} = |V| - |E| + |F| \tag{A.1}$$

where  $|V|$ ,  $|E|$  and  $|F|$  are respectively the cardinality of the set of vertices, edges and faces of the map. It depends only on the genus  $\mathfrak{h}$  of the surface in which the map is embedded. If we consider maps not connected, they are drawn on several surfaces (one for each connected component) and the Euler characteristic of the map is  $2K - 2\mathfrak{h} = |V| - |E| + |F|$ , where  $K$  is the number of connected components.

Different maps can correspond to a single graph, even if the maps have different genus, as in figure A.3.

Maps that can be drawn on the sphere are said to be *planar*. Every planar map can be drawn on the plane without edge crossing from the stereographic projection and the face that contains the point at infinity is called external.

### A.2.1 Fat-graphs

The additional information that allows to obtain a map from a graph is the cyclic ordering of edges near a vertex. Indeed when we draw a graph we fix this ordering and this is all we need to determine its embedding.

A convenient way to specify a cyclic ordering of the edges is using the *fat-graphs* representation in which edges are drawn as opposite oriented double lines. Then these double lines will meet at a vertex in such a way that the ordering is now fixed: if we

---

<sup>1</sup>These topological symmetries form a group called the mapping class group of the oriented genus- $\mathfrak{h}$  surface, generated by transformations called Dehn twists [62].

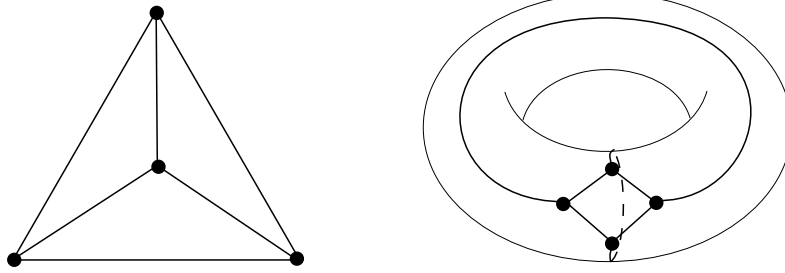


Figure A.3: The complete graph  $K_4$  drawn on the sphere and on the torus corresponds to two maps of different genus.

arrive at a vertex on an oriented line, we leave it by the first line on the right. The lines form disjoint cycles that correspond to the faces of the map (see figure A.4).

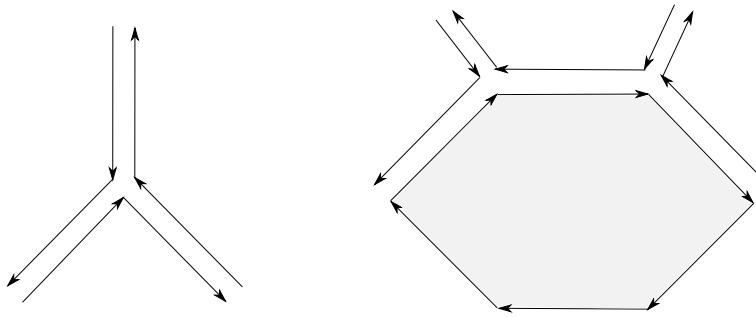


Figure A.4: On the left, three edges that meet at a vertex defining a cyclic ordering. On the right, a face.

### A.2.2 Automorphism group

The *automorphism group*  $\text{Aut}(\mathcal{G})$  of the map  $\mathcal{G}$  is the collection of all functions from  $\mathcal{G}$  to itself such that:

1. The set of vertices is mapped to itself
2. The set of edges is mapped to itself
3. The cyclic ordering that defines faces is preserved at every vertex.

A map  $\mathcal{G}$  can be considered as obtained from contracting half-edges attached to single vertices. Then the order of  $\text{Aut}(\mathcal{G})$  is given by the following formula

$$\frac{1}{|\text{Aut}(\mathcal{G})|} = C \prod_i \frac{1}{i^{V_i} V_i!} \tag{A.2}$$

where  $C$  is the combinatorial factor labelling how many distinct contractions of the half-edges lead to the same graph and  $i^{V_i}V_i!$  is the order of the automorphism group of the set of stars to be contracted to produce such map. For example the order of the automorphism group of the one-vertex map in figure A.5 is 6: there is only one way to obtain it contracting a one-vertex map with 6 half-edges ( $C = 1$ ), and  $V_3 = 1, V_i = 0$  for every  $i \neq 3$ .

### A.2.3 Dual map

The dual map  $\mathcal{G}^*$  of a map  $\mathcal{G}$  is embedded in the same surface and is constructed associating to every face of  $\mathcal{G}$  a dual vertex and to every edge a dual edge in such a way that they connect dual vertices on the two sides of the edges of  $\mathcal{G}$ . The automorphism group of a graph and of its dual is the same. Note that  $\mathcal{G}^{**} = \mathcal{G}$ . For an example of the dual map of a one-vertex map embedded in the torus, see figure A.5.

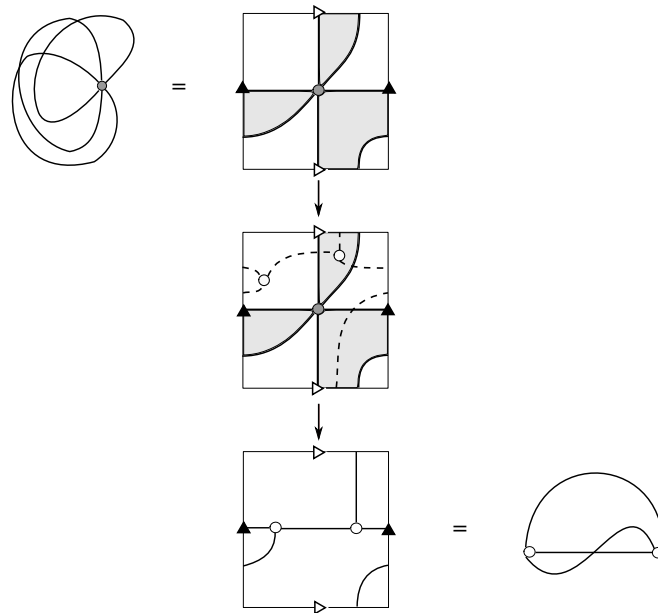


Figure A.5: At the left top corner there is a one-vertex map of genus 1 with 3 edges. We can draw it on the torus, as at the top of the middle column, where the torus is as usual seen as the quotient space of the square where black and white arrows indicate how to glue the sides. This map has two faces both of degree 3 corresponding to the filled and non filled region. Then we construct the dual map by inserting a dual vertex (white circle) in every face. Dual edges are represented as shaded lines and connect dual vertices on the two sides of the edges of the one-vertex map. The figure at the bottom of the middle column is the resulting dual map with one face, drawn on the torus. If we draw it on the plane as in the right bottom corner, non-planarity imposes that its edges intersect not only in their endpoints.

## Appendix B

# The Tutte polynomial

The Tutte polynomial of a graph is a polynomial in two variables which plays an important role in graph theory since it encodes a lot of information about the graph. Given a graph  $G = (V, E)$  we define the Tutte polynomial of  $G$  as

$$T_G(x, y) = \sum_{A \subseteq E} (x - 1)^{K(A) - K(E)} (y - 1)^{K(A) + |A| - |V|} \quad (\text{B.1})$$

where the sum is over all spanning subgraphs  $(V, A)$  and  $K(E)$  and  $K(A)$  denotes respectively the number of connected components of  $G$  and  $(V, A)$ .

As an example we compute the Tutte polynomial for the cycle graph with four vertices,  $G = C_4$ . As depicted in figure B.1 this graph has 16 spanning subgraphs<sup>1</sup>. The subgraph with no edges counts as  $(x - 1)^3$ , the four subgraphs with one edge as  $(x - 1)^2$ , the six with two edges as  $(x - 1)$ , the four with three edges as 4 and the one with four edges as  $(y - 1)$ . Then the Tutte polynomial of  $C_4$  is

$$T_{C_4}(x, y) = (x - 1)^3 + 4(x - 1)^2 + 6(x - 1) + 4 + (y - 1) = x^3 + x^2 + x + y. \quad (\text{B.2})$$

The definition of the Tutte polynomial implies that if a graph  $G$  is the disjoint union of two graphs  $G = G_1 \cup G_2$  then  $T_G(x, y) = T_{G_1}(x, y) \times T_{G_2}(x, y)$ . Then in what follows we will restrict to the class of connected graphs ( $K(E) = 1$ ). We refer to [63] for a complete description of the Tutte polynomial and its properties. Here we will discuss the relation of the Tutte polynomial to the partition function of the Potts model and of spanning forests, and then illustrate the spanning trees expansion.

### B.1 Relation with the Potts model and spanning forests

From its definition (B.1), the Tutte polynomial is easily related to the partition function of the Potts model in the Fortuin-Kasteleyn representation introduced in section 1.3.2,

$$Z_G^{\text{FK}}(q, \vec{v}) = \sum_{A \subseteq E} q^{k(A)} \prod_{(ij) \in A} v_{ij}. \quad (\text{B.3})$$

---

<sup>1</sup>In general a graph with  $|E|$  edges has  $2^{|E|}$  spanning subgraphs corresponding to the binary choice of taking or not an edge in the subgraph.

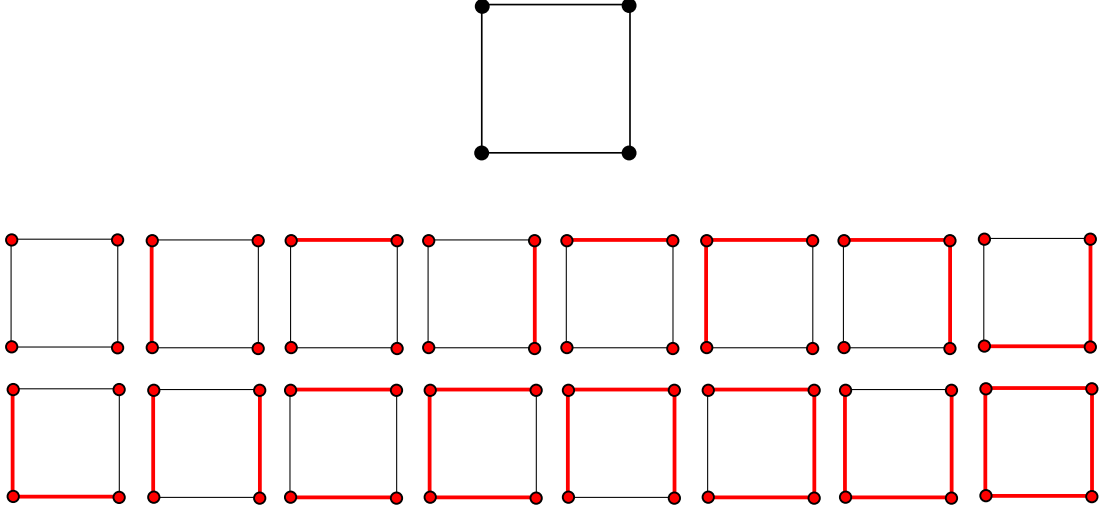


Figure B.1: The 16 spanning subgraphs of  $C_4$ . Elements of the subgraphs are marked in red.

Indeed we have

$$T_G(x, y) = (x - 1)^{-1}(y - 1)^{-|V|} Z_G^{\text{FK}}((x - 1)(y - 1), y - 1) \quad (\text{B.4})$$

where we give a uniform weight  $y - 1$  to the edges of the subgraph.

Specializations of the Tutte polynomial permit to obtain a lot of precise information about a graph. In particular evaluations of  $T_G(x, y)$  at  $x = 1, y = 1$  or both give the generating functions for connected spanning subgraphs, spanning forests and spanning trees. From (B.4) these correspond to three  $q \rightarrow 0$  limit of the Potts model [16]. Setting  $x = 1$  in (B.1) we have

$$\begin{aligned} T_G(1, y) &= \sum_{A \subseteq E} 0^{K(A)-1} (y - 1)^{K(A)+|A|-|V|} \\ &= \sum_{\substack{A \subseteq E \\ K(A)=1}} (y - 1)^{1-|V|+|A|}. \end{aligned} \quad (\text{B.5})$$

This corresponds to the generating function of connected spanning subgraphs

$$C_G(\vec{v}) = \sum_{\substack{A \subseteq E \\ K(A)=1}} \prod_{(ij) \in A} v_{ij} \quad (\text{B.6})$$

since  $C_G(y - 1) = (y - 1)^{|V|-1} T_G(1, y)$ . Using (B.4) we see that if we take the limit  $q \rightarrow 0$  with  $\vec{v}$  fixed in (B.3) we have

$$\lim_{q \rightarrow 0} q^{-1} Z_G^{\text{FK}}(q, \vec{v}) = C_G(\vec{v}). \quad (\text{B.7})$$

Consider now the evaluation at  $y = 1$ :

$$T_G(x, 1) = \sum_{A \subseteq E} (x-1)^{K(A)-1} 0^{K(A)+|A|-|V|}. \quad (\text{B.8})$$

This corresponds to a sum over spanning forests with a weight  $x - 1$  per connected component since the cyclomatic number (the number of independent cycles)  $c(A) = K(A) + |A| - |V|$  is forced to be equal to zero. If we define more generally the generating function for spanning forests as

$$Z_G^{\text{forest}}(t, \vec{w}) = \sum_{\substack{A \subseteq E \\ c(A)=0}} t^{K(A)} \prod_{(ij) \in A} w_{ij}, \quad (\text{B.9})$$

then

$$(x-1)T_G(x, 1)|_{x=t+1} = Z_G^{\text{forest}}(t, 1). \quad (\text{B.10})$$

In the Fortuin-Kasteleyn representation the generating function for spanning forests is achieved by considering the limit  $q \rightarrow 0, \vec{v} \rightarrow 0$  with fixed  $\vec{w} = \vec{v}/q$

$$\lim_{q \rightarrow 0} q^{-|V|} Z_G^{\text{FK}}(q, q\vec{w}) = \sum_{\substack{A \subseteq E \\ c(A)=0}} \prod_{(ij) \in A} w_{ij} = Z_G^{\text{forest}}(1, \vec{w}). \quad (\text{B.11})$$

Let us note also that if we have a uniform coupling  $w$  in the formula above, then  $w$  can be regarded as the inverse of the fugacity of the trees:

$$Z_G^{\text{forest}}(t, 1) = t^{|V|} Z_G^{\text{forest}}\left(1, \frac{1}{t}\right). \quad (\text{B.12})$$

As a last specialization that is of interest for our purposes we consider the generating polynomial of spanning trees. Starting from  $C_G(\vec{v})$ , we redefine the weight of edges  $\vec{v} \rightarrow \lambda \vec{v}$  and then take the limit  $\lambda \rightarrow 0$ . This selects from connected spanning subgraphs those having the fewer number of edges: trees, that have  $|A| = |V| - 1$ . Then we define the generating function of spanning trees as

$$Z_G^{\text{tree}}(\vec{v}) = \lim_{\lambda \rightarrow 0} \lambda^{1-|V|} C_G(\lambda \vec{v}) = \sum_{\substack{A \subseteq E \\ |A|=|V|-1}} \prod_{(ij) \in A} v_{ij}. \quad (\text{B.13})$$

Alternatively we can obtain this partition function from that of spanning forests  $Z_G^{\text{forest}}(1, \vec{w})$  where we replace  $\vec{w}$  by  $\lambda \vec{w}$  and take the limit  $\lambda \rightarrow \infty$

$$Z_G^{\text{tree}}(\vec{w}) = \lim_{\lambda \rightarrow \infty} \lambda^{1-|V|} Z_G^{\text{forest}}(1, \lambda \vec{w}). \quad (\text{B.14})$$



## B.2 Spanning trees expansion

The first definition given by Tutte of his polynomial was a generating function of spanning trees counted according to their activities (if the graph is connected, as we are assuming) [64]. To explain his definition we have to give some preliminary notions.

Consider a graph  $G$  and a spanning tree  $T$  over it. Call an edge internal if it belongs to  $T$  and external otherwise. Define the fundamental cycle of an external edge  $e$  as the set of edges  $f$  such that  $T \setminus \{f\} \cup \{e\}$  is a spanning tree. Analogously define the fundamental cocycle of an internal edge  $e$  as the set of edges  $f$  such that  $T \setminus \{e\} \cup \{f\}$  is a spanning tree. Recall from section A.1 that the notation  $T \setminus \{e\}$  means the deletion of the edge  $e$  in the graph  $T$ . See figure B.2 for examples of fundamental cycle and cocycle.

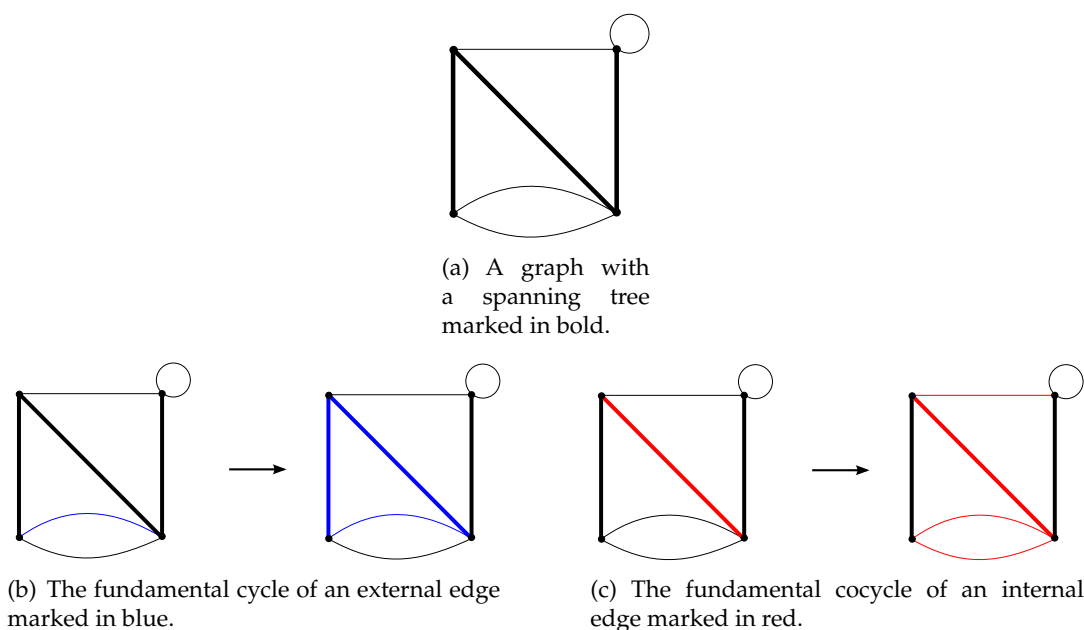


Figure B.2: Examples of fundamental cycle and cocycle for edges of the graph in figure B.2(a).

Note that the fundamental cycle of an external edge  $e$  contains only internal edges apart from  $e$  and the fundamental cocycle of an internal edge  $e'$  contains only external edges apart from  $e'$ . Further, if  $e$  is external and  $e'$  is internal, then  $e'$  is in the fundamental cycle of  $e$  if and only if  $e$  is in the fundamental cocycle of  $e'$ .

Given a graph  $G$ , choose an arbitrary fixed linear order of the edge set  $E$ , that is number increasingly the edges from first to last. Then take a spanning tree  $T$  over it. We say that an external edge is active if it is minimal in its fundamental cycle. In a similar way an internal edge is active if minimal in its fundamental cocycle.

Then the spanning trees expansion of the Tutte polynomial (B.1) is

$$T_G(x, y) = \sum_{T \prec G} x^{i(T)} y^{e(T)} \quad (\text{B.15})$$

where the sum  $T \prec G$  means over spanning trees  $T$  of  $G$  and  $i(T)$  and  $e(T)$  are respectively the number of active internal and external edges. This result is quite surprising since it states that the sum in (B.15) does not depend on the linear order chosen to assign activities. For a proof of this theorem we refer to [63].

Remark that using the spanning trees expansion of the Tutte polynomial, the partition function for unrooted spanning forests with a weight one to edges (B.10) becomes

$$Z_G^{\text{forest}}(t, 1) = t \sum_{T \prec G} (1+t)^{i(T)}. \quad (\text{B.16})$$

Here we do not have to count external active edges and we weight the configurations with  $(1+t)$  to the number of internal active edges.

However this notion of activity is not the only possible one. The choice of a linear order is not convenient to be used in the context of random planar graphs, in which we are interested in. We present then the notion due to O. Bernardi that characterizes the Tutte polynomial using the embeddings of the graphs.

### B.2.1 Definition for embedded graphs

If we turn to embedded graphs<sup>2</sup> the notion of activities can be changed in such a way to not depend anymore on the linear ordering and to be automatically encoded in the drawing of a graph on a surface.

Consider a graph  $\mathcal{G}$  with a distinguished half-edge (root), and a spanning tree  $T$  embedded on a surface. Starting from the root, consider a walk around the tree that follows internal edges and crosses external edges. Then number the edges according to their order of appearance around the tree. We call this ordering the  $(\mathcal{G}, T)$ -order. We say now that an external edge is embedding-active if it is minimal in its fundamental cycle according to the  $(\mathcal{G}, T)$ -order. Analogously we define an internal edge embedding-active if minimal in its fundamental cocycle according to this ordering.

For the determination of the embedding-active edges of a rooted version of the graph presented in figure B.2(a), see figure B.3.

Now we can express the Tutte polynomial of a graph  $G$  that have  $\mathcal{G}$  as any of its rooted embeddings, as [65]

$$T_G(x, y) = \sum_{T \prec G} x^{\mathcal{I}(T)} y^{\mathcal{E}(T)} \quad (\text{B.17})$$

where  $\mathcal{I}(T)$  and  $\mathcal{E}(T)$  are respectively the number of internal and external embedding-active edges chosen according to the  $(\mathcal{G}, T)$ -order. For example figure B.3 corresponds to a term  $xy^3$  in the Tutte polynomial of that graph. We remark that (B.17) does not depend on the choice of the rooted embedding.

When we consider the ensemble of random planar graphs, as generated by random matrices, we have an explicit embedding structure that, upon the choice of a root, establish the embedding-active edges. For an example of counting embedding-active edges

<sup>2</sup>For the difference between a graph and an embedded graph (called also map), see section A.2.

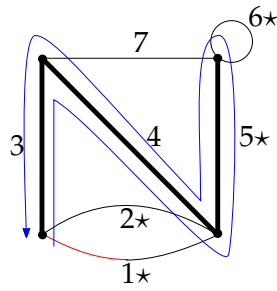


Figure B.3: The walk along the tree that starts from the root (red half-edge) is marked in blue. We order the edges according to their order of appearance around the tree and mark the resulting embedding-active edges with a star.

in a rooted random planar graph see figure B.4. This embedded graph corresponds to a term  $x^4y^3$  in the summand of (B.17).

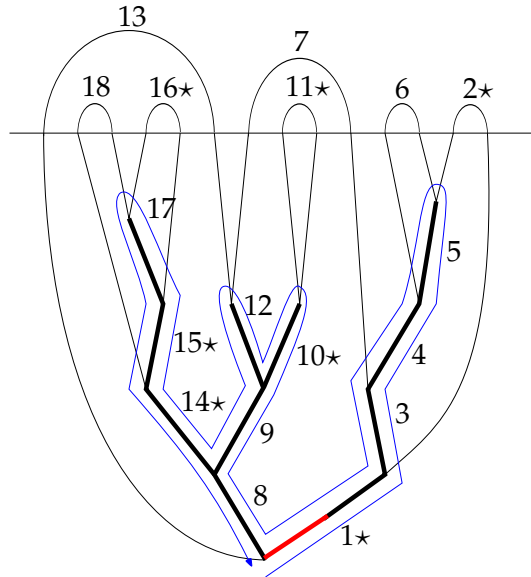
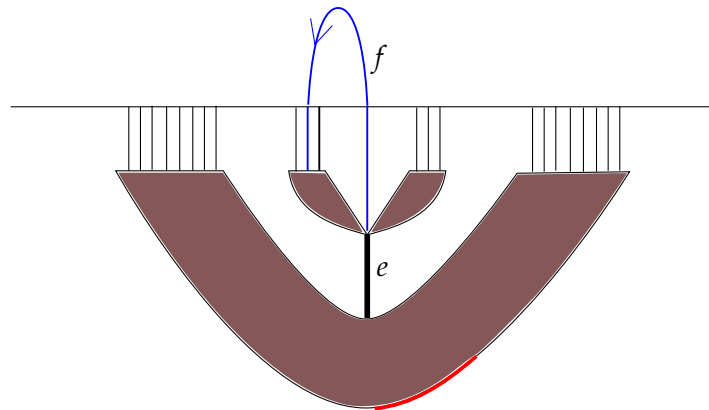


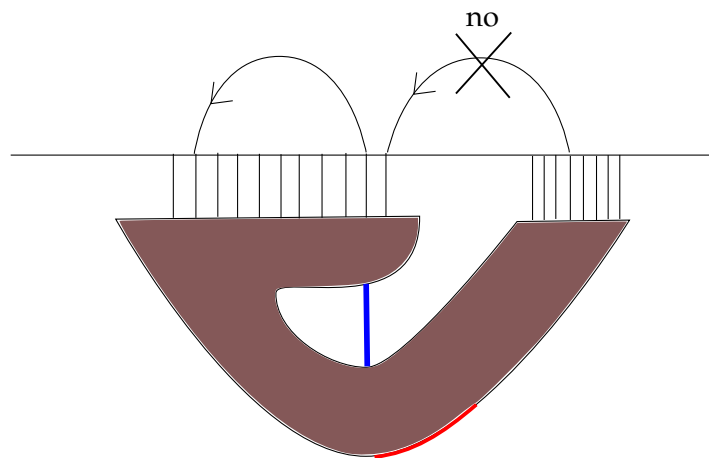
Figure B.4: A rooted cubic random planar graph with embedding-active edges marked with a star. It has 4 internal and 3 external embedding-active edges. As before the root is in red and the walk along the tree in blue. The external edges form link patterns on the boundary of the upper half-plane.

We remark that on random planar graphs we can understand the general form of configurations that have internal or external embedding-active edges. Indeed notice that drawing the edge containing the root first gives a hierarchical structure where we can distinguish parental relations between edges. For example we will say that in figure (B.4) the edges 9 and 14 are born from 8. Moreover we can orient the arcs forming a link pattern, say from right to left, without altering their counting in order to consider

only matching of an half-arc with other on its left. We will say that an external edge will go out of a an internal edge and goes into another one (or the same) according to this orientation. Then the only possible configurations that lead to an external (resp. internal) embedding-active edge are the ones depicted in figure B.5(a) (resp. B.5(b)). The deep reason underlying the simplification of the possible configurations is a consequence of the interplay of the degrees of freedom of the lattice and of the matter model, the reason why we could study the combinatorial models of chapters 5 and 6.



(a) An external edge  $f$  going out of an internal edge  $e$  (dark bold) is active if and only if it goes into an internal edge equal to  $e$ , or born from  $e$  on the left of  $f$ .



(b) An internal edge is active if and only if all the external edges composing its fundamental cocycle are oriented as going out of edges born from (or equal to) itself.

Figure B.5: The configurations that lead to internal and external embedding-active edges on random planar graphs. Filled regions correspond to arbitrary configurations and the the root is marked in red.

If we rewrite the partition function for spanning forests on a graph  $G$  (B.16) using

embedding-activities, we have

$$Z_G^{\text{forest}}(t, 1) = t \sum_{T \prec G} (1+t)^{I(T)}. \quad (\text{B.18})$$

Then we can sum over random planar graphs this partition function where  $G$  is replaced by the embedded graph  $\mathcal{G}$  for which the sum in the r.h.s. is naturally defined: for every  $\mathcal{G}$  we have to choose a root and, given its spanning trees, count the internal embedding-active edges.

# Bibliography

- [1] G. 't Hooft, "Planar Diagram Theory For Strong Interactions", *Nucl. Phys. B* **72** (1974) 461–473.
- [2] E. Brezin, C. Itzykson, G. Parisi, and J. Zuber, "Planar Diagrams", *Commun. Math. Phys.* **59** (1978) 35–51.
- [3] V. Kazakov, "Ising model on a dynamical planar random lattice: exact solution", *Phys. Lett. A* **119** (1986) 140–144.
- [4] J. Ambjørn, J. Bergfinnur, and T. Jonsson, *Quantum Geometry: A Statistical Field Theory Approach*. Cambridge University Press, 1997.
- [5] P. D. Francesco, P. Ginsparg, and J. Zinn-Justin, "2D Gravity and Random Matrices", *Phys. Rept.* **254** (1994) 1–133, [arXiv:hep-th/9306153v2](https://arxiv.org/abs/hep-th/9306153v2).
- [6] V. Knizhnik, A. Polyakov, and A. Zamolodchikov, "Fractal structure of 2d-quantum gravity", *Mod. Phys. Lett. A* **3** (1988) 819–826.
- [7] E. Wigner, "On the statistical distribution of the widths and spacings of nuclear resonance levels", *Proc. Cambridge Philos. Soc.* **47** (1951) 790–798.
- [8] T. Guhr, A. Mueller-Groeling, and H. A. Weidenmueller, "Random Matrix Theories in Quantum Physics: Common Concepts", *Phys. Rept.* **229** (1998) 189–425, [arXiv:cond-mat/9707301v1](https://arxiv.org/abs/cond-mat/9707301v1).
- [9] P. Moerbeke, "Integrable Lattices: Random Matrices and Random Permutations", in *Random matrix models and their applications*, P. Bleher and A. R. Its, eds., pp. 321–406. Cambridge University Press, 2001. [arXiv:math/0010135v1](https://arxiv.org/abs/math/0010135v1).
- [10] M. Mehta, *Random Matrices: Revised and Enlarged Second Edition*. Academic Press, 1990.
- [11] J. Harer and D. Zagier, "The Euler characteristics of the moduli space of curves", *Inven. Math.* **85** (1986) 457–485.
- [12] P. Zinn-Justin, "The General  $O(n)$  Quartic Matrix Model and its application to Counting Tangles and Links", *Commun. Math. Phys.* **238** (2003) 287–304, [arXiv:math-ph/0106005](https://arxiv.org/abs/math-ph/0106005).

- [13] P. D. Francesco, “Matrix Model Combinatorics: Applications to Folding and Coloring”, [arXiv:math-ph/9911002](https://arxiv.org/abs/math-ph/9911002).
- [14] M. Bousquet-Mélou and G. Schaeffer, “The degree distribution in bipartite planar maps: applications to the ising model”, [arXiv:math/0211070v2](https://arxiv.org/abs/math/0211070v2).
- [15] O. Bernardi and M. Bousquet-Mélou, “Counting colored planar maps: algebraicity results”, [arXiv:0909.1695v1](https://arxiv.org/abs/0909.1695v1).
- [16] A. Sokal, “The multivariate tutte polynomial (alias potts model) for graphs and matroids”, in *Surveys in Combinatorics*, B. S. Webb, ed., pp. 173–226. Cambridge University Press, 2005. [arXiv:math/0503607v1](https://arxiv.org/abs/math/0503607v1).
- [17] S. Caracciolo, J. L. Jacobsen, H. Saleur, A. D. Sokal, and A. Sportiello, “Fermionic field theory for trees and forests”, *Phys. Rev. Lett.* **93** (2004) 080601, [arXiv:cond-mat/0403271](https://arxiv.org/abs/cond-mat/0403271).
- [18] I. Kostov and M. Staudacher, “Multicritical Phases of the  $O(n)$  model on a Random Lattice”, *Nucl. Phys. B* **384** (1992) 459–483, [arXiv:hep-th/9203030v1](https://arxiv.org/abs/hep-th/9203030v1).
- [19] T. Walsh and A. Lehman, “Counting rooted maps by genus.I”, *J. Comb. Theory* **13** (1972) 192–218.
- [20] A. Goupil and G. Schaeffer, “Factoring  $n$ -cycles and counting maps of given genus”, *Europ. J. Combinatorics* **19(7)** (1998) 819–834.
- [21] S. Caracciolo and A. Sportiello, “Spanning Forests on Random Planar Lattices”, *J. Statist. Phys.* **135** (2009) 1063–1104, [arXiv:0903.4432](https://arxiv.org/abs/0903.4432).
- [22] P. D. Francesco, “Matrix Models, 2D Quantum Gravity and Graph Combinatorics”, [arXiv:math-ph/0406013](https://arxiv.org/abs/math-ph/0406013). Lectures given at the summer school “Applications of random matrices in physics”, Les Houches.
- [23] D. Bessis, “A new method in the combinatorics of the topological expansion”, *Comm. Math. Phys.* **69** (1979) 147–163.
- [24] N. J. A. Sloane, “The on-line encyclopedia of integer sequences.” Published on-line. <http://www.research.att.com/~njas/sequences>.
- [25] I. Kostov, “ $O(n)$  Vector Model on a Planar Random Lattice: Spectrum of Anomalous Dimensions”, *Mod. Phys. Lett. A4* **3** (1989) 217–226.
- [26] V. Kazakov, “Exactly solvable Potts models, bond and tree-like percolation on dynamical (random) planar lattice”, *Nucl. Phys. B (Proc. Supp.)* **4** (1988) 93–97.
- [27] I. Kostov and B. Duplantier, “Geometrical Critical Phenomena on a Random Surface of Arbitrary genus”, *Nucl. Phys. B* **340** (1989) 491–541.

- [28] I. Kostov and M. Gaudin, “ $O(n)$  Vector Model on a Fluctuating Planar Lattice: Some Exact Results”, *Phys. Lett. B* **220** (1989) 200–206.
- [29] B. Eynard and C. Kristjansen, “Exact solution of the  $O(n)$  model on a random lattice”, *Nucl. Phys. B* **455** (1995) 577–618, [arXiv:hep-th/9506193v1](#).
- [30] J. Zinn-Justin and B. Eynard, “The  $O(n)$  Model on a Random Surface: Critical Points and Large Order Behaviour”, *Nucl. Phys. B* **386** (1992) 558–591, [arXiv:hep-th/9204082](#).
- [31] N. Muskhelishvili, *Singular Integral Equations*. Dover Publications, 2nd edition, 1992.
- [32] B. Lass, “Démonstration combinatoire de la formule de Harer-Zagier”, *C. R. Acad. Sci. Paris Sér. I Math.* **333(3)** (2001) 155–160.
- [33] I. P. Goulden and A. Nica, “A direct bijection for the Harer-Zagier formula”, *J. Combin. Theory Ser. A* **111(2)** (2005) 224–238.
- [34] S. K. Lando, A. K. Zvonkin, and D. Zagier, *Graphs on surfaces and their applications*. Springer, 2004.
- [35] R. Bacher and A. Vdovina, “Counting 1-vertex triangulations of oriented surfaces”, *Discrete Math.* **246** (2002) no. 1-3, 13–27, [arXiv:math/0110025](#).
- [36] J. Cardy, “Conformal Field Theory and Statistical Mechanics”, [arXiv:0807.3472v1](#). Lectures given at the summer school “Exact Methods in Low-Dimensional Statistical Physics and Quantum Computing”, Les Houches.
- [37] B. Nienhuis, “Exact Critical Point and Critical Exponents of  $O(n)$  Models in Two Dimensions”, *Phys. Rev. Lett.* **49** (1982) 1062–1065.
- [38] R. Baxter, S. Kelland, and F. Wu, “Equivalence of the potts model or Whitney polynomial with an ice-type model”, *J. Phys. A: Math. Gen.* **9** (1976) 397–406.
- [39] B. Nienhuis, “Coulomb gas formulation of two-dimensional phase transitions”, in *Phase transitions and critical phenomena*, C. Domb and J. Lebowitz, eds., vol. 11, pp. 1–54. Academic Press, New York, 1987.
- [40] J. Daul, “Q-states Potts model on a random planar lattice”, [arXiv:hep-th/9502014v1](#).
- [41] P. Zinn-Justin, “The dilute Potts model on random surfaces”, *J. Statist. Phys.* **98** (2001) 245–264, [arXiv:cond-mat/9903385v2](#).
- [42] B. Eynard and G. Bonnet, “The Potts- $q$  random matrix model : loop equations, critical exponents, and rational case”, *Phys. Lett. B* **463** (1999) 273–279, [arXiv:hep-th/9906130v1](#).



- [43] B. Duplantier, “Conformal Random Geometry”, in *Mathematical Statistical Physics*, A. Bovier, F. Dunlop, F. den Hollander, A. van Enter, and J. Dalibard, eds., pp. 101–217. Elsevier B.V., Les Houches, July, 2005. [arXiv:math-ph/0608053](#).
- [44] F. David, “Conformal field theories coupled to 2d gravity in the conformal gauge”, *Mod. Phys. Lett.* **A3** (1988) 1651–1659.
- [45] B. Duplantier and S. Sheffield, “Liouville Quantum Gravity and KPZ”, [arXiv:0808.1560](#).
- [46] F. David and M. Bauer, “Another derivation of the geometrical KPZ relations”, [arXiv:0810.2858](#).
- [47] B. Duplantier, “Two-dimensional copolymers and exact conformal multifractality”, *Phys. Rev. Lett.* **82** (1999) 880–883.
- [48] R. Baxter, *Exactly Solved Models in Statistical Mechanics*. Academic Press, New York, 1982.
- [49] J. L. Jacobsen, A. D. Sokal, and J. Salas, “Spanning forests and the  $q$ -state Potts model in the limit  $q \rightarrow 0$ ”, *J. Stat. Phys.* **119** (2005) 1153–1281, [arXiv:cond-mat/0401026v2](#).
- [50] J. L. Jacobsen and H. Saleur, “The arboreal gas and the supersphere sigma model”, *Nucl. Phys. B* **716** (2005) 439–461, [arXiv:cond-mat/0502052v1](#).
- [51] J. L. Jacobsen and H. Saleur, “The antiferromagnetic transition for the square-lattice Potts model”, *Nucl. Phys. B* **743** (2006) 207–248, [arXiv:cond-mat/0512058v1](#).
- [52] Y. Deng, T. M. Garoni, and A. D. Sokal, “Ferromagnetic phase transition for the spanning-forest model ( $q \rightarrow 0$  limit of the Potts model) in three or more dimensions”, *Phys. Rev. Lett.* **98** (2007) 030602, [arXiv:cond-mat/0610193v2](#).
- [53] A. Bedini, S. Caracciolo, and A. Sportiello, “Phase transition in the spanning-hyperforest model on complete hypergraphs”, *Nucl. Phys. B* **882** (2009) 493–516, [arXiv:0906.4503v1](#).
- [54] R. L. Graham, D. E. Knuth, and O. Patashnik, *Concrete Mathematics*. Addison-Wesley, 1994.
- [55] V. Gurarie, “Logarithmic Operators in Conformal Field Theory”, *Nucl. Phys. B* **410** (1993) 535–549, [arXiv:hep-th/9303160v2](#).
- [56] H. Saleur, “Polymers and percolation in two dimensions and twisted  $N = 2$  supersymmetry”, *Nucl. Phys. B* **382** (1992) 486–531, [arXiv:hep-th/9111007v1](#).
- [57] I. Kostov and M. Mehta, “Random surfaces of arbitrary genus: Exact results for  $d = 0$  and  $d = -2$  dimensions”, *Nucl. Phys. B.* **189** (1987) 118–124.

- [58] B. Duplantier and F. David, "Exact partition functions and correlation functions of multiple Hamiltonian walks on the Manhattan lattice", *J. Stat. Phys* **51** (1988) 327–434.
- [59] J. Distler and H. Kawai, "Conformal Field Theory and 2-D Quantum Gravity or Who's Afraid of Joseph Liouville?", *Nucl. Phys. B* **321** (1989) 509–527.
- [60] J. Zinn-Justin, *Quantum Field Theory and Critical Phenomena*. Oxford Univ. Press, 1989.
- [61] A. Zvonkin, "Matrix Integrals and Map Enumeration: An Accessible Introduction", *Mathematical and Computer Modelling* **26** (1997) 281–304.
- [62] B. Farb and D. Margalit, *A Primer on Mapping Class Groups*.  
<http://www.math.utah.edu/~margalit/primer/>.
- [63] B. Bollobas, *Modern Graph Theory*. Springer, 2002.
- [64] W. Tutte, "A contribution to the theory of chromatic polynomials", *Canad. J. Math* **6** (1954) 80–91.
- [65] O. Bernardi, "A characterization of the Tutte polynomial via combinatorial embeddings", *Annals of Combinatorics* **12** (2008) 139–153, [arXiv:math/0608057v1](https://arxiv.org/abs/math/0608057v1).

# Ringraziamenti

Ringrazio innanzitutto il prof. Sergio Caracciolo per avermi permesso di svolgere questo lavoro di tesi, per i preziosi consigli e il supporto. Ringrazio poi in particolar modo Andrea Sportiello per essere stato sempre presente e aver stimolato la mia curiosità scientifica. Ho appreso molto da lui.

Un grazie particolare va anche a chi mi è stato vicino durante questi cinque anni di Università. Per prima la mia famiglia, che mi ha sempre appoggiato e sostenuto affinché potessi portare avanti serenamente gli studi; non saprei con le parole come rendere giustizia di quanto gli sia debitore. Poi Laura, che mi è stata sempre accanto, si è dimostrata rispettosa dei miei impegni, e si è sorbita i miei monologhi di fisica, grazie.

Ringrazio i miei amici più cari, il Tres e Luca, i compagni di musica, Ale, Pablo, Comi, Paolo, Bosca, Robi, Mauro, Tanz, Pera, Betti, le serate passate con voi sono state davvero importanti. Ringrazio anche il maestro Pacho, da cui, oltre che la musica, spero di aver appreso la determinazione nel cercare di fare ciò che piace nella vita, fregandosene di cosa pensano gli altri.

Ringrazio poi i compagni di LCM, Gian, Vittore, Davide, Jacopo, Buddino, Emanuele, non avrei potuto trovare un gruppo e un posto migliore in Università. Un grazie va anche agli altri amici dell'Università, Ale Motta (con cui ho passato interminabili pomeriggi a studiare, un grazie particolare va a lui), Ulisse (con cui ho condiviso parecchi interessi), Davide, Margherita, Pier, Ale Amato, Enrico, Pietro, Sara, Simona, Arianna, Marco e tutti gli altri con cui ho studiato e scherzato fino ad oggi. Mi sembra assurdo che stia finendo...